ISSN: 2146-1414

MIRT

Molecular Imaging and Radionuclide Therapy

February 2019 Volume 28 Issue 1 www.tsnm.org

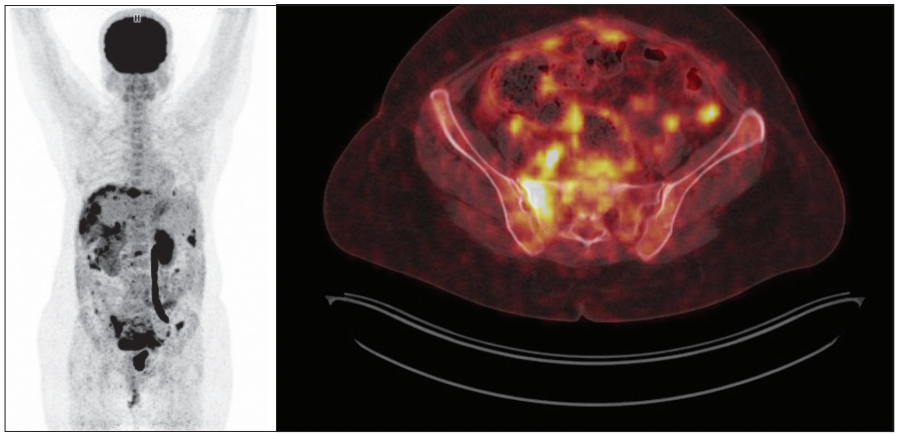

"Official Journal of the Turkish Society of Nuclear Medicine"

galenos yayınevi

TURKISH SOCIETY OF NUCLEAR MEDICINE 1975

MIRT

Molecular Imaging and Radionuclide Therapy

Scientific Advisory Board

MIRT

Molecular Imaging and Radionuclide Therapy

Turkish Society of Nuclear Medicine
Cinnah Caddesi Pilot Sokak No: 10/12 Çankaya 06650 Ankara, Turkey **Phone:** +90 312 441 00 45 **Fax:** +90 312 441 12 95 **Web:** www.tsnm.org **E-mail:** dernekmerkezi@tsnm.org
"Formerly Turkish Journal of Nuclear Medicine"

The paper used to print this journal conforms to ISO 9706: 1994 standard (Requirements for Permanence). The National Library of Medicine suggests that biomedical publications be printed on acid-free paper (alkaline paper). Reviewing the articles' conformity to the publishing standards of the Journal, typesetting, reviewing and editing the manuscripts and abstracts in English, creating links to source data, and publishing process are realized by Galenos.

Galenos Publishing House
Owner and Publisher
Erkan Mor

Publication Coordinator
Burak Sever

Web Coordinators
Soner Yıldırım
Turgay Akpınar

Graphics Department
Ayda Alaca
Çiğdem Birinci
Gülşah Özgül

Project Coordinators
Eda Kolukısa
Hatice Balta
Lütfiye Ayhan İrtem
Sedanur Sert
Zeynep Altındağ

Project Assistants
Gamze Aksoy
Nurcan Acarçağ

Finance Coordinator
Sevinç Çakmak

Research&Development
Kerim Sancar Ölmez
Mert Köse

Publisher Contact
Address: Molla Gürani Mah. Kaçamak Sk. No: 21/1
34093 İstanbul, Turkey
Phone: +90 (212) 621 99 25 **Fax:** +90 (212) 621 99 27
E-mail: info@galenos.com.tr/yayin@galenos.com.tr
Web: www.galenos.com.tr

Printing at: Özgün Ofset Ticaret Ltd. Şti.
Yeşilce Mah. Aytekin Sk. No: 21 34418 4. Levent, İstanbul, Turkey
Phone: +90 (212) 280 00 09
Printing Date: 18 March 2019
ISSN: 2146-1414 **E-ISSN:** 2147-1959
International scientific journal published quarterly.

MIRT

Molecular Imaging and Radionuclide Therapy

ABOUT US

Molecular Imaging and Radionuclide Therapy (formerly Turkish Journal of Nuclear Medicine) is the official publication of Turkish Society of Nuclear Medicine.

Focus and Scope

Molecular Imaging and Radionuclide Therapy (Mol Imaging Radionucl Ther, MIRT) is a double-blind peer-review journal published in English language. It publishes original research articles, reviews, editorials, short communications, letters, consensus statements, guidelines and case reports with a literature review on the topic, interesting images in the field of molecular imaging, multimodality imaging, nuclear medicine, radionuclide therapy, radiopharmacy, medical physics, dosimetry and radiobiology. MIRT is published three times a year (February, June, October). Audience: Nuclear medicine physicians, medical physicists, radiopharmaceutical scientists, radiobiologists.

The editorial policies are based on the "Recommendations for the Conduct, Reporting, Editing, and Publication of Scholarly Work in Medical Journals (ICMJE Recommendations)" by the International Committee of Medical Journal Editors (2016, archived at http://www.icmje.org/) rules.

Open Access Policy

This journal provides immediate open access to its content on the principle that making research freely available to the public supports a greater global exchange of knowledge.

Open Access Policy is based on rules of Budapest Open Access Initiative (BOAI) (http://www.budapestopenaccessinitiative.org/). By "open access" to [peer-reviewed research literature], we mean its free availability on the public internet, permitting any users to read, download, copy, distribute, print, search, or link to the full texts of these articles, crawl them for indexing, pass them as data to software, or use them for any other lawful purpose, without financial, legal, or technical barriers other than those inseparable from gaining access to the internet itself. The only constraint on reproduction and distribution, and the only role for copyright in this domain, should be to give authors control over the integrity of their work and the right to be properly acknowledged and cited.

Permission Requests

Instructions for Authors

Instructions for authors are published in the journal and on the website http://mirt.tsnmjournals.org

Manuscripts can only be submitted electronically through the Journal Agent website (http://www.journalagent.com/mirt/?plng=eng) after creating an account. This system allows online submission and review.

All published volumes in full text can be reached free of charge through the website http://mirt.tsnmjournals.org

Material Disclaimer

Scientific and legal responsibilities pertaining to the papers belong to the authors. Contents of the manuscripts and accuracy of references are also the author's responsibility. The Turkish Society of Nuclear Medicine, the Editor, the Editorial Board or the publisher do not accept any responsibility for opinions expressed in articles.

Financial expenses of the journal are covered by Turkish Society of Nuclear Medicine.

Correspondence Address

Editor-in-Chief, Prof. Zehra Özcan, MD,

Ege University, Medical School, Department of Nuclear Medicine, İzmir, Turkey

Phone: +90 312 441 00 45

Fax: +90 312 441 12 97

E-mail: editor@tsnmjournals.org

Web page: http://mirt.tsnmjournals.org

Publisher Corresponding Address

Galenos Yayınevi Tic. Ltd. Şti.

Address: Molla Gürani Mah. Kaçamak Sk. No: 21/1 34093

Fındıkzade, İstanbul, Turkey

Phone: +90 212 621 99 25

Fax: +90 212 621 99 27

E-mail: info@galenos.com.tr

The journal is printed on an acid-free paper.

MIRT

Molecular Imaging and Radionuclide Therapy

INSTRUCTIONS TO AUTHORS

Molecular Imaging and Radionuclide Therapy (Mol Imaging Radionucl Ther, MIRT) publishes original research articles, short communications, reviews, editorials, case reports with a literature review on the topic, interesting images, consensus statements, guidelines, letters in the field of molecular imaging, multimodality imaging, nuclear medicine, radionuclide therapy, radiopharmacy, medical physics, dosimetry and radiobiology. MIRT is published by the Turkish Society of Nuclear Medicine three times a year (February, June, October). The journal is printed on an acid-free paper.

Molecular Imaging and Radionuclide Therapy does not charge any article submission or processing fees.

GENERAL INFORMATION

MIRT commits to rigorous peer review, and stipulates freedom from commercial influence, and promotion of the highest ethical and scientific standards in published articles. Neither the Editor(s) nor the publisher guarantees, warrants or endorses any product or service advertised in this publication. All articles are subject to review by the editors and peer reviewers. If the article is accepted for publication, it may be subjected to editorial revisions to aid clarity and understanding without changing the data presented.

Manuscripts must be written in English and must meet the requirements of the journal. The journal is in compliance with the uniform requirements for manuscripts submitted to biomedical journals published by the International Committee of Medical Journal Editors (NEJM 1997; 336:309-315, updated 2016). Manuscripts that do not meet these requirements will be returned to the author for necessary revision before the review. Authors of manuscripts requiring modifications have a maximum of two months to resubmit the revised text. Manuscripts returned after this deadline will be treated as new submissions.

It is the authors' responsibility to prepare a manuscript that meets ethical criteria. The Journal adheres to the principles set forth in the Helsinki Declaration October 2013 (https://www.wma.net/policies-post/wma-declaration-of-helsinki-ethical-principles-for-medical-research-involving-human-subjects/) and holds that all reported research involving "Human beings" conducted in accordance with such principles.

Reports describing data obtained from research conducted in human participants must contain a statement in the MATERIALS AND METHODS section indicating approval by the ethical review board (including the approval number) and affirmation that INFORMED CONSENT was obtained from each participant.

All manuscripts reporting experiments using animals must include a statement in the MATERIALS AND METHODS section giving assurance that all animals have received humane care in compliance with the Guide for the Care and Use of Laboratory Animals (www.nap.edu) and indicating approval by the ethical review board.

If the study should have ethical approval, authors asked to provide ethical approval in order to proceed the review process. If they provide approval, review of the manuscript will continue.

In case report(s) and interesting image(s) a statement regarding the informed consent of the patients should be included in the manuscript and the identity of the patient(s) should be hidden.

Subjects must be identified only by number or letter, not by initials or names. Photographs of patients' faces should be included only if scientifically relevant. Authors must obtain written consent from the patient for use of such photographs.

In cases of image media usage that potentially expose patients' identity requires obtaining permission for publication from the patients or their parents/guardians.

If the proposed publication concerns any commercial product, the author must include in the cover letter a statement indicating that the author(s) has (have) no financial or other interest with the product or explaining the nature of any relations (including consultancies) between the author(s) and editor the manufacturer or distributor of the product.

All submissions will be screened by Crossref Smilarity Check powered by "iThenticate". Manuscripts with an overall similarity index of greater than 25%, or duplication rate at or higher than 5% with a single source will be returned back to authors.

MANUSCRIPT CATEGORIES

1. Original Articles

2. Short Communications are short descriptions of focused studies with important, but very straightforward results.

3. Reviews address important topics in the field. Authors considering the submission of uninvited reviews should contact the editor in advance to determine if the topic that they propose is of current potential interest to the Journal. Reviews will be considered for publication only if they are written by authors who have at least three published manuscripts in the international peer reviewed journals and these studies should be cited in the review. Otherwise only invited reviews will be considered for peer review from qualified experts in the area.

4. Editorials are usually written by invitation of the editor by the editors on current topics or by the reviewers involved in the evaluation of a submitted manuscript and published concurrently with that manuscript.

5. Case Report and Literature Reviews are descriptions of a case or small number of cases revealing a previously undocumented disease process, a unique unreported manifestation or treatment of a known disease process, unique unreported complications of treatment regimens or novel and important insights into a condition's pathogenesis, presentation, and/or management. The journal's policy is to accept case reports only if it is accompanied by a review of the literature on the related topic. They should include an adequate number of images and figures.

6. Interesting Image

One of the regular parts of Molecular Imaging and Radionuclide Therapy is a section devoted to interesting images. Interesting image(s) should describe case(s) which are unique and include interesting findings adding insights into the interpretation of patient images, a condition's pathogenesis, presentation, and/or management.

7. Consensus Statements or Guidelines may be submitted by professional societies. All such submissions will be subjected to peer review, must be modifiable in response to criticisms, and will be published only if they meet the Journal's usual editorial standards.

8. Letters to the Editor may be submitted in response to work that has been published in the Journal. Letters should be short commentaries related to specific points of agreement or disagreement with the published work.

Note on Prior Publication

Articles are accepted for publication on the condition that they are original, are not under consideration by another journal, or have not been previously

MIRT
Molecular Imaging and Radionuclide Therapy

published. Direct quotations, tables, or illustrations that have appeared in copyrighted material must be accompanied by written permission for their use from the copyright owner and authors. Materials previously published in whole or in part shall not be considered for publication. At the time of submission, authors must report that the manuscript has not been published elsewhere. Abstracts or posters displayed at scientific meetings need not be reported.

MANUSCRIPT SUBMISSION PROCEDURES

MIRT only accepts electronic manuscript submission at the web site http://www.journalagent.com/mirt/. After logging on to the website Click the 'online manuscript submission' icon. All corresponding authors should be provided with a password and a username after entering the information required. If you already have an account from a previous submission, enter your username and password to submit a new or revised manuscript. If you have forgotten your username and/or password, please send an e-mail to the editorial office for assistance. After logging on to the article submission system please read carefully the directions of the system to give all needed information and attach the manuscript, tables and figures and additional documents.

All Submissions Must Include:

1. Completed Copyright Assignment & Disclosure of Potential Conflict of Interest Form; This form should be downloaded from the website (provided in the author section), filled in thoroughly and uploaded to the website during the submission.
2. All manuscripts describing data obtained from research conducted in human participants must be accompanied with an approval document by the ethical review board.
3. All manuscripts reporting experiments using animals must include approval document by the animal ethical review board.
4. All submissions must include the authorship contribution form which is signed by all authors.

Authors must complete all online submission forms. If you are unable to successfully upload the files please contact the editorial office by e-mail.

MANUSCRIPT PREPARATION

General Format

The Journal requires that all submissions be submitted according to these guidelines:

- Text should be double spaced with 2.5 cm margins on both sides using 12-point type in Times Roman font.
- All tables and figures must be placed after the text and must be labeled.
- Each section (abstract, text, references, tables, figures) should start on a separate page.
- Manuscripts should be prepared as a word document (*.doc) or rich text format (*.rtf).
- Please make the tables using the table function in Word.
- Abbreviations should be defined in parenthesis where the word is first mentioned and used consistently thereafter.
- Results should be expressed in metric units. Statistical analysis should be done accurately and with precision. Please consult a statistician if necessary.
- Authors' names and institutions should not be included in the manuscript text and should be written only in the title page.

Title Page

The title page should be a separate form from the main text and should include the following:

- Full title (in English and in Turkish). Turkish title will be provided by the editorial office for the authors who are not Turkish speakers.
- Authors' names and institutions.
- Short title of not more than 40 characters for page headings.
- At least three and maximum eight keywords. (in English and in Turkish). Do not use abbreviations in the keywords. Turkish keywords will be provided by the editorial office for the authors who are not Turkish speakers. If you are not a native Turkish speaker, please reenter your English keywords to the area provided for the Turkish keywords. English keywords should be provided from http://www.nlm.nih.gov/mesh (Medical Subject Headings) while Turkish keywords should be provided from http://www.bilimterimleri.com.
- Word count (excluding abstract, figure legends and references).
- Corresponding author's e-mail and address, telephone and fax numbers.
- Name and address of person to whom reprint requests should be addressed.

Original Articles

Authors are required to state in their manuscripts that ethical approval from an appropriate committee and informed consents of the patients were obtained.

Original Articles should be submitted with a structured abstract of no more than 250 words. All information reported in the abstract must appear in the manuscript. The abstract should not include references. Please use complete sentences for all sections of the abstract. Structured abstract should include background, objective, methods, results and conclusions. Turkish abstract will be provided by the editorial office for the authors who are not Turkish speakers. If you are not a native Turkish speaker, please reenter your English abstract to the area provided for the Turkish abstract.

- Introduction
- Materials and Methods
- Results
- Discussion
- Study Limitations
- Conclusion

May be given for contributors who are not listed as authors, or for grant support of the research.

References should be cited in numerical order (in parentheses) in the text and listed in the same numerical order at the end of the manuscript on a separate page or pages. The author is responsible for the accuracy of references. Examples of the reference style are given below. Further examples will be found in the articles describing the Uniform Requirements for Manuscripts Submitted to Biomedical Journals (Ann Intern Med.1988; 208:258-265, Br Med J. 1988; 296:401-405). The titles of journals should be abbreviated according to the style used in the Index Medicus. Journal Articles and Abstracts: Surnames and initials of author's name, title of the article, journal name, date, volume number, and pages. All authors should be listed regardless of number. The citation of unpublished papers, observations or personal communications is not permitted. Citing an abstract is

not recommended. Books: Surnames and initials of author's names, chapter title, editor's name, book title, edition, city, publisher, date and pages.

Sample References

Journal Article: Sayit E, Söylev M, Capa G, Durak I, Ada E, Yilmaz M. The role of technetium-99m-HMPAO-labeled WBC scintigraphy in the diagnosis of orbital cellulitis. Ann Nucl Med 2001;15:41-44.

Erselcan T, Hasbek Z, Tandogan I, Gumus C, Akkurt I. Modification of Diet in Renal Disease equation in the risk stratification of contrast induced acute kidney injury in hospital inpatients. Nefrologia 2009 doi: 10.3265/Nefrologia.2009.29.5.5449.en.full.

Article in a journal published ahead of print: Ludbrook J. Musculovenous pumps in the human lower limb. Am Heart J 2009;00:1-6. (accessed 20 February 2009).

Lang TF, Duryea J. Peripheral Bone Mineral Assessment of the Axial Skeleton: Technical Aspects. In: Orwoll ES, Bliziotes M (eds). Osteoporosis: Pathophsiology and Clinical Management. New Jersey, Humana Pres Inc, 2003;83-104.

Books: Greenspan A. Orthopaedic Radiology a Pratical Approach. 3th ed. Philadelphia, Lippincott Williams Wilkins 2000, 295-330.

Website: Smith JR. 'Choosing Your Reference Style', Online Referencing 2(3), http://orj.sagepub.com (2003, accessed October 2008).

- Tables

Tables must be constructed as simply as possible. Each table must have a concise heading and should be submitted on a separate page. Tables must not simply duplicate the text or figures. Number all tables in the order of their citation in the text. Include a title for each table (a brief phrase, preferably no longer than 10 to 15 words). Include all tables in a single file following the manuscript.

– Figure Legends

Figure legends should be submitted on a separate page and should be clear and informative.

– Figures

Number all figures (graphs, charts, photographs, and illustrations) in the order of their citation in the text. At submission, the following file formats are acceptable: AI, EMF, EPS, JPG, PDF, PPT, PSD, TIF. Figures may be embedded at the end of the manuscript text file or loaded as separate files for submission. All images MUST be at or above intended display size, with the following image resolutions: Line Art 800 dpi, Combination (Line Art + Halftone) 600 dpi, Halftone 300 dpi. Image files also must be cropped as close to the actual image as possible.

Short Communications:

Short communications should be submitted with a structured abstract of no more than 200 words. These manuscripts should be no longer than 2000 words, and include no more than two figures and tables and 20 references. Other rules which the authors are required to prepare and submit their manuscripts are the same as described above for the original articles.

Review Articles:

- Title page (see above)
- Abstract: Maximum 250 words; without structural divisions; in English and in Turkish . Turkish abstract will be provided by the editorial office for the authors who are not Turkish speakers. If you are not a native Turkish speaker, please reenter your English abstract to the area provided for the Turkish abstract.
- Text
- Conclusion
- Acknowledgements (if any)
- References

Editorial:

- Title page (see above)
- Abstract: Maximum 250 words; without structural divisions; in English and in Turkish. Turkish abstract will be provided by the editorial office for the authors who are not Turkish speakers. If you are not a native Turkish speaker, please re enter your English abstract to the area provided for the Turkish abstract.
- Text
- References

Case Report and Literature Review

- Title page (see above)
- Abstract: Approximately 100-150 words; without structural divisions; in English and in Turkish. Turkish abstract will be provided by the editorial office for the authors who are not Turkish speakers. If you are not a native Turkish speaker, please re-enter your English abstract to the area provided for the Turkish abstract.
- Introduction
- Case report
- Literature Review and Discussion
- References

Interesting Image:

No manuscript text is required. Interesting Image submissions must include the following:

Title Page: (see Original article section)

Abstract: Approximately 100-150 words; without structural divisions; in English and in Turkish. Turkish abstract will be provided by the editorial office for the authors who are not Turkish speakers. If you are not a native Turkish speaker, please re-enter your English abstract to the area provided for the Turkish abstract.

Image(s): The number of images is left to the discretion of the author. (See Original article section)

Figure Legend: Reference citations should appear in the legends, not in the abstract. Since there is no manuscript text, the legends for illustrations should be prepared in considerable detail but should be no more than 500 words total. The case should be presented and discussed in the Figure legend section.

References: Maximum eight references (see original article section).

Letters to the Editor:

- Title page (see above)
- Short comment to a published work, no longer than 500 words, no figures or tables.
- References no more than five.

Consensus Statements or Guidelines: These manuscripts should typically be no longer than 4000 words and include no more than six figures and tables and 120 references.

MIRT
Molecular Imaging and Radionuclide Therapy

INSTRUCTIONS TO AUTHORS

Proofs and Reprints

Proofs and a reprint orders are sent to the corresponding author. The author should designate by footnote on the title page of the manuscript the name and address of the person to whom reprint requests should be directed. The manuscript when published will become the property of the journal.

Archiving

The editorial office will retain all manuscripts and related documentation (correspondence, reviews, etc.) for 12 months following the date of publication or rejection.

Submission Preparation Checklist

As part of the submission process, authors are required to check off their submission's compliance with all of the following items, and submissions may be returned to authors that do not adhere to these guidelines.

1. The submission has not been previously published, nor is it before another journal for consideration (or an explanation has been provided in Comments to the Editor).
2. The submission file is in Microsoft Word, RTF, or WordPerfect document file format. The text is double-spaced; uses a 12-point font; employs italics, rather than underlining (except with URL addresses); and the location for all illustrations, figures, and tables should be marked within the text at the appropriate points.
3. Where available, URLs for the references will be provided.
4. All authors should be listed in the references, regardless of the number.
5. The text adheres to the stylistic and bibliographic requirements outlined in the Author Guidelines, which is found in About the Journal.
6. English keywords should be provided from http://www.nlm.nih.gov/mesh(Medical Subject Headings), while Turkish keywords should be provided fromhttp://www.bilimterimleri.com
7. The title page should be a separate document from the main text and should be uploaded separately.
8. The "Affirmation of Originality and Assignment of Copyright/The Disclosure Form for Potential Conflicts of Interest Form" and Authorship Contribution Form should be downloaded from the website, filled thoroughly and uploaded during the submission of the manuscript.

TO AUTHORS

Copyright Notice

The author(s) hereby affirms that the manuscript submitted is original, that all statement asserted as facts are based on author(s) careful investigation and research for accuracy, that the manuscript does not, in whole or part, infringe any copyright, that it has not been published in total or in part and is not being submitted or considered for publication in total or in part elsewhere. Completed Copyright Assignment & Affirmation of Originality Form will be uploaded during submission. By signing this form;

1. Each author acknowledges that he/she participated in the work in a substantive way and is prepared to take public responsibility for the work.
2. Each author further affirms that he or she has read and understands the "Ethical Guidelines for Publication of Research".
3. The author(s), in consideration of the acceptance of the manuscript for publication, does hereby assign and transfer to the Molecular Imaging and Radionuclide Therapy all of the rights and interest in and the copyright of the work in its current form and in any form subsequently revised for publication and/or electronic dissemination.

Privacy Statement

The names and email addresses entered in this journal site will be used exclusively for the stated purposes of this journal and will not be made available for any other purpose or to any other party.

Peer Review Process

1. The manuscript is assigned to an editor, who reviews the manuscript and makes an initial decision based on manuscript quality and editorial priorities.
2. For those manuscripts sent for external peer review, the editor assigns at least two reviewers to the manuscript.
3. The reviewers review the manuscript.
4. The editor makes a final decision based on editorial priorities, manuscript quality, and reviewer recommendations.
5. The decision letter is sent to the author.

Contact Address

All correspondence should be directed to the Editorial Office:
Cinnah Caddesi Pilot Sokak No:10/12 06650 Çankaya / Ankara, Turkey
Phone: +90 312 441 00 45
Fax: +90 312 441 12 97
E-mail: info@tsnmjournals.org

MIRT
Molecular Imaging and Radionuclide Therapy

CONTENTS

Original Articles

Interesting Images

Letter to the Editor

Original Article
Mol Imaging Radionucl Ther 2019;28:1-7 DOI:10.4274/mirt.galenos.2018.88528

Effect of PET Image Reconstruction Techniques on Unexpected Aorta Uptake

PET Görüntü Rekonstrüksiyon Tekniklerinin Beklenmeyen Aorta Tutulumu Üzerinde Etkisi

Hassan Hirji[1], Keith Sullivan[2], Imran Lasker[3], Mhd S. Sharif[4], Andre Nunes[3], Chris Shepherd[3], Wai-lup Wong[3], Bal Sanghera[3]

[1]*Northwick Park Hospital, Department of Rheumatology, London, England*
[2]*University of Hertfordshire, London, England*
[3]*Paul Strickland Scanner Centre, Mount Vernon Hospital, London, England*
[4]*University of East London, London, England*

Abstract

Objectives: To determine if unexpected aorta uptake seen in some patients is influenced by popular modern reconstruction algorithms using semi-quantitative and qualitative analysis.

Methods: Twenty-five consecutive patients without suspected vascular disease were selected for ^{18}F-FDG positron emission tomography/computed tomography (PET/CT) scanning and images of the aorta were created using iterative reconstruction (IT), IT + time of flight (TOF), IT + TOF + point spread function correction (referred collectively as UHD) with and without metal artefact reduction (MAR) algorithms. An experienced radiologist created aorta and blood pool (BP) regions of interests then copied these to all reconstructions for accurate positioning before recording target aorta standardized-uptake-values (SUV_{max}) and background BP SUV_{mean}. Furthermore, target-to-background ratio (TBR_{max}) was defined by aorta SUV_{max}-to-BP SUV_{mean} ratio for more analysis.

Results: For aorta SUV_{max} with IT, IT + TOF, UHD, UHD + MAR reconstructions the mean ± standard deviation recorded were 2.15±0.43, 2.25±0.51, 2.25±0.45 and 2.09±0.4, respectively. Values for BP SUV_{mean} were 1.61±0.31, 1.58±0.28, 1.58±0.28 and 1.47±0.25, respectively. Likewise, for TBR_{max} these were 1.35±0.19, 1.43±0.21, 1.43±0.19, 1.43±0.18, respectively. ANOVA analysis revealed no significant differences for aorta SUV_{max} (F(0.86) p=0.46), BP SUV_{mean} (F(1.22) p=0.31) or TBR_{max} (F(0.99) p=0.4). However, the qualitative visual analysis revealed significant differences between IT + TOF with UHD (p=0.02) or UHD + MAR (p=0.02).

Conclusion: Reconstruction algorithm effect on aorta SUV_{max} or BP SUV_{mean} or TBR_{max} was not statistically significant. However, qualitative visual analysis showed significant differences between IT + TOF as compared with UHD or UHD + MAR reconstructions. Harmonization of techniques with a larger patient cohort is recommended in future clinical trials.

Keywords: Positron emission tomography, computed tomography, aorta, blood pool, quantitative, qualitative, analysis

Öz

Amaç: Yarı-kantitatif ve kalitatif analiz kullanarak bazı hastalarda görülen beklenmedik aorta tutulumunun popüler modern rekonstrüksiyon algoritmalarından etkilenip etkilenmediğini belirlemektir.

Yöntem: Vasküler hastalık şüphesi olmayan 25 ardışık hasta ^{18}F-FDG pozitron emisyon tomografi/bilgisayarlı tomografi (PET/BT) görüntüleme için seçildi ve iterative rekonstrüksiyon (IT), IT + time of flight (TOF), IT + TOF + point spread function düzeltme ile, metal artefact reduction (MAR) algoritmasıyla ve bu algoritma kullanılmaksızın, aorta görüntüleri oluşturuldu. Deneyimli bir uzman aorta ve kan havuzu ROI'lerini oluşturarak bunları hedef aort SUV_{maks} ve arka plan (BP) $SUV_{ortalama}$ değerlerini kaydetmeden önce doğru pozisyonu sağlamak için tüm rekonstrüksiyonlara kopyaladı. Buna ek olarak, hedef-BP oranı (TBR_{maks}), aorta SUV_{maks}-BP $SUV_{ortalama}$ oranı kullanılarak, ileri analiz için hesaplandı.

Bulgular: Ortalama ± standart deviasyon aorta SUV_{maks} değeri IT, IT + TOF, UHD, UHD + MAR rekonstrüksiyonları ile 2,15±0,43, 2,25±0,51, 2,25±0,45 ve 2,09±0,4 olarak saptandı. BP $SUV_{ortalama}$ için bu değerler 1,61±0,31, 1,58±0,28, 1,58±0,28 ve 1,47±0,25 idi. Benzer şekilde,

Address for Correspondence: Bal Sanghera MD, Paul Strickland Scanner Centre, Mount Vernon Hospital, London, England
Phone: +01923844392 E-mail: bal.sanghera@nhs.net ORCID ID: orcid.org/0000-0003-0206-7834
Received: 12.03.2018 **Accepted:** 14.09.2018

TBR_{maks} için bu değerler 1,35±0,19, 1,43±0,21, 1,43±0,19, 1,43±0,18 olarak belirlendi. ANOVA analizi aorta SUV_{maks} (F(0,86) p=0,46), BP $SUV_{ortalama}$ (F(1,22) p=0,31) veya TBR_{maks} (F(0,99) p=0,4) arasında istatistik olarak anlamlı fark saptamadı. Bununla birlikte kalitatif görsel analiz, UHD (p=0,02) ya da UHD + MAR (p=0,02) rekonstrüksiyonları ile yapılan IT + TOF arasında anlamlı farklılık ortaya koydu.

Sonuç: Rekonstrüksiyon algoritmalarının aorta SUV_{maks} veya BP $SUV_{ortalama}$ ya da TBR_{maks} üzerinde etkisi istatistiki olarak anlamlı değildi. Ancak kalitatif görsel analiz, UHD ya da UHD + MAR rekonstrüksiyonları ile yapılan IT + TOF arasında anlamlı farklılık ortaya koydu. İleride yapılacak klinik çalışmalarda daha geniş bir hasta grubu ile tekniklerin harmonizasyonu önerilir.

Anahtar kelimeler: Pozitron emisyon tomografi, bilgisayarlı tomografi, aorta, kantitatif, kalitatif, analiz

Introduction

PET technological scanning innovations (1) have increased rapidly over the last decade leading to improved diagnostic imaging capability. Examples include routine clinical introduction of time-of-flight (TOF) scanning (2), point-spread-function correction (PSF) (3), metal artefact reduction (MAR) (4), gating (5), dose reduction techniques (6), application to radiotherapy treatment planning (7), continuous bed motion, digital detectors etc. (8). These have all contributed significantly to widespread adoption of PET as a popular clinical diagnostic imaging tool in the patient pathway today (9).

A recognised caveat of introducing new advances in scanning technology is the necessity to compare images against scanners incorporating older and less sophisticated equipment. Corresponding concerns in image interpretation can arise e.g. with PET/computed tomography (CT) superseding PET only systems (10) or with new PET magnetic resonance imaging systems (11). For PET this comparison can apply equally to visual qualitative analysis and semi-quantitative analysis utilizing standardized uptake values (SUV).

An increasing recognized challenge exists in qualitative and quantitative comparison of patient scans across PET/CT vendors and device-dependent image reconstruction algorithms. PET scanner harmonization against a standard has been widely used for SUV comparison between scanners and is commonly employed in multi-centre clinical trials to reduce bias (12) leading to more reliable and reproducible results. It has also been proposed that different reconstructions be applied for optimizing qualitative and quantitative analysis (13) with a review of modern harmonization strategies (14) to address differences described above.

Specifically, in the case of PET qualitative analysis, some clinicians have commented on unexpected apparent increased physiological uptake that simulates disease in the aorta and great vessels (15,16). The full cause of these observations is unclear and may comprise of multiple, complex factors including patient physiology and scanner hardware/software configuration. Further, this effect can be exacerbated by the introduction of modern imaging algorithms e.g. PSF modelling which has the potential to boost focal uptake. The role of ^{18}F-FDG in diagnosis of vascular disease (17) may be undermined with the potential to mistake image reconstruction effects as PET false positives (18). Accordingly, introduction of new technology initially has the potential to lead to loss of confidence in reporting with potential misdiagnosis and unneeded further tests possibly leading to poor utilization of funding & resources (19).

A thorough analysis of all factors thought to be responsible for apparent increased aorta uptake is challenging clinically and beyond the scope of this publication. In response, we investigated the effect of PET reconstruction techniques on ^{18}F-FDG aorta uptake, in a clinical setting, to establish if apparent increased uptake in patients without known vascular disease is influenced by modern popular algorithms. We investigated 25 consecutive patients scanned using iterative reconstruction (IT), IT + TOF, IT + TOF + PSF referred to as UHD with and without MAR algorithms for a range of aorta and blood pool (BP) SUV. Aorta uptake target-to-background ratio (TBR), defined as TBR_{max}=Aorta SUV_{max}/BP SUV_{mean}, is a commonly used metric for assessment of vasculitis and was also investigated. We compared differences between reconstruction algorithms in terms of semi-quantitative analysis and by qualitative visual assessment.

Materials and Methods

Twenty-five consecutive patients were selected who underwent routine PET/CT studies at our centre. Exclusion criteria included non-^{18}F-FDG scans and subjects with suspected large vessel vasculitis, aortitis or thoracic aortic grafts to minimize bias arising in vascular disease. Patients with metallic implants in the required fields of view, including pacemakers, were not included due to the potential for artefacts in attenuation correction.

Subjects scanned with a Siemens Biograph mCT 64 slice PET/CT scanner were asked to fast for six hours prior to ^{18}F-FDG injection. Blood glucose was recorded prior to injection with an upper limit of 10 mmol/dL applied. Patients were injected with 4.5 MBq/kg ^{18}F-FDG and following a

typical 90 minute uptake period scans were acquired for 3 min per bed. Subject weight average ± standard deviation (SD) was 77.1±19.8 kg, injected activity 355.6±90.5 MBq and age 62.7±11.3 years, respectively. The scanner was calibrated with recommended QA regimes implemented and daily QA pass before clinical use to ensure accuracy and consistency of scanning was maintained. Clinical IR algorithms consisted of 2 iterations and 21 subsets with a 5 mm smoothing filter and zoom of 1 on a 200x200 matrix yielding a 4.07x4.07x3 mm^3 voxel size.

CT acquisition without contrast media was performed from the skull base to the proximal femora. Acquisition settings included tube potential 120 kVp, automatic current modulation, revolution time 0.5 s, collimation 16x1.2 mm, pitch 0.8 and slice thickness 3 mm. Patients were asked to breathe gently during CT and PET acquisition with CT data was used for attenuation correction and anatomical localization.

2D regions of interest (ROI) were hand created by a clinician in the aorta using trans-axial CT slices for anatomic localization (Figure 1a). ROIs were transferred to PET UHD reconstructions and adjusted if necessary to avoid adjacent activity before application *in situ* to other reconstructions. Aorta ROI (Figure 1b), and mediastinal BP ROI (Figure 1c), were acquired at the upper part of the descending aorta just below the arch where the descending aorta has a continuous circular wall. These were delineated by the outer voxels of the aortic wall and the outermost voxels of blood within the aorta at that level, respectively. Care was taken to exclude any mediastinal lymph nodes or other avid pathology within the ROI.

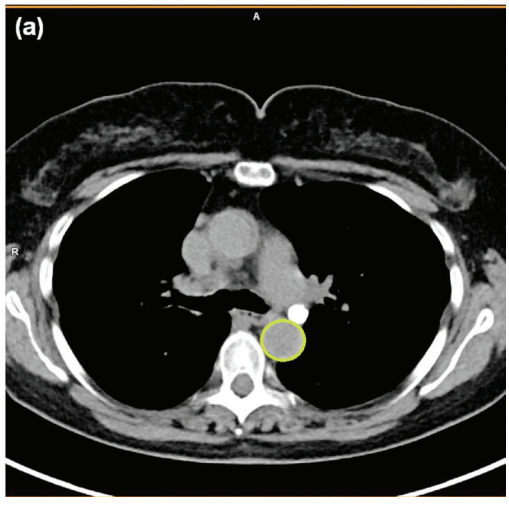

Figure 1a. Typical regions of interest placement for the aorta guided by computed tomography

Two ROIs per patient (aorta SUV_{max} and BP SUV_{mean}) per image reconstruction technique applied were generated and including TBR_{max} estimation amounted to 300 measurements in total across all reconstructions and all patients. Qualitative and semi-quantitative analysis was implemented on a Siemens dedicated workstation (Syngo. via, Siemens, Erlangen, Germany).

Semi-quantitative Analysis

For semi-quantitative comparison, ROI defined aorta SUV_{max} and BP SUV_{mean} standardized to body weight were recorded using IT, IT + TOF, UHD and UHD + MAR reconstruction algorithms. TBR_{max} derived from these SUV were then calculated.

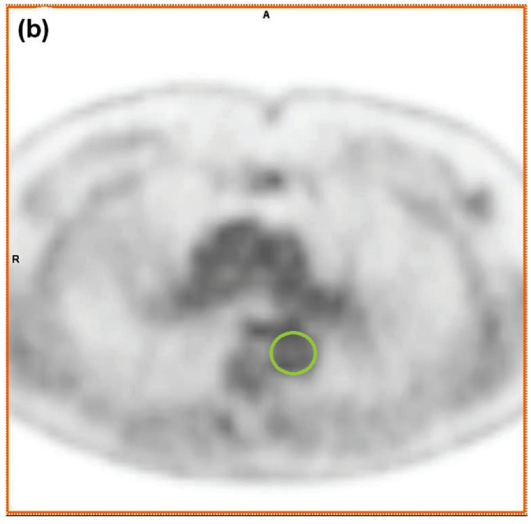

Figure 1b. Aorta regions of interest copied to positron emission tomography slice

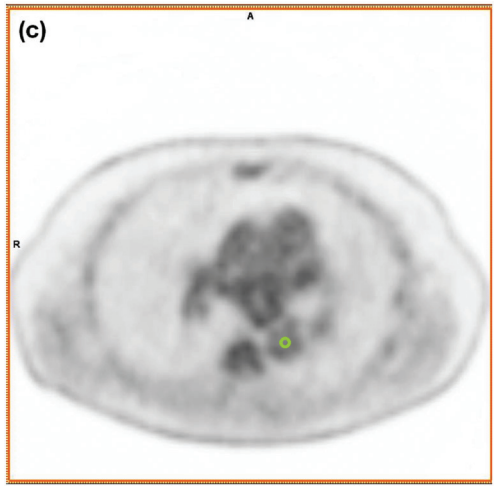

Figure 1c. Typical positron emission tomography blood pool regions of interest

Data were investigated using one-way analysis of variance (ANOVA) revealing any statistically significant differences between means of independent reconstruction algorithms. Fischer's least significant difference post-hoc test was applied to identify which, if any, reconstruction algorithm means were statistically different within these respective groups.

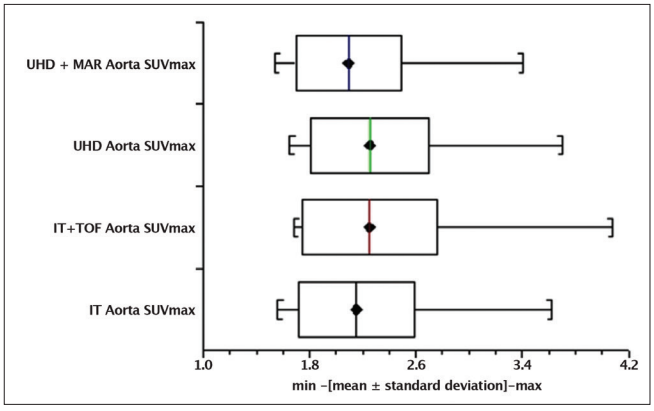

Figure 2. Aorta SUV_{max} distributions with different reconstructions

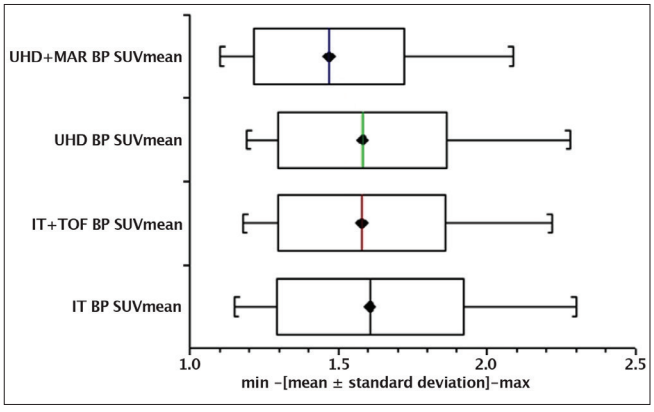

Figure 3. Blood pool SUV_{mean} distributions with different reconstructions

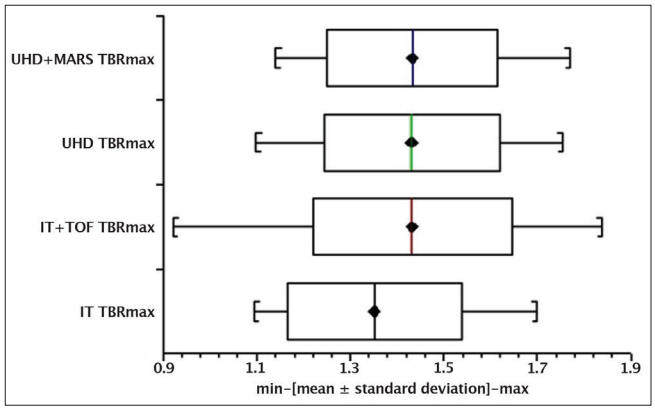

Figure 4. Target-to-background ratio maximum distributions with different reconstructions

Qualitative Analysis

Visual comparison was made by a radiologist with 1.5 years experience of PET/CT reporting, using images reconstructed by IT + TOF as the standard as compared to more recent UHD or UHD + MAR. A scoring system, for UHD or UHD + MAR in comparison with respective IT + TOF scans, was adopted such that a score of '1' depicted aorta markedly less avid, '2' specified aorta slightly less avid, '3' represented no discernible difference, '4' indicated aorta is slightly more avid while '5' signified aorta markedly more avid.

The scoring system led to a parametric preference scale from which a mean and 95% confidence interval (CI) were evaluated. A consistent preference for 1 scan in the direction indicated by the coding at a 5% level was suggested when the 95% CI did not cross 0 and was consistent with a 1-sample t-test.

This project involving comparison and quality assurance of existing techniques was classified as an audit under NHS Research and Development Guidelines 2006, and therefore NHS Research and Ethics Committee approval was not required. All scans once identified as eligible under the suitability criteria were anonymized by a technician prior to further analysis by a clinician.

Results

Semi-quantitative

A box and whisker plot (Figure 2) represented aorta SUV_{max} recorded in ROI measurements collected from the 25 patients scanned. The mean ± SD for IT, IT + TOF, UHD, UHD + MAR reconstructions was 2.15±0.43, 2.25±0.51, 2.25±0.45 and 2.09±0.4, respectively. Likewise, Figure 3 represents these parameters for BP SUV_{mean} with mean ± SD values of 1.61±0.31, 1.58±0.28, 1.58±0.28 and 1.47±0.25, respectively. Similarly, Figure 4 reveals TBR_{max} mean ± SD values of 1.35±0.19, 1.43±0.21, 1.43±0.19, 1.43±0.18, respectively.

The Shapiro-Wilkes test established non-normal behaviour in reconstruction algorithm SUV distributions necessitating log transformations for further statistical analysis. ANOVA revealed no statistically significant differences between the means of independent reconstruction algorithms investigated for aorta SUV_{max} ($F(0.86)$ $p=0.46$), BP SUV_{mean} ($F(1.22)$ $p=0.31$) or TBR_{max} ($F(0.99)$ $p=0.4$).

Qualitative

The appearance of standard IT + TOF reconstructions was compared with UHD or UHD + MAR algorithms and in each case the radiologist's qualitative scoring response ranged from '1' i.e. aorta markedly less avid, through to '5' i.e.

aorta markedly more avid yielding a score mean ± SD with associated p values of 3.28±0.58, p=0.02 or 3.29±0.59, p=0.02 for UHD or UHD + MAR, respectively, when compared with IT + TOF reconstructions.

Discussion

Complicated automated approaches have been used elsewhere to perform segmentation typically using CT to define the aorta (20) initially. In this publication, exotic segmentation software techniques were not available while fixed uptake thresholds proved unreliable for defining aorta or BP structure accurately. Segmentation was performed manually by a trained and experienced clinician using hand drawn ROIs for delineation of relevant structures. This pragmatic approach enabled ROIs to be accurately mapped to other reconstructed scans ensuring reproducibility of placement for accurate SUV measurements.

Pre-clinical PET image reconstruction has been reported to heavily influence atherosclerotic plaque ^{18}F-FDG SUV in a rabbit model (21). Clinical application of different PET reconstruction methods in oncology is known to influence SUV semi-quantification with variability introduced in SUV_{max} and SUV_{mean} (22). TBR_{max} traditionally used as a quantitative measure in vascular imaging as the ratio of vessel wall SUV_{max} to the BP SUV_{mean} is known to be a reliable index (23). As a ratio of SUVs it minimizes variability associated with patient weight, injected activity and post injection uptake times that may influence individual SUV. Therefore, TBR_{max} was also included as a metric along with individual SUVs recorded. SUV_{peak} though claimed to be more reproducible (24) is not used in widespread routine clinical practice and accordingly this publication focused on SUV_{max}, SUV_{mean} and TBR_{max} indices for quantitative investigation.

Box and whisker plots (Figures 2, 3, 4) depict minimum, maximum, mean ± SD for Aorta SUV_{max}, BP SUV_{mean} and TBR_{max} with individual reconstructions, respectively. The uptake values presented in this publication are consistent with those reported elsewhere (25). In this study, no significant statistical differences were observed with different reconstruction algorithms for Aorta SUV_{max} or BP SUV_{mean} or TBR_{max} using ANOVA tests on log transformed data; suggesting that image reconstruction did not heavily influence aorta structure uptake values in our cohort of patients without known vascular disease. This result implies that unexpected enhanced uptake seen in more sensitive and accurate modern scanners is possibly related to atherosclerotic plaques not seen in earlier generation machines. The aetiology of this is not yet fully understood and may involve macrophage activity (16) warranting further investigation.

For qualitative evaluation, a trained radiologist compared IT + TOF against UHD or UHD + MAR using the scoring system described earlier. A mean value of 3.28±0.58 was scored for UHD, and 3.29±0.59 for UHD + MAR. In both cases, statistically significant differences of p=0.02 were noted confirming that UHD or UHD + MAR algorithms influenced visual assessment as compared to more traditional IT and TOF reconstruction alone.

It is recognized that there can be a disparity of results in publications dealing with aorta uptake and image interpretation using ^{18}F-FDG PET scanning, highlighting the subtlety of imaging this structure. One must also be careful to understand and interpret the effects of the image reconstruction software applied to generally diffuse aorta uptake compared with the more focal uptake typical in oncology. A systematic review article highlighting ^{18}F-FDG PET uptake in patients with aortic aneurysms demonstrated conflicting results regarding prediction of aneurysm rupture and growth between studies (26). Similarly, no differences were seen in ^{18}F-FDG uptake between heavily and non-heavily calcified aneurysms (27). This intricacy is also revealed in CT angiography studies where aortic signal-to-noise and contrast ratio measurements on patients reconstructed with and without Adaptive Statistical Iterative Reconstruction revealed contradictory qualitative evaluation between reviewers (28).

Our study reflected the existing complexity reported in this field showing semi-quantitative aorta related structure uptake seen in some patients without known vascular disease is not statistically influenced by reconstruction technique. However, some caution must be exercised as our results also confirmed that new image reconstruction techniques can influence the visual appearance of aorta geometry (28), though differences were relatively small. Incongruity between quantitative and qualitative analysis has been observed in healthcare research studies and documented previously (29) supporting the findings of this study. To maintain efficacy and reduce bias from all possible sources described earlier, some form of harmonisation is recommended to ensure consistency in PET vascular imaging (12,14,26) in future investigations.

Study Limitations

This study dealt with the consequence of manipulating various commonly used image reconstruction parameters in a clinical setting to investigate their effect on quantitative and qualitative aspects of unexpected aorta uptake in PET/CT images. The intention was not to characterize or optimize all possible parameters e.g. partial volume

correction, post filter, image matrix size as this was beyond the scope of this publication.

In terms of direct study limitations, a single radiologist created ROIs and took all measurements and performed qualitative evaluations. Ideally consensus agreement between 2 reporters would have the potential for reducing any inherent bias in results. A single image slice in each case was used to define ROIs for characterizing aorta wall, or BP and it is acknowledged that TBR values can be susceptible to partial volume effect (30) in PET scans.

However, for each patient different reconstruction techniques used in this study were applied robustly to the same ROIs on the same slice supporting accurate data acquisition and analysis with minimal additional bias. All analysis was validated by a trained and experienced statistician. We recommend a larger cohort of patients for a more detailed investigation of reconstruction parameters influencing apparent aorta ^{18}F-FDG uptake in future investigations.

Conclusions

Modern PET/CT systems can show unexpected aortic wall uptake in patients without known vascular disease. In this study, we identified that qualitative analysis revealed statistically significant differences between traditional IT + TOF reconstructions and UHD with or without MAR algorithms; indicating that image reconstruction does influence subjective image interpretation. However, quantitatively our study demonstrated little effect of reconstruction algorithm on Aorta SUV_{max}, BP SUV_{mean} or TBR_{max}. Consequently, a need for PET scan harmonization is recommended with a larger study cohort in future multi-centre studies.

Ethics

Ethics Committee Approval: Anonymized audit and non-required.

Informed Consent: Anonymized audit and non-required.

Peer-review: Externally and internally peer-reviewed.

Authorship Contributions

Concept: H.H., K.S., I.L., M.S.S., A.N., C.S., W.W., B.S., Design: H.H., K.S., I.L., M.S.S., A.N., C.S., W.W., B.S., Data Collection or Processing: H.H., K.S., I.L., M.S.S., A.N., C.S., W.W., B.S., Analysis or Interpretation: H.H., K.S., I.L., B.S., Literature Search: H.H., K.S., I.L., M.S.S., A.N., C.S., W.W., B.S., Writing: H.H., K.S., I.L., M.S.S., A.N., C.S., W.W., B.S.

Conflict of Interest: No conflict of interest was declared by the authors.

Financial Disclosure: The authors declared that this study received no financial support.

References

1. Torres EI. PET/CT: underlying physics, instrumentation, and advances. Radiologia 2017;59:431-445.
2. Vandenberghe S, Mikhaylova E, D'Hoe E, Mollet P, Karp JS. Recent developments in time-of-flight PET. EJNMMI Phys 2016;3:3.
3. Kawashima K, Kato K, Tomabechi M, Matsuo M, Otsuka K, Ishida K, Nakamura R, Ehara S. Clinical evaluation of (18)F fludeoxyglucose positron emission tomography/CT using point spread function reconstruction for nodal staging of colorectal cancer. Br J Radiol 2016;89:20150938.
4. Schabel C, Gatidis S, Bongers M, Hüttig F, Bier G, Kupferschlaeger J, Bamberg F, la Fougère C, Nikolaou K, Pfannenberg C. Improving CT-Based PET Attenuation Correction in the Vicinity of Metal Implants by an Iterative Metal Artifact Reduction Algorithm of CT Data and Its Comparison to Dual-Energy-Based Strategies: A Phantom Study. Invest Radiol 2017;52:61-65.
5. Hess M, Buther F, Schafers K. Data-Driven Methods for the Determination of Anterior Posterior Motion in PET. IEEE Trans Med Imaging 2017;36:422-432.
6. Rui X, Cheng L, Long Y, Fu L, Alessio AM, Asma E, Kinahan PE, De Man B. Ultra-low dose CT attenuation correction for PET/CT: analysis of sparse view data acquisition and reconstruction algorithms. Phys Med Biol 2015;60:7437-7460.
7. Mattoli MV, Massaccesi M, Castelluccia A, Scolozzi V, Mantini G, Calcagni ML. The predictive value of (18)F-FDG PET-CT for assessing the clinical outcomes in locally advanced NSCLC patients after a new induction treatment: low-dose fractionated radiotherapy with concurrent chemotherapy. Radiat Oncol 2017;12:4.
8. van der Vos CS, Koopman D, Rijnsdorp S, Arends AJ, Boellaard R, van Dalen JA, Lubberink M, Willemsen ATM, Visser EP. Quantification, improvement, and harmonization of small lesion detection with state-of-the-art PET. Eur J Nucl Med Mol Imaging 2017;44:4-16.
9. Walrand S, Hesse M, Jamar F. Update on novel trends in PET/CT technology and its clinical applications. Br J Radiol 2016;25:20160534.
10. Landis KG, Use of PET/CT scanning in cancer patients: technical and practical considerations Proc (Bayl Univ Med Cent) 2005;18:321-330.
11. Oprea-Lager DE, Yaqub M, Pieters IC, Reinhard R, van Moorselaar RJ, van den Eertwegh AJ. A Clinical and Experimental Comparison of Time of Flight PET/MRI and PET/CT Systems. Mol Imaging Biol 2015;17:714-725.
12. Boellaard R, Delgado-Bolton R, Oyen WJ, Giammarile F, Tatsch K, Eschner W, Verzijlbergen FJ, Barrington SF, Pike LC, Weber WA, Stroobants S, Delbeke D, Donohoe KJ, Holbrook S, Graham MM, Testanera G, Hoekstra OS, Zijlstra J, Visser E, Hoekstra CJ, Pruim J, Willemsen A, Arends B, Kotzerke J, Bockisch A, Beyer T, Chiti A, Krause BJ. FDG PET/CT:EANM procedure guidelines for tumour imaging: version 2.0. Eur J Nucl Med Mol Imaging 2015;42:328-354.
13. Lasnon C, Salomon T, Desmonts C, Dô P, Oulkhouir Y, Madelaine J, Aide N. Generating harmonized SUV within the EANM EARL accreditation program: software approach versus EARL-compliant reconstruction. Ann Nucl Med 2017;31:125-134.
14. Aide N, Lasnon C, Veit-Haibach P, Sera T, Sattler B, Boellaard R. EANM EARL harmonization strategies in PET quantification: from daily practice to multicentre oncological studies. Eur J Nucl Med Mol Imaging 2017;44:17-31.
15. Sarji AS. Physiological uptake in FDG PET simulating disease. Biomed Imaging Interv J 2006;2:e59.
16. Kemna MJ, Bucerius J, Drent M, Vöö S, Veenman M, van Paassen P, Tervaert JW, van Kroonenburgh MJ. Aortic 18F-FDG uptake in patients suffering from granulomatosis with polyangiitis. Eur J Nucl Med Mol Imaging 2015;42:1423-1429.

17. Chrapko BE, Chrapko M, Nocuń A, Stefaniak B, Zubilewicz T, Drop A. Role of 18F-FDG PET/CT in the diagnosis of inflammatory and infectious vascular disease. Nucl Med Rev Cent East Eur 2016;19:28-36.
18. Safaie E, Matthews R, Bergamaschi R. PET scan findings can be false positive. Tech Coloproctol 2015;19:329-330.
19. Mytton OT, Velazquez A, Banken R, Mathew JL, Ikonen TS, Taylor K, Painter F, Jean-Baptiste R, Poon A, Ruelas E. Introducing new technology safely. Qual Saf Health Care 2010;19(Suppl 2):i9-14.
20. Bauer C, Sun S, Sun W, Otis J, Wallace A, Smith BJ, Sunderland JJ, Graham MM, Sonka M, Buatti JM, Beichel RR. Automated measurement of uptake in cerebellum, liver, and aortic arch in full-body FDG PET/CT scans. Med Phys 2012;39:3112-3123.
21. Zhao QM, Zhao X, Feng TT, Zhang MD, Zhuang XC, Zhao XC, Zhang XX, Su G. Monitoring of atherosclerosis evolution by detection of inflammatory states of aortae in a rabbit model using 18F-FDG -PET/CT. Q J Nucl Med Mol Imaging 2014;58:440-450.
22. Riegler G, Karanikas G, Rausch I, Hirtl A, El-Rabadi K, Marik W, Pivec C, Weber M, Prosch H, Mayerhoefer M. Influence of PET reconstruction technique and matrix size on qualitative and quantitative assessment of lung lesions on [18F]-FDG-PET: A prospective study in 37 cancer patients. Eur J Radiol 2017;90:20-26.
23. Bucerius J, Hyafil F, Verberne HJ, Slart RH, Lindner O, Sciagra, R, Agostini D, Übleis C, Gimelli A, Hacker M. Cardiovascular Committee of the European Association of Nuclear Medicine (EANM). Position paper of the Cardiovascular Committee of the European Association of Nuclear Medicine (EANM) on PET imaging of atherosclerosis. Eur J Nucl Med Mol Imaging 2016;43:780-792.
24. Brendle C, Kupferschläger J, Nikolaou K, la Fougère C, Gatidis S, Pfannenberg C. Is the standard uptake value (SUV) appropriate for quantification in clinical PET imaging? - Variability induced by different SUV measurements and varying reconstruction methods. Eur J Radiol 2015;84:158-162.
25. Van der Valk FM, Verweij SL, Zwinderman KAH, Strang AC, Kaiser Y, Marquering HA, Nederveen AJ, Stroes ES, Verberne HJ, Rudd JH. Thresholds for Arterial Wall Inflammation Quantified by 18F-FDG PET Imaging: Implications for Vascular Interventional Studies. JACC Cardiovascular Imaging 2016;9:1198-1207.
26. Timur UT, van Herwaarden JA, Mihajlovi D, De Jong P, Mali W, Moll FL. 18F-FDG PET scanning of abdominal aortic aneurysms and correlation with molecular characteristics: a systematic review. EJNMMI Res 2015;5:76.
27. Kotze CW, Menezes LJ, Endozo R, Groves AM, Ell PJ, Yusuf SW. Increased Metabolic Activity in Abdominal Aortic Aneurysm Detected by 18F-Fluorodeoxyglucose (18F-FDG) Positron Emission Tomography/Computed Tomography (PET/CT). Eur J Vasc Endovasc Surg 2009;38:93-99.
28. Cornfeld D, Israel G, Detroy E, Bokhari J, Mojibian H. Impact of Adaptive Statistical Iterative Reconstruction (ASIR) on Radiation Dose and Image Quality in Aortic Dissection Studies: A Qualitative and Quantitative Analysis. AJR Am J Roentgenol 2011;196:W336-340.
29. Wagner KD, Davidson PJ, Pollini RA, Strathdee SA, Washburn R, Palinkas LA. Reconciling incongruous qualitative and quantitative findings in mixed methods research: Exemplars from research with drug using populations. Int J Drug Policy 2012;23:54-61.
30. Burg S, Dupas A, Stute S, Dieudonné A, Huet P, Le Guludec D, Buvat I. Partial volume effect estimation and correction in the aortic vascular wall in PET imaging. Phys Med Biol 2013;58:7527-7542.

Original Article
Mol Imaging Radionucl Ther 2019;28:8-14 DOI:10.4274/mirt.galenos.2018.00710

The Role of ^{18}F-FDG PET/CT in Detecting Ovarian Cancer Recurrence in Patients with Elevated CA-125 Levels

CA-125 Düzeylerinde Artış Olan Over Kanserli Hastalarda Rekürrens Saptamada ^{18}F-FDG PET/BT'nin Rolü

Arzu Cengiz[1], Zehra Pınar Koç[2], Pelin Özcan Kara[2], Yakup Yürekli[1]

[1]*Aydın Adnan Menderes University Faculty of Medicine, Department of Nuclear Medicine, Aydın, Turkey*
[2]*Mersin University Faculty of Medicine, Department of Nuclear Medicine, Mersin, Turkey*

Abstract

Objectives: To investigate the role of ^{18}F-FDG positron emission tomography/computed tomography (PET/CT) in detection of recurrence in ovarian cancer patients with increased CA-125 levels.

Methods: Fifty-two patients (30-80 years old, mean: 58.5±10.6 years) who had been histopathologically diagnosed with ovarian cancer, underwent ^{18}F-FDG PET/CT imaging for re-staging due to elevation of CA-125 levels were included in this retrospective study. ^{18}F-FDG PET/CT findings were compared with histopathological, radiological and clinical follow-up results.

Results: CA-125 levels ranged between 35.2-2740 U/mL (N: 0-35 U/mL). Recurrent disease was detected in 45 of 52 patients on PET/CT imaging. There were three false negative and one false positive result. In addition to abdominal and pelvic lesions, 14 distant metastatic lesions (brain, lung, liver and bone metastasis) were identified correctly on PET/CT imaging. Sensitivity, specificity, positive and negative predictive value and accuracy of ^{18}F-FDG PET/CT were calculated as 94%, 75%, 98%, 50% and 96%, respectively.

Conclusion: ^{18}F-FDG PET/CT is a useful imaging method that can be used in detection of ovarian cancer recurrence in patients with elevated CA-125 levels. Since this modality offers whole body imaging, distant metastases could be detected in addition to abdominal and pelvic lesions thus contributing to patient management.

Keywords: Ovarian cancer, ^{18}F-FDG PET/CT, tumor, markers

Öz

Amaç: Bu çalışmanın amacı, serum CA-125 düzeylerinde artış olan over kanserli hastalarda rekürrens saptamada ^{18}F-FDG pozitron emisyon tomografi/bilgisayarlı tomografinin (PET/BT) rolünü araştırmaktır.

Yöntem: Bu retrospektif çalışmaya histopatolojik olarak over kanseri tanısı almış, CA-125 düzeylerinde artış nedeniyle yeniden evreleme amacıyla ^{18}F-FDG PET/BT yapılan 52 hasta (30-80 yaş, ortalama: 58,5±10,6 yaş) dahil edildi. ^{18}F-FDG PET/BT bulguları histopatolojik bulgular veya radyolojik ve klinik izlem sonuçlarıyla karşılaştırıldı.

Bulgular: CA-125 düzeyleri 35,2-2740 U/mL (N: 0-35 U/mL) aralığındaydı. PET/BT görüntülerinde rekürren hastalık 52 hastanın 45'inde gösterildi. Üç yanlış negatif, bir yanlış pozitif sonuç elde edildi. Abdominal ve pelvik lezyonlara ilave olarak 14 uzak metastaz (beyin, akciğer, karaciğer ve kemik metastazı) PET/BT ile doğru olarak gösterildi. Duyarlılık, özgüllük, pozitif ve negatif öngörü değeri ve doğruluk sırasıyla %94, %75, %98, %50 ve %96 idi.

Sonuç: ^{18}F-FDG PET/BT, serum CA-125 düzeylerinde artış olan over kanserli hastalarda rekürrens saptamada kullanılabilecek yararlı bir yöntemdir. Tüm vücut görüntüleme yöntemi olması nedeniyle abdominal ve pelvik lezyonların yanında uzak metastazları da saptayarak bu hastaların izlemine katkıda bulunabilir.

Anahtar kelimeler: Over kanseri, ^{18}F-FDG PET/BT, tümör, belirteçler

Address for Correspondence: Arzu Cengiz MD, Aydın Adnan Menderes University Faculty of Medicine, Department of Nuclear Medicine, Aydın, Turkey
Phone: +90 256 444 12 56 E-mail: arzukincengiz@gmail.com ORCID ID: orcid.org/0000-0003-2110-4450
Received: 07.11.2018 **Accepted:** 13.02.2019

Introduction

Ovarian cancer is the fourth leading cause of cancer death among women (1). It is usually diagnosed at advanced stages thus having poor prognosis. In spite of effective treatment and complete response, recurrence may occur in 50-80% of these patients (2,3,4). Early detection of recurrence is important for patient management.

CA-125 is a high-molecular weight glycoprotein that is expressed at the cell-surface of epithelial cells. Serum CA-125 levels are the reference method for the detection of ovarian carcinoma recurrences with a very high positive predictive value (PPV). Nevertheless, CA-125 is not specific for ovarian cancer in addition to not being sensitive especially for small-volume disease (5,6).

^{18}F-FDG positron emission tomography/computed tomography (PET/CT) is a noninvasive, highly accurate imaging method both in staging and in follow-up of many cancers including ovarian cancer. ^{18}F-FDG PET/CT has a very high sensitivity rate (85-100%) for detection of recurrence in ovarian cancer (7).

The aim of this retrospective study is to investigate the role of ^{18}F-FDG PET/CT in detection of recurrence in ovarian cancer patients with increased CA-125 levels.

Materials and Methods

Patient Population

All patients who underwent ^{18}F-FDG PET/CT for restaging due to high CA-125 levels (N: 0-35 U/mL) from March 2013 to December 2016 were retrospectively evaluated. A total of 52 patients (30-80 years; mean 58.5±10.6) were analyzed in two different institutions. All patients had undergone surgery (3-94 month ago) and chemotherapy or radiotherapy prior to PET/CT imaging. ^{18}F-FDG PET/CT findings were compared with histopathological, radiological and clinical follow-up findings in at least 6 months.

The Local Ethics Committee of Adnan Menderes University approved the study (protocol number: 2018/1487, date: 27.09.2018).

^{18}F-FDG PET/CT Imaging

All patients' fasting blood sugar levels were less than 180 mg/dL prior to imaging. After intravenous administration of 270-370 MBq (7.3-10 mCi) ^{18}F-FDG, patients rested in a quiet room. Oral contrast was given to all patients. ^{18}F-FDG PET/CT imaging was performed after a resting period of 60 minutes by using Siemens (Biograph mCT 20) and General Electric (GE, Discovery 610) PET/CT scanners. The CT scan data were collected at 120 kV and 50 mAs. The PET acquisitions were obtained from the head to the midthighs at the rate of 2 minute per frame.

All ^{18}F-FDG PET/CT imaging were evaluated visually and semi-quantitatively by two nuclear medicine physicians. For semi-quantitative evaluation, maximum standardized uptake values (SUV_{max}) were calculated for all pathological lesions. The lesions with a $SUV_{max} \geq 2.5$ at the site of pathologic changes on CT imaging were accepted as malignant lesions.

Data Analysis

PET/CT findings were compared with histopathologic findings (n=10) and serial conventional imaging methods and/or clinical follow-up results (n=42). If the lesion could not be histopathologically confirmed then those with decreased CA-125 levels following ovarian cancer treatment (chemotherapy or radiation therapy) and/or lesions verified by serial imaging methods including PET/CT were accepted as true positive (TP). If PET/CT findings were normal and no recurrence was detected during serial imaging or clinical follow-up then the result was classified as true negative (TN). If PET/CT findings were normal but recurrence was detected by serial imaging methods or clinical follow-up, then the results were defined as false negative (FN). Positive PET/CT results that were proved to be benign or due to a secondary malignancy were classified as false positive (FP). Patients who had both TP and FP findings were classified as TP in the patient based analysis.

Statistical Analysis

The sensitivity, specificity, PPV and negative predictive values (NPV) and accuracy were calculated by standard statistical formulas.

Results

A total of 52 patients with a diagnosis of ovarian cancer were included in the study. The main tumor type was serous carcinoma/adenocarcinoma (n=39, 75%), followed by clear cell carcinoma (n=3, 6%), endometroid carcinoma (n=3, 6%), mucinous carcinoma (n=3, 6%), undifferentiated carcinoma (n=2, 4%), granulosa cell tumor (n=1, 2%) and primitive neuroectodermal tumor (n=1, 2%). CA-125 levels ranged between 35.2-2740 U/mL (mean 341±564 U/mL).

^{18}F-FDG PET/CT detected a hypermetabolic nodular lesion in the lung suggesting metastasis in one patient. Serial contrast-enhanced CT scans did not reveal any nodule following non-specific treatment and CA-125 levels also decreased, therefore, the PET/CT result was accepted as FP.

There were 3 FN results in the study: In one patient there was a hypometabolic cystic lesion on pelvic images but CA-

125 levels decreased after chemotherapy (patient no: 8). In another patient PET/CT imaging did not show any lesions except mildly hypermetabolic (SUV_{max}: 2.7) millimetric lymph nodes with benign appearance in the mediastinum suggesting reactive enlargement, however, serial PET/CT imaging detected progression and CA-125 levels increased progressively (patient no: 17). In the third patient, PET/CT imaging did not reveal any hypermetabolic lesions but serial CT imaging detected local recurrence (patient no: 40). In this patient, recurrence was confirmed by biopsy during follow-up.

Fourteen distant metastasis were detected correctly in 12 patients on ^{18}F-FDG PET/CT imaging (8 of them liver, 2 bone, 2 lung, one pleura, and one brain metastasis). Two patients with positive ^{18}F-FDG PET/CT findings are illustrated in Figures 1, 2.

According to patient-based analysis; the sensitivity, specificity, PPV, NPV and accuracy of ^{18}F-FDG PET/CT in detecting ovarian cancer recurrence in patients with elevated CA-125 levels were calculated as 94%, 75%, 98%, 50% and 96%, respectively.

Detailed results of PET/CT imaging and final diagnosis of all patients are shown in Table 1.

The patients were divided into two different groups as those with CA-125 elevation less than 100 U/mL (n=22) and those with ≥100 U/mL (n=30). The sensitivity and specificity rates of PET/CT imaging according to CA-125 levels are shown in Table 2. Because there is no TN result in patients with CA-125 levels ≥100, specificity could not be calculated in this group.

Discussion

Early detection of tumor recurrence is important in ovarian cancer patients due to its close relation with prognosis and the choice of appropriate treatment. Even after effective treatment and complete response, the recurrence rate is 50-80% in these patients (2,3,4,8).

In addition to clinical examination and imaging modalities, CA-125 measurements are also used for monitoring disease progression in patients with ovarian cancer. Nevertheless, several benign diseases such as infections may cause elevation in CA-125, and it is not reliable in detecting disease recurrence due to its high FN results (6,9). In this study, the patient with a TN finding had an infection at the operation site and the high CA-125 level was attributed to this infection.

Although, CT and magnetic resonance imaging (MRI) are the most commonly used imaging methods to detect recurrent ovarian cancer; their contribution is limited in small-volume recurrent lesions or metastatic deposits on visceral surfaces. CT has low sensitivity (25-50%) for detection of peritoneal metastases smaller than 1 cm (7,10).

^{18}F-FDG PET/CT has been shown to be superior to CT and MRI in detection of recurrent ovarian cancer. It might specify recurrent ovarian cancer approximately 6 months prior to CT (11). In a meta-analysis, the authors evaluated diagnostic performance of CA-125, PET, PET/CT and MRI in 34 recurrent ovarian cancers, and they reported that CA-125 had the highest specificity (93%) while PET/CT had the highest sensitivity (91%). They also showed that diffusion weight MRI is showing promise in detecting small volume peritoneal disease and may be used complementary to

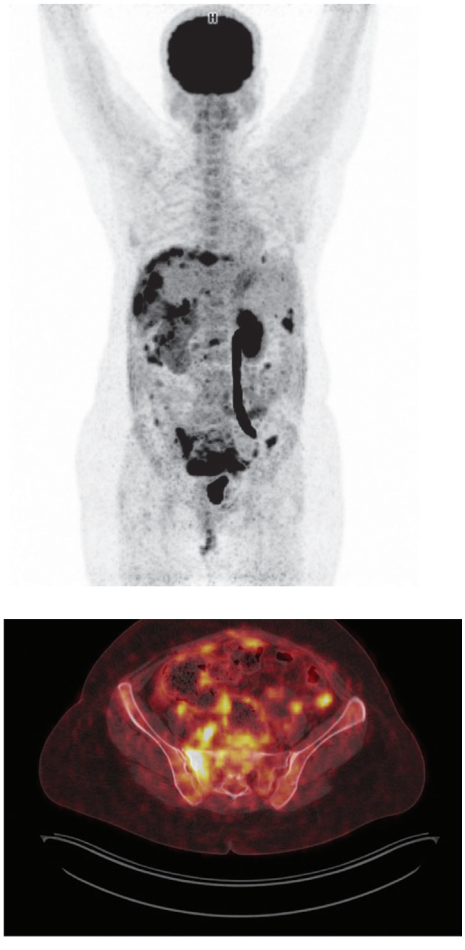

Figure 1. Maximum intensity projection (A) and axial fused positron emission tomography/computed tomography (B) images of a 47-year-old patient with stage 1B serous ovarian carcinoma (patient no: 24) show widespread peritoneal involvement and mesenteric implants (SUV_{max}: 15.5), lymph nodes (SUV_{max}: 7.4), hypermetabolic lytic lesions in the sacrum and L3 vertebra (SUV_{max}: 16.5) suggestive of metastasis. The patient received chemotherapy, her serial positron emission tomography/computed tomography images showed regression and CA-125 levels decreased progressively

PET. The pooled sensitivity and specificity did not show any statistical significance between PET alone and PET/CT in this study (12).

The reported sensitivity and specificity of ^{18}F-FDG PET/CT imaging ranged from 80-100% and 42%-100%, respectively, in detecting recurrent disease (4,7,13,14). Fagotti et al. (15) reported the sensitivity, specificity, NPV, PPV, and accuracy of ^{18}F-FDG PET/CT in recurrent ovarian cancer as 93.0%, 55.6%, 83.3%, 76.9% and 78.6%, respectively. In the same study, authors reported the sensitivity, specificity, PPV, NPV and accuracy rates for laparoscopy as 95%, 64%, 80.8%, 88.9% and 83.1%, respectively (15). In another study, Sari et al. (16) investigated the role of ^{18}F-FDG PET/CT in recurrent ovarian cancer with high tumor markers or suspicious lesions on CT and they reported the sensitivity, specificity and accuracy of PET/CT as 96.1%, 100% and 97%, respectively.

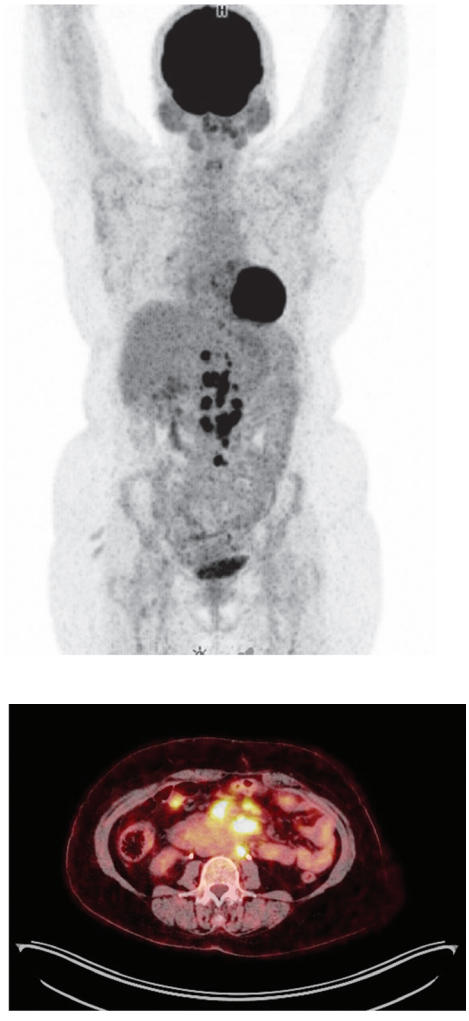

Figure 2. Maximum intensity projection (A) and axial fused positron emission tomography/computed tomography (B) images of a 49 year-old patient with serous carcinoma (patient no: 26) show increased ^{18}F-FDG uptake in para-aortic and celiac lymph nodes (SUV_{max}: 18.3) and mesenteric implants (4.2). Peritoneal biopsy confirmed malignancy in this patient

In this study, sensitivity, specificity, PPV, NPV and accuracy of ^{18}F-FDG PET/CT in detecting ovarian cancer recurrence in patients with elevated CA-125 levels were 94%, 75%, 98%, 50% and 96%, respectively, which were concordant with the literature. Compared to previous studies, NPV is relatively low in our study. Cystic or necrotic lesions and low grade tumor may result in FN ^{18}F-FDG PET/CT imaging findings (4). A hypometabolic cystic lesion on pelvic images was one of the FN results. ^{18}F-FDG PET has a lower sensitivity in detection of primary or recurrent mucinous carcinoma, but all FN results were from patients with a diagnosis of serous carcinoma in this study. These results may be attributed to low grade tumor or early disease progression and small lesion size at the time of PET/CT imaging. In accordance with our results, Risum et al. (17) found high sensitivity (97%) for ^{18}F-FDG PET/CT in patients with high CA-125 levels although they reported relatively low NPV rate (43%) due to micro or cystic/mucinous lesions.

Recurrences were primarily detected in peritoneal cavity and retroperitoneal lymph nodes in 75% of patients with ovarian cancer (18). In our study, we concordantly detected peritoneal and retroperitoneal metastases in majority of patients (41/52, 79%). PET/CT may not be able to demonstrate diffuse peritoneal involvement or small volume disease and small or necrotic lymph nodes (19,20). Rubini et al. (21) investigated the role of ^{18}F-FDG PET/CT in diagnosis of peritoneal carcinomatosis in patients with ovarian cancer and they reported the sensitivity, specificity, accuracy, PPV and NPV of ^{18}F-FDG PET/CT as 85%, 92.31%, 88.61%, 91.89% and 85.71%, respectively. In a meta-analysis which included eighteen studies, authors compared the diagnostic performances of CT, MRI and PET/CT for detection of metastatic lymph nodes in patients with ovarian cancer and they concluded that ^{18}F-FDG PET/CT is more accurate (sensitivity, 73.2%; specificity, 96.7%) than CT and MRI (sensitivity, 42.6% and 54.7%; specificity, 95.0% and 88.3%) (22).

One of the main advantages of PET/CT is the information about the extent and location of recurrence. Early diagnosis of recurrence and exact localization of metastatic disease are crucial for determination of the best treatment strategy. In a study, the authors reported that PET/CT findings changed clinical management in 58% of patients (23). We detected fourteen distant metastasis correctly in 12 patients with ^{18}F-FDG PET/CT in addition to abdominal and pelvic peritoneal metastasis in our study.

Table 1. Positron emission tomography/computed tomography imaging findings and final diagnosis of all patients

No	Primary tumor	CA-125 U/mL	LN's above diaphragm SUV_{max}	LN's below diaphragm SUV_{max}	Peritoneum SUV_{max}	Local recurrence SUV_{max}	Distant metastasis SUV_{max}	Final result
1	Serous carcinoma	37.5	-	11.9	-	-	-	TP
2	Serous carcinoma	1501	-	8.8	9	-		TP
3	Mucinous carcinoma	186	-	-	2.7	-	-	TP
4	Clear cell carcinoma	87.4	22.4	29.7	24.5	-	Liver 23.1	TP
5	Serous carcinoma	306	-	-	7.3	-	-	TP
6	Serous carcinoma	388.9	-	11	7.2	-	-	TP
7	Serous carcinoma	46.9	-	9.7	-	9.7	-	TP
8	Serous carcinoma	228	-	-	-	-	-	FN
9	Serous carcinoma	2740	8.1	19.4	7.2	6.7	Liver 18.0	TP
10	Serous carcinoma	799	-	22.1	13.3	-	-	TP
11	Serous carcinoma	129	-	-	-	-	Lung 4.0	FP
12	Serous carcinoma	546	-	3.2	-	-	-	TP
13	Clear cell carcinoma	155	-	7.5	12.6	-	-	TP
14	Serous carcinoma	85.6	-	2.6	11.9	-	-	TP
15	Serous carcinoma	1000	-	-	10.5	-	-	TP
16	Serous carcinoma	307	-	-	9.9	-	-	TP
17	Serous carcinoma	97.3	-	-	-	-	-	FN
18	Serous carcinoma	287	4.3	12.3	-	12.3	-	TP
19	Serous carcinoma	402	9.3	3.3	-	-	Pleura 14.8	TP
20	Mucinous carcinoma	77	-	-	-	-	-	TN
21	Serous carcinoma	57.7	7.3	19.4	-	-	-	TP
22	Serous carcinoma	265	-	3.8	10.3	-	-	TP
23	Serous carcinoma	35.8	7.7	6.6	-	-	Brain 14.2	TP
24	Serous carcinoma	135	4.0	7.4	15.5	-	Bone 16.5	TP
25	Serous carcinoma	239	9.9	13.9	9.9	-	Liver 11.7	TP
26	Serous carcinoma	566	-	18.3	4.2	-	-	TP
27	Serous carcinoma	123	7.7	8.5	11.1	-	-	TP
28	Endometrioid carcinoma	255	-	11.7	-	-	-	TP
29	Endometrioid carcinoma	990	-	11.6	-	22.3	-	TP
30	Serous carcinoma	44.7	-	11.4		-	-	TP
31	Serous carcinoma	921	-	-	10.5	-	-	TP
32	Serous carcinoma	100	-	-	13.9	-	-	TP
33	Serous carcinoma	77	-	-	4.1	-	-	TP
34	Endometrioid carcinoma	76	-	-	-	-	-	TN
35	Serous carcinoma	229	-	-	12.9	-	-	TP
36	Serous carcinoma	35.2	-	-	4.3	-	-	TP
37	Serous carcinoma	46	-	3.9	-	-	Lung 6.6	TP
38	Serous carcinoma	86	-	2.7	-	-	-	TP
39	Serous carcinoma	2678	-	-	-	-	Liver 8.3	TP
40	Serous carcinoma	36.2	-	-	-	-	-	FN

41	Mucinous carcinoma	64	-	-	10.5	-	-	TP
42	PNET	53.7	-	8.4	-	-	-	TP
43	Clear cell carcinoma	83	-	4.4	-	-	-	TP
44	Serous adenocarcinoma	144	8.5	17.1	-	-	Lung 4.2 Liver 9.6	TP
45	Undifferentiated carcinoma	45	-	-	4.1	-	Liver, 15.8	TP
46	Serous adenocarcinoma	1086	-	-	-	22.2	-	TP
47	Undifferentiated carcinoma	41	-	-	-	-	Bone 18 Liver 14.1	TP
48	Serous adenocarcinoma	282	-	-	3.8	8.9	-	TP
49	Serous carcinoma	91.9	-	-	4.8	-	-	TP
50	Granulosa cell tumor	76.9	-	-	-	-	-	TN
51	Serous carcinoma	162	-	-	-	11.3	-	TP
52	Serous adenocarcinoma	247	-	-	12.9	-	Liver 7.5	TP

TP: True positive, FP: False positive, TN: True negative, FN: False negative, PNET: Primitive neuroectodermal tumor, SUV: Standardited uptake values

Table 2. Detailed results of ^{18}F-FDG positron emission tomography/computed tomography according to CA-125 levels

CA-125 levels (U/mL)	TP (n)	FP (n)	TN (n)	FN (n)	Sensitivity %	Specificity %
<100	17	0	3	2	89	100
≥100	28	1	0	1	97	-

TP: True positive, FP: False positive, TN: True negative, FN: False negative

Study Limitations

The main limitation of our study is its retrospective design. Patients were included from two different institutions and imaging techniques could not be standardized. Besides, pathological confirmation of ^{18}F-FDG positive lesions could not be performed in all patients.

Conclusion

In conclusion, ^{18}F-FDG PET/CT is a useful imaging method that can be used in detection of ovarian cancer recurrence in patients with elevated CA-125 levels. Since this modality offers whole body imaging, distant metastases could be detected in addition to abdominal and pelvic lesions thus contributing to patient management.

Ethics

Ethics Committee Approval: The study were approved by the Adnan Menderes University of Local Ethics Committee (protocol number: 2018/1487).

Informed Consent: Consent form was filled out by all participants.

Peer-review: Externally and internally peer-reviewed.

Authorship Contributions

Surgical and Medical Practices: A.C., Z.P.K., P.Ö.K., Y.Y., Concept: A.C., Design: A.C., Data Collection or Processing: A.C., Z.P.K., P.Ö.K., Y.Y., Analysis or Interpretation: A.C., Z.P.K., P.Ö.K., Literature Search: A.C., Writing: A.C., Y.Y.

Conflict of Interest: No conflict of interest was declared by the authors.

Financial Disclosure: The authors declared that this study received no financial support.

References

1. Cannistra SA. Cancer of the ovary. N Engl J Med 2004;351:2519-2529.
2. Berek JS, Tropé C, Vergote I. Surgery during chemotherapy and at relapse of ovarian cancer. Ann Oncol 1999;10(Suppl 1):3-7.
3. Pignata S, Cecere SC, Du Bois A, Harter P, Heitz F. Treatment of recurrent ovarian cancer. Ann Oncol 2017;28(Suppl 8):vii51-vii56.
4. Son H, Khan SM, Rahaman J, Cameron KL, Prasad-Hayes M, Chuang L, Machac J, Heiba S, Kostakoglu L. Role of FDG PET/CT in staging of recurrent ovarian cancer. Radiographics. 2011;31:569-583.
5. Niloff JM, Knapp RC, Lavin PT, Malkasian GD, Berek JS, Mortel R, Whitney C, Zurawski VR Jr, Bast RC Jr. The CA 125 assay as a predictor of clinical recurrence in epithelial ovarian cancer. Am J Obstet Gynecol. 1986;155:56-60.
6. Kruse V, Cocquyt V, Borms M, Maes A, Van de Wiele C. Serum tumor markers and PET/CT imaging for tumor recurrence detection. Ann Nucl Med 2013;27:97-104.
7. Pannu HK, Bristow RE, Cohade C, Fishman EK, Wahl RL. PET-CT in recurrent ovarian cancer: initial observations. Radiographics 2004;241:209-223.
8. von Georgi R, Schubert K, Grant P, Münstedt K. Post-therapy surveillance and after-care in ovarian cancer. Eur J Obstet Gynecol Reprod Biol 2004;1142:228-233.

9. Meyer T, Rustin GJ. Role of tumor markers in monitoring epithelial ovarian cancer. Br J Cancer 2000;83:1535-1538.
10. Kim HJ, Kim JK, Cho KS. CT features of serous surface papillary carcinoma of the ovary. ARJ Am J Roentgenol 2004;183:1721-1724.
11. Fulham MJ, Carter J, Baldey A, Hicks RJ, Ramshaw JE, Gibson M. The impact of PET-CT in suspected recurrent ovarian cancer: A prospective multi-centre study as part of the Australian PET Data Collection Project. Gynecol Oncol 2009;112:462-468.
12. Gu P, Pan LL, Wu SQ, Sun L, Huang G. CA 125, PET alone, PET-CT, CT and MRI in diagnosing recurrent ovarian carcinoma: a systematic review and meta-analysis. Eur J Radiol 2009;71:164-174.
13. Kim CK, Park BK, Choi JY, Kim BG, Han H. Detection of recurrent ovarian cancer at MRI: comparison with integrated PET/CT. J Comput Assist Tomogr 2007;316:868-875.
14. Cho SM, Ha HK, Byun JY, Lee JM, Kim CJ, Nam-Koong SE, Lee JM. Usefulness of FDG PET for assessment of early recurrent epithelial ovarian cancer. Am J Roentgenol 2002;179:391-395.
15. Fagotti A, Fanfani F, Rossitto C, Lorusso D, De Gaetano AM, Giordano A, Vizzielli G, Scambia G. A treatment selection protocol for recurrent ovarian cancer patients: the role of FDG-PET/CT and staging laparoscopy. Oncology 2008;75:152-158.
16. Sari O, Kaya B, Kara PO, Gedik GK, Celik C, Ozbek O, Serdengecti M. The role of FDG-PET/CT in ovarian cancer patients with high tumor markers or suspicious lesion on contrast-enhanced CT in evaluation of recurrence and/or in determination of intraabdominal metastases. Rev Esp Med Nucl Imagen Mol 2012;31:3-8.
17. Risum S, Høgdall C, Markova E, Berthelsen AK, Loft A, Jensen F, Høgdall E, Roed H, Engelholm SA. Influence of 2-(18F) fluoro-2-deoxy-D-glucose positron emission tomography/computed tomography on recurrent ovarian cancer diagnosis and on selection of patients for secondary cytoreductive surgery. Int J Gynecol Cancer 2009;19:600-604.
18. Gadducci A, Cosio S, Zola P, Landoni F, Maggino T, Sartori E. Surveillance procedures for patients treated for epithelial ovarian cancer: a review of the literature. Int J Gynecol Cancer 2007;171: 21-31.
19. Choi HJ, Roh JW, Seo SS, Lee S, Kim JY, Kim SK, Kang KW, Lee JS, Jeong JY, Park SY. Comparison of the accuracy of magnetic resonance imaging and positron emission tomography/ computed tomography in the presurgical detection of lymph node metastases in patients with uterine cervical carcinoma: a prospective study. Cancer 2006;106:914-922.
20. Sironi S, Messa C, Mangili G, Zangheri B, Aletti G, Garavaglia E, Vigano R, Picchio M, Taccagni G, Maschio AD, Fazio F. Integrated FDG PET/CT in patients with persistent ovarian cancer: correlation with histologic findings. Radiology 2004;233:433-440.
21. Rubini G, Altini C, Notaristefano A, Merenda N, Rubini D, Ianora AA, Asabella AN. Role of 18F-FDG PET/CT in diagnosing peritoneal carcinomatosis in the restaging of patient with ovarian cancer as compared to contrast enhanced CT and tumor marker Ca-125. Rev Esp Med Nucl Imagen Mol 2014;331:22-27.
22. Yuan Y, Gu ZX, Tao XF, Liu SY. Computer tomography, magnetic resonance imaging, and positron emission tomography or positron emission tomography/computer tomography for detection of metastatic lymph nodes in patients with ovarian cancer: a meta-analysis. Eur J Radiol 2012;815:1002-1006.
23. Simcock B, Neesham D, Quinn M, Drummond E, Milner A, Hicks RJ. The impact of PET/CT in the management of recurrent ovarian cancer. Gynecol Oncol 2006;103:271-276.

Original Article
Mol Imaging Radionucl Ther 2019;28:15-20 DOI:10.4274/mirt.galenos.2018.60490

The Correlation of Clinicopathological Findings and Neutrophil-to-Lymphocyte and Platelet-to-Lymphocyte Ratios in Papillary Thyroid Carcinoma

Papiller Tiroid Kanserli Hastalarda Nötrofil/Lenfosit ve Trombosit/Lenfosit Oranlarının Kliniko-Patolojik Bulgularla İlişkisi

Yeşim Ceylan[1], Kamil Kumanlıoğlu[2], Aylin Oral[2], Yeşim Ertan[3], Zehra Özcan[2]

[1]*Adıyaman Faculty of Medicine Training and Research Hospital, Department of Nuclear Medicine, Adıyaman, Turkey*
[2]*Ege University Faculty of Medicine, Department of Nuclear Medicine, İzmir, Turkey*
[3]*Ege University Faculty of Medicine, Department of Pathology, İzmir, Turkey*

Abstract

Objectives: Inflammatory markers such as neutrophil-to-lymphocyte ratio (NLR) and platelet-to-lymphocyte ratio (PLR) have been recently introduced as potential biomarkers for tumor pathogenesis, development and prognosis in solid tumors. Our aim was to assess the correlation of clinicopathological features and NLR and PLR in patients with papillary thyroid carcinoma (PTC).

Methods: A total of 201 papillary thyroid carcinoma patients were divided into groups with a cut-off preoperative median NLR and PLR value of 1,92 and 123.9, respectively. The correlation of NLR and PLR and clinicopathological features including age, tumor size, extra-thyroidal extension, thyroid capsule invasion, surgical margin positivity, multifocality, bilaterality of the patients were analyzed.

Results: The mean NLR and PLR were 2.11±0.94, 129.69±42.81, respectively. Larger tumor size and higher positivity of extra-thyroidal spread were correlated with higher NLR values. No significant relationship was found between NLR and age, presence of thyroid capsule invasion, surgical margin positivity, multifocality, bilaterality, and lymph node metastasis. Also no significant association was observed between the clinicopathological features and PLR.

Conclusion: High NLR was found to correlate with tumor size and extra-thyroidal extension. NLR may be used as a marker to determine the clinical behavior of disease in patients with papillary thyroid carcinoma (PTC).

Keywords: Neutrophil-to-lymphocyte ratio, platelet-to-lymphocyte ratio, papillary thyroid carcinoma

Öz

Amaç: Son yıllarda nötrofil/lenfosit oranı (NLO) ve trombosit/lenfosit oranı (TLO) gibi enflamatuvar belirteçlerin solid tümör patogenezinde, gelişmesinde ve prognozunda etkili olduğuna dair çalışmalar mevcuttur. Bu çalışmada tiroid papiller kanserinin (PTK) kliniko-patolojik özellikleri ile NLO ve TLO arasındaki ilişkinin retrospektif olarak incelenmesi amaçlanmıştır.

Yöntem: Çalışmaya dahil edilen 201 hasta preoperatif medyan NLO (grup 1 <1,92 ve grup 2 ≥1,92) ve medyan TLO (grup 1 <123,9 ve grup 2 ≥123,9) değerlerine göre gruplara ayrıldı. NLO ve TLO ile hastaların yaş, tümör boyutu, ekstra-tiroidal yayılım, tiroid kapsül invazyonu, cerrahi sınır pozitifliği, multifokalite, bilateralite gibi kliniko-patolojik özellikleri arasındaki ilişki değerlendirildi.

Bulgular: Ortalama NLR ve PLR sırasıyla 2,11±0,94, 129,69±42,81 idi. Verilerin istatiksel analizi preoperatif yüksek NLO ile tümör boyutu (p=0,002) ve ekstra-tiroidal yayılım (p=0,028) arasında anlamlı ilişki bulunduğunu gösterdi. Yaş, tiroid kapsül invazyonu, cerrahi sınır pozitifliği,

Address for Correspondence: Yeşim Ceylan MD, Adıyaman Faculty of Medicine Training and Research Hospital, Department of Nuclear Medicine, Adıyaman, Turkey Phone: +90 507 707 18 89 E-mail: dryesimceylan@gmail.com ORCID ID: orcid.org/0000-0002-9677-5307
Received: 08.08.2018 **Accepted:** 19.12.2018

multifokalite, bilateralite ile NLO arasında ise ilişki saptanmadı (p>0,05). TLO ile kliniko-patolojik özellikler arasında anlamlı istatistiksel ilişki gösterilemedi (p>0,05).

Sonuç: Çalışmamız PTK de NLO ile tümör boyutu ve ekstra-tiroidal yayılım arasında istatistiksel olarak anlamlı ilişki bulunduğunu göstermektedir. NLO'nun diğer bazı solid tümörlerde olduğu gibi PTK olgularında hastalığın klinik davranışını belirlemek için yararlı bir belirteç olarak kullanılabileceği düşünülmektedir.

Anahtar kelimeler: Nötrofil/lenfosit oranı, trombosit/lenfosit oranı, papiller tiroid kanseri

Introduction

It has been demonstrated that inflammation might play an important role in cancer development and progression (1). The interaction between cancer and inflammation is assumed to be complicated and based on different physiological processes such as miscellaneous inflammatory cells, mediators and signaling pathways in cancer tissue (2). It has been indicated that cancer-related inflammatory response leads to proliferation and survival of tumor cells, angiogenesis and finally to cancer progression by affecting tumor microenvironment in numerous tumors (3). The increase of pro-inflammatory cytokine is regarded to be indicative of disease prognosis and patient response to the tumor. Thus, systemic inflammatory markers including C-reactive protein (CRP), albumin concentration, neutrophil-to-lymphocyte ratio (NLR), platelet-to-lymphocyte ratio (PLR) may have potential roles as prognostic biomarkers (4).

NLR, which is simply measured by a routine peripheral blood test, has been widely used as an indicator of general immunoreactivity. It has been studied in various tumors and found to be useful as a prognostic indicator, estimating overall and recurrence free survival in some solid tumors such as esophagus, stomach, pancreas, colon, ovary, kidney, lung and prostate cancers (5,6,7). However, studies examining the role of NLR in thyroid cancer with an increasing frequency worldwide are limited. In the current study, we aimed to evaluate the correlation of clinicopathological features and inflammatory indicators in papillary thyroid cancer.

Materials and Methods

Patients

The study group included papillary thyroid carcinoma patients referred to Department of Nuclear Medicine between January 2015 and December 2016. Those patients with confirmed diagnosis of thyroid papillary carcinoma greater than 1 cm on a detailed histopathological examination and total blood count analysis just prior to thyroid surgery (within a 2 days interval) were selected. Patients with co-existing hematologic diseases, additional tumors, acute myocardial infarction or coronary revascularization in the last 6 months, acute infectious diseases, chronic drug (steroids etc.) use that could affect blood analysis, presence of lymphocytic infiltration suggesting thyroiditis on histopathology and abnormal white blood cells (WBC) measurements were excluded from the study. The medical records of all patients were examined and those without symptoms of acute infections and normal blood cells were included. The final study population included a total of 201 patients. Demographic characteristics of the patients (age, gender), clinical records including histopathologic findings, and pre-operative complete blood count results were obtained. All surgical specimens were examined in detail for certain pathologic features including tumor size, presence of thyroid capsule invasion, extra-thyroidal extension, surgical margin positivity, bilateral involvement, presence of multifocal tumor and lymph node metastasis. We used complementary data achieved by ultrasound and post ablation whole body iodine scan to assess lymph node involvement as neck dissection was not routinely performed to all patients. Complete blood count analyzes; hemoglobin level, WBC, neutrophil and lymphocyte counts were obtained by using a Dyn Ruby Cell (ABBOTT, USA) hematology analyzer. The NLR was calculated by dividing the absolute neutrophil count by the absolute lymphocyte count; similarly, the PLR was calculated by dividing the absolute platelet count by the absolute lymphocyte count. We formed 2 cohort groups according to the values above and below the median value of NLR and PLR. These groups were compared in terms of the aforementioned clinicopathologic characteristics.

The study was approved by the Ege University of Local Ethics Committee (protocol number: 17-12.1/33).

Statistical Analysis

Statistical Package for Social Sciences version 15.0 (SPSS Inc., Chicago, IL, USA) was used for statistical analysis. Kolmogorov-Smirnov test was used to determine if sample data is normally distributed. The Mann-Whitney U test was then used to compare the continuous variables which did not show normal distribution. The correlation between the nominal variables was compared with the chi-square test. P

value less than 0.05 was considered statistically significant.

Results

An overview of patient characteristics is shown in Table 1. The mean age of the study population was 47.1±14.3 years, and the female/male ratio was 155/46. Two of the patients had distant metastatic involvement (lung) and 57 had cervical lymph node metastases.

The mean NLR and PLR were 2.11±0.94 and 129.69±42.81, respectively. The patients were divided into two groups according to the median NLR as those below (group 1) and above (group 2) 1.92. When clinic-pathologic features were compared by using chi-square and Mann-Whitney U tests, larger tumor size (group 1: 2.24±1.14 cm; group 2: 2.79±1.49 cm, p=0.002), and higher positivity of extra-thyroidal spread (group 1: 3 patients, group 2: 11 patients, p=0.028) were found to be statistically related with the higher values of NLR in group 2. Statistical analyses did not reveal a significant correlation between NLR and age (<45 years, ≥45 years), presence of thyroid capsule invasion, surgical border positivity, multifocality, bilaterality, lymph node metastasis (Table 2). When the cohort was also divided into two groups according to median PLR (PLR <123,9 and PLR ≥123,9), no statistically significant correlation was detected with clinic-pathologic features (Table 3).

Discussion

It has been widely recognized that inflammation and cancer are closely related to each other as inflammation has both cancer-inhibiting and neoplasia modelling properties (8,9,10). The inflammatory effect on tumor pathogenesis, which was first described by Rudolf Virchow, has been recognized as an important concept also for the development and proliferation of the tumor by reducing response to anticancer agents (11,12). In recent studies, there is growing evidence on the effect of inflammation on cancer pathogenesis, progression and response to treatment (2,12). Inflammation, cytokines and chemokines induce tumor proliferation, angiogenesis and metastasis by CRP and neutrophil induction. In addition, it is considered to play an important role in the development and proliferation of the tumor by reducing the response to anticancer agents (2). The physiologic response of leukocytes to stress results in an increase in the number of neutrophils and a decrease in the number of lymphocytes (13). The inflammatory cytokines, leukocytes and phagocytic mediators that cause neutrophil release, lead to DNA damage. It inhibits

Table 1. Demographic characteristics and hematological data of papillary thyroid carcinoma patients

	Mean ± SD	Minimum - Maximum
Age (years)	47.10±14.32	19-83
Sex		
Female (n, %)	155 (77.1%)	
Male (n, %)	46 (22.9%)	
Neutrophils	4.40±1.32	1.95-8.88
Lymphocytes	2.23±0.65	0.87-4.68
Platelets	271.28±64.35	138.00-466.00
NLR	2.11±0.94	0.78-8.28
PLR	129.69±42.81	56.11-311.49

SD: Standard deviation, NLR: Neutrophil-to-lymphocyte ratio, PLR: Platelet-to-lymphocyte

Table 2. Association of preoperative neutrophil-to-lymphocyte ratio with clinicopathological characteristics of papillary thyroid carcinoma

	Total	NLR <1.92	NLR ≥1.92	p
Total	201 (100%)	100 (49.8%)	101 (50.2%)	
Age				
<45 years	81 (40.3%)	40 (49.4%)	41 (50.6%)	0.932
≥45 years	120 (59.7%)	60 (50.0%)	60 (50.0%)	
Sex				
Female	155 (77.1%)	76 (49.0%)	79 (51.0%)	0.708
Male	46 (22.9%)	24 (52.2%)	22 (47.8%)	
Tumor size (cm)	2.51±1.35	2.24±1.13	2.79±1.48	**0.002***
Capsule invasion				
Yes	75 (37.3%)	37 (49.3%)	38 (50.7%)	0.927
No	126 (62.7%)	63 (50.0%)	63 (50.0%)	
Multifocality				
Yes	80 (39.8%)	41 (51.3%)	39 (48.8%)	0.730
No	121 (60.2%)	59 (48.8%)	62 (51.2%)	
Bilaterality				
Yes	60 (100%)	32 (53.3%)	28 (46.7%)	0.508
No	141 (100%)	68 (48.2%)	73 (51.8%)	
Surgical margin positivity				
Yes	19 (9.5%)	10 (52.6%)	9 (47.4%)	0.792
No	182 (90%)	90 (49.5%)	92 (50.5%)	
Extra-thyroidal spread				
Yes	14 (7.0%)	3 (21.4%)	11 (78.6%)	**0.028***
No	187 (93.0%)	97 (51.9%)	90 (48.1%)	
Lymph node metastasis				
Yes	57 (28.4%)	26 (45.6%)	31 (54.4%)	0.460
No	144 (71.6%)	74 (51.4%)	70 (48.6%)	

NLR: Neutrophil-to-lymphocyte ratio, *p<0.05

apoptosis and induces tumor angiogenesis resulting in tumor growth, progression, and metastasis. On the other hand, lymphocytes also play a major role in the prevention of tumor growth and immunity (10).

Recently some studies pointed out that elevated blood NLR that can be easily calculated from blood tests might be used to predict some aggressive features in a variety of cancers (5,6,7). In the current study, we aimed to examine the value of NLR and PLR in papillary thyroid cancers in which the current relevant literature is quite limited (14,15,16).

In the current study patients with papillary thyroid carcinoma, we have noted a statistically significant association between high preoperative NLR value and size and extra-thyroidal extension of the tumor. This observation was in agreement with the study of Manatakis et al. (8) indicating that the high levels of NLR was associated with extra-thyroidal invasion. Also, Liu et al. (16) showed the correlation of high preoperative NLR values with increased tumor size and recurrence risk in differentiated thyroid cancers. Several additional studies have also supported the correlation of tumor size and increasing NLR (14,15,16). However, in our study, pathologic findings other than tumor size and extra-thyroidal extension did not appear to be inter-related. Moreover, no correlation was found between PLR and clinic-pathologic features of thyroid tumors. This inconsistent observation might be related to several factors related to the study population and methodology. Moreover, as inflammation is a slow process and most of the study patients herein represent early stage of the disease, no significant correlation between inflammation

Table 3. Association of preoperative platelet-to-lymphocyte with clinicopathological characteristics of papillary thyroid carcinoma

	Total	PLR <123.9	PLR ≥123.9	p
Total	201 (100%)	100 (49.8%)	101 (50.2%)	
Age				
<45 years	81 (40.3%)	44 (54.3%)	37 (45.7%)	0.287
≥45 years	120 (59.7%)	56 (46.7%)	64 (53.3%)	
Sex				
Female	155 (77.1%)	72 (46.5%)	83 (53.5%)	0.086
Male	46 (22.9%)	28 (60.9%)	18 (39.1%)	
Tumor size (cm)	2.51±1.35	2.46±1.36	2.56±1.33	0.309
Capsule invasion				
Yes	75 (37.3%)	34 (45.3%)	41 (54.7%)	0.334
No	126 (62.7%)	66 (52.4%)	60 (47.6%)	
Multifocality				
Yes	80 (39.8%)	44 (55.0%)	36 (45.0%)	0.226
No	121 (60.2%)	56 (46.3%)	65 (53.7%)	
Bilaterality				
Yes	60 (100%)	35 (58.3%)	25 (41.7%)	0.112
No	141 (100%)	65 (46.1%)	76 (53.9%)	
Surgical margin positivity				
Yes	19 (9.5%)	9 (47.4%)	10 (52.6%)	0.827
No	182 (90%)	91 (50.0%)	91 (50.0%)	
Extra-thyroidal spread				
Yes	14 (7.0%)	8 (57.1%)	6 (42.9%)	0.566
No	187 (93.0%)	92 (49.2%)	95 (50.8%)	
Lymph node metastasis				
Yes	57 (28.4%)	32 (56.1%)	25 (43.9%)	0.254
No	144 (71.6%)	68 (47.2%)	76 (52.8%)	

PLR: Platelet-to-lymphocyte

and NLR was noted. In the study of Manatakis et al. (8), the study group (205 patients) included those cases with tumors smaller than 1 cm and those with co-existing thyroiditis. Actually this is divergent from our cases as we have excluded smaller tumors and those with thyroiditis. In the study of Gong et al. (14), the median NLR used as a cut-off value was 2.0 that is similar to our study. They have found a positive correlation between high NLR and lymph node metastasis, multifocality and tumor size. However it should be noted that these NLR values obtained in the studies focusing on thyroid carcinoma are lower than those in previous studies focusing on solid tumors. As an example, Templeton et al. (17) found the median NLR value as 4 in a meta-analysis with solid tumors. Moreover, it should also be considered that there has been no clear validation of the cut-off values used in the literature (14). Regarding the correlation between disease extension and NLR, Manatakis et al. (8) and Gong et al. (14) found an association between the presence of lymph node metastases, which is not supported in our series. As stated above, this might be linked to the differences in the study population and the number of patients with lymph node involvement in their series which is obviously smaller than ours. On contrary to this, Kim et al. (15) have indicated lack of evidence for the association between NLR and the clinicopathological findings of the tumor based on 1066 female patients. However, they have found a significant correlation between high pre-operative PLR and lymph node metastasis. In the current study, while a significant correlation between NLR and tumor size and extra-thyroidal extension was noted, an association with PLR was not detected. In most of the previous studies, both NLR and PLR were found to be valuable in several solid tumors (18,19,20,21). Costantini et al. (22) suggested that production of bone marrow-stimulating cytokines as a result of inflammatory response to malignancy may play an important role in the regulation of platelet counts in neoplasms (23). Platelets can give rise to angiogenesis and extra-vasation of tumor cells by releasing vascular endothelial growth factor (VEGF) (24). VEGF and various growth factors have been suggested to induce angiogenesis and vascularization resulting in the increase of tumor growth rates (25). Some proinflammatory cytokines, such as IL-1 and IL-6, also cause megakaryocyte proliferation resulting in thrombocytosis (24,25).

Several clinical studies showed that high PLR correlates with worse clinicopathological features in patients with HCC (26,27). Deng et al. (28) performed a literature search in PubMed, Web of Science and Embase. This meta-analysis included 13 studies involving 4.621 patients. The result indicated that the elevated PLR level was associated with lymph node metastasis, higher tumor stage, deeper tumor invasion and longer tumor length, indicating that the level of PLR is important for predicting clinicopathological features. Most of the studies have been performed in esophagus, ovary, breast, prostate, stomach, colorectal and hepatocellular carcinomas with limited studies focusing on thyroid cancer (29,30). Previously Kim et al. (15) documented elevated PLR in association with increased risk of lateral lymph node involvement. However, when combining NLR and PLR, they were not able to support the correlation of these markers with prognostic factors in papillary thyroid carcinoma. A high preoperative PLR is associated with poor prognosis in operable colorectal and pancreatic cancers (19), and a high preoperative NLR is poor prognostic marker in some cancers, including gastric, pancreatic, colorectal, cholangiocarcinoma, lung and ovarian cancers (6). But only a few studies have evaluated the significance of the NLR and also PLR in thyroid cancer. Measurement of the PLR and NLR were cost-effective, safe, and readily available so we evaluated the association between preoperative NLR and PLR and the clinicopathological characteristics of patients with PTC. Unfortunately; it should be considered that this study has some limitations related to the limited number of patients and retrospective study design. Also, NLR and PLR values are not specific for inflammation process and may be affected by many factors. Moreover, lack of standard cut-off values for NLR and PLR also appear to be important to validate these observations. Another limitation is that patients who had PTC below 1 cm have not been investigated in this study although tumors below 1 cm may have metastasis or extra-thyroidal invasion. Further studies including thyroid papillary microcarcinomas may provide future guidance.

Conclusion

In the current analysis, we identified a statistically significant correlation between NLR and tumor size and extra-thyroidal extension. However, no evidence of correlation with these features and PLR was observed. The current results indicate NLR, which is a quite simple and inexpensive test, as a potential marker to determine clinical behavior in papillary thyroid carcinoma patients.

Ethics

Ethics Committee Approval: The study was approved by the Ege University of Local Ethics Committee (protocol number: 17-12.1/33).

Informed Consent: Retrospective study.

Peer-review: Externally and internally peer-reviewed.

Authorship Contributions

Surgical and Medical Practices: Y.C., Z.Ö., Y.E., A.O.,

Concept: Y.C., Z.Ö., Design: Y.C., Z.Ö., Data Collection or Processing: Y.C., Analysis or Interpretation: Y.C., Z.Ö., K.K., Literature Search: Y.C., Z.Ö., Writing: Y.C., Z.Ö.

Conflict of Interest: No conflict of interest was declared by the authors.

Financial Disclosure: The authors declared that this study received no financial support.

References

1. Whiteside TL. The tumor microenvironment and its role in promoting tumor growth. Oncogene 2008;27:5904-5912.
2. Mantovani A, Allavena P, Sica A, Balkwill F. Cancer related inflammation. Nature 2008;454:436-444.
3. Li X, Ma X, Tang L, Wang B, Chen L, Zhang F, Zhang X. Prognostic value of neutrophil-to-lymphocyte ratio in urothelial carcinoma of the upper urinary tract and bladder: a systematic review and meta-analysis. Oncotarget 2017;8:62681-62692.
4. de Visser KE, Coussens LM. The inflammatory tumor microenvironment and its impact on cancer development. Contrib Microbiol 2006;13:118-137.
5. Moore MM, Chua W, Charles KA, Clarke SJ, Inflammation and cancer: causes and consequences. Clin Pharmacol Ther 2010;87;504-508.
6. Liu CL, Lee JJ, Liu TP, Chang YC, Hsu YC, Cheng SP. Blood neutrophil-to-lymphocyte ratio correlates with tumor size in patients with differentiated thyroid cancer. J Surg Oncol 2013;107:493-497.
7. Hsueh C, Tao L, Zhang M, Cao W, Gong H, Zhou J, Zhou L. The prognostic value of preoperative neutrophils, platelets, lymphocytes, monocytes and calculated ratios in patients with laryngeal squamous cell cancer. Oncotarget 2017;8:60514-60527.
8. Manatakis DK, Tseleni-Balafouta S, Balalis D, Soulou VN, Korkolis DP, Sakorafas GH, Plataniotis G, Gontikakis E. Association of Baseline Neutrophil-to-Lymphocyte Ratio with Clinicopathological Characteristics of Papillary Thyroid Carcinoma. Int J Endocrinol 2017;2017:8471235.
9. Tong YS, Tan J, Zhou XL, Song YQ, Song YJ. Systemic immune-inflammation index predicting chemoradiation resistance and poor outcome in patients with stage III non-small cell lung cancer. J Transl Med 2017;15:221.
10. Dunn GP, Old LJ, Schreiber RD. The Immunobiology of Cancer Immunosurveillance and Immunoediting. Immunity 2004;21:137-148.
11. Mantovani A, Allavena P, Sica A, Balkwill F. Cancer-related inflammation. Nature 2008;454:436-444.
12. Colotta F, Allavena P, Sica A, Garlanda C, Mantovani A. Cancer-related inflammation, the seventh hallmark of cancer: links to genetic instability. Carcinogenesis 2009;30:1073-1081.
13. Jilma B, Blann A, Pernerstorfer T, Stohlawetz P, Eichler HG, Vondrovec B, Amiral J, Richter V, Wagner OF. Regulation of adhesion molecules during human endotoxemia. No acute effects of aspirin. Am J Respir Crit Care Med 1999;159:857-863.
14. Gong W, Yang S, Yang X, Guo F. Blood preoperative neutrophil-to-lymphocyte ratio is correlated with TNM stage in patients with papillary thyroid cancer. Clinics (Sao Paulo) 2016;71:311-314.
15. Kim SM, Kim EH, Kim BH, Kim JH, Park SB, Nam YJ, Ahn KH, Oh MY, Kim WJ, Jeon YK, Kim SS, Kim YK, Kim IJ. Association of the Preoperative Neutrophil-to-lymphocyte Count Ratio and Platelet-to-Lymphocyte Count Ratio with Clinicopathological Characteristics in Patients with Papillary Thyroid Cancer. Endocrinol Metab (Seoul) 2015;30:494-501.
16. Liu JF, Ba L, Lv H, Lv D, Du JT, Jing XM, Yang NJ, Wang SX, Li C, Li XX. Association between neutrophil-to-lymphocyte ratio and differentiated thyroid cancer: a meta-analysis. Sci Rep 2016;6:38551.
17. Templeton AJ, Ace O, McNamara MG, Al-Mubarak M, Vera-Badillo FE, Hermanns T, Seruga B, Ocaña A, Tannock IF, Amir E. Prognostic Role of Platelet to Lymphocyte Ratio in Solid Tumors: A Systematic Review and Meta-Analysis. Cancer Epidemiol Biomarkers Prev 2014;23:1204-1212.
18. Roxburgh CS, McMillan DC. Role of systemic inflammatory response in predicting survival in patients with primary operable cancer. Future Oncol 2010;6:149-163.
19. Smith RA, Bosonnet L, Raraty M, Sutton R, Neoptolemos JP, Campbell F, Ghaneh P. Preoperative platelet-lymphocyte ratio is an independent significant prognostic marker in resected pancreatic ductal adenocarcinoma. Am J Surg 2009;197:466-472.
20. Sharma R, Hook J, Kumar M, Gabra H. Evaluation of an inflammation-based prognostic score in patients with advanced ovarian cancer. Eur J Cancer 2008;44:251-256.
21. Feng JF, Huang Y, Chen QX. Preoperative platelet lymphocyte ratio (PLR) is superior to neutrophil lymphocyte ratio (NLR) as a predictive factor in patients with esophageal squamous cell carcinoma. World J Surg Oncol 2014;12:58.
22. Costantini V, Zacharski LR, Moritz TE, Edwards RL. The platelet count in carcinoma of the lung and colon. Thromb Haemost 1990;64:501-505.
23. Gu D, Szallasi A. Thrombocytosis Portends Adverse Prognosis in Colorectal Cancer: A Meta-Analysis of 5,619 Patients in 16 Individual. Anticancer Res 2017;37:4717-4726.
24. Patruno R, Arpaia N, Gadaleta CD, Passantino L, Zizzo N, Misino A, Lucarelli NM, Catino A, Valerio P, Ribatti D, Ranieri G. VEGF concentration from plasma activated platelets rich correlates with microvascular density and grading in canine mast cell tumour spontaneous model. J Cell Mol Med 2008;13:555-561.
25. Peduzzi P, Concato J, Kemper E, Holford TR, Feinstem AR. A simulation study of the number of events per variable in logistic regression analysis. J Clin Epidemiol 1996;49:1373-1379.
26. Goh BK, Kam JH, Lee SY, Chan CY, Allen JC, Jeyaraj P, Cheow PC, Chow PK, Ooi LL, Chung AY. Significance of neutrophil-to-lymphocyte ratio, platelet-to-lymphocyte ratio and prognostic nutrition index as preoperative predictors of early mortality after liver resection for huge (>/=10 cm) hepatocellular carcinoma. J Surg Oncol 2016;113:621-627.
27. Song W, Wang K, Zhong FP, Fan YW, Peng L, Zou SB. Clinicopathological and prognostic significance of platelet-to-lymphocyte ratio in patients with hepatocellular carcinoma. Oncotarget 2016;7:81830-81838.
28. Deng J, Zhang P, Sun Y, Peng P, Huang Y. Prognostic and clinicopathological significance of platelet to lymphocyte ratio in esophageal cancer: a meta-analysis. J Thorac Dis 2018;10:1522-1531.
29. Jiang K, Lei J, Chen W, Gong Y, Luo H, Li Z, Gong R, Zhu J. Association of the preoperative neutrophil-to- lymphocyte and platelet-to-lymphocyte ratios with lymph node metastasis and recurrence in patients with medullary thyroid carcinoma. Medicine (Baltimore) 2016;95:5079.
30. Kim JY, Park T, Jeong SH, Jeong CY, Ju YT, Lee YJ, Hong SC, Ha WS, Choi SK, Jung EJ. Prognostic importance of baseline neutrophil to lymphocyte ratio in patients with advanced papillary thyroid carcinomas. Endocrine 2014;46:526-531.

Original Article
Mol Imaging Radionucl Ther 2019;28:21-26 DOI:10.4274/mirt.galenos.2018.09825

The Role of Pre-ablative Stimulated Thyroglobulin and Thyroglobulin/Thyroid-Stimulating Hormone Ratio for Predicting Metastasis in Thyroid Cancer

Tiroid Kanserinde Pre-ablatif Stimüle Tiroglobulin ve Tiroglobulin/Tiroid Uyarıcı Hormon Oranının Metastaz Tahminindeki Rolü

Fadime Demir[1], Fikri Selçuk Şimşek[2], Tansel Ansal Balcı[2]

[1]*Tokat Gaziosmanpaşa University Faculty of Medicine, Department of Nuclear Medicine, Tokat, Turkey*
[2]*Fırat University Faculty of Medicine, Department of Nuclear Medicine, Elazığ, Turkey*

Abstract

Objectives: In this study, we aimed to investigate the predictive value of pre-ablative stimulated thyroglobulin (Tg) and Tg/thyroid-stimulating hormone (TSH) to identify lymph node metastasis (LNM) or distant metastases (DM) prior to radioactive iodine (RAI) treatment.

Methods: Patients without metastasis were included in group 1 (n=100), those with LNM were included in group 2 (n=83), and those with DM constituted group 3 (n=23). Tg and TSH values were measured approximately 4 hours prior to RAI ablation therapy.

Results: There was a significant difference between group 3 and other groups (group 1 and group 2) in terms of Tg (p<0.001) and Tg/TSH (p<0.001). For Tg level and Tg/TSH ratio, the areas under ROC were 0.990 [95% confidence interval (CI): 0.979-1] and 0.991 (95% CI: 0.981-1), respectively. The cut-off points for Tg and Tg/TSH were 102 ng/mL and 1.06, respectively.

Conclusion: Our results suggest that Tg and Tg/TSH values can be used to predict DM. On the other hand, our study indicates that patients should be carefully evaluated for LNM even when Tg levels are low.

Keywords: Thyroid cancer, thyroglobulin, metastasis

Öz

Amaç: Bu çalışmada, radyoaktif iyot (RAİ) tedavisi öncesi lenf nodu metastazını veya uzak metastazları belirlemek için pre-ablatif stimüle tiroglobulin (Tg) ve Tg/tiroid-uyarıcı hormonun (Tg/TSH) prediktif değerini araştırmayı amaçladık.

Yöntem: Grup 1'e (n=100) metastaz saptanmayan hastalar, grup 2'ye (n=83) lenf nodu metastazı olan hastalar ve grup 3'e (n=23) uzak metastazı olan hastalar dahil edildi. Tg ve TSH değerleri RAİ tedavisinden yaklaşık 4 saat önce ölçüldü.

Bulgular: Grup 3 ile diğer gruplar (grup 1 ve grup 2) arasında Tg (p<0,001) ve Tg/TSH (p<0,001) açısından anlamlı fark vardı. Tg seviyesi ve Tg/TSH oranı için ROC eğrisi altındaki alanlar sırasıyla 0,990 (%95 güven aralığı: 0,979-1) ve 0,991 (%95 güven aralığı: 0,981-1) idi. Tg ve Tg/TSH için kesme noktaları sırasıyla 102 ng/mL ve 1,06 ng/mL idi.

Sonuç: Çalışmamıza göre Tg ve Tg/TSH değerleri uzak metastaz için prediktif bir değer olarak kullanılabilir. Öte yandan, çalışmamız lenf nodu metastazının düşük Tg seviyelerinde bile dikkatli bir şekilde değerlendirilmesi gerektiğini düşündürmektedir.

Anahtar kelimeler: Tiroid kanseri, tiroglobulin, metastaz

Address for Correspondence: Fadime Demir MD, Tokat Gaziosmanpaşa University Faculty of Medicine, Department of Nuclear Medicine, Tokat, Turkey
Phone: +90 530 419 70 80 E-mail: drfadimedemir@hotmail.com ORCID ID: orcid.org/0000-0002-9799-6398
Received: 21.11.2018 **Accepted:** 12.03.2019

Introduction

Thyroid cancer is the most common endocrine malignancy worldwide, with a rapidly inceraseing incidence rate (1). Thyroid carcinomas are classified as differentiated or undifferentiated according to their histologic type. Differentiated thyroid carcinomas (DTC) account >90% of thyroid cancer. The standard treatments for DTC include total thyroidectomy (TT), radioactive iodine (RAI) ablation therapy (patients with a tumor >1 cm in size) and long-term thyroid stimulating hormone (TSH) suppression therapy (2). DTC has a relatively good prognosis with 10-year survival rates of 92-98%. Nevertheless, cervical lymph node metastases (LNM) develop in 53% and distant metastases (DM) in 10% of patients (3,4). The RAI dose to administer can be chosen either empirically (100-200 mCi) or by lesional or whole-body dosimetry if available, in order to limit the whole-body retention to 80 mCi at 48 hours and 200 cGy to the bone marrow (5). The most common method is empiric administration in which the radioiodine dose is based primarily on the extent of the tumor. The potential disadvantage of empiric dosing is that individual patients may be under- or over-dosed (6). Presence of LNM and DM are significant determinants for empirical dose planning. LNM or DM can be detected by using clinical evaluation, as well as surgical, radiological and diagnostic iodine-131 (I-131) whole-body scan (WBS) findings. However, it will be more appropriate if diagnostic tools are performed after a risk assessment or clinical suspicion. Thyroglobulin (Tg) is the specific marker of thyroid tissue. Tg levels significantly decrease after surgical removal of thyroid tissue, while Tg levels remain high in case of residual tissue or DM in thyroid cancer (7). Endogenous TSH can stimulate Tg release from the thyroid bed or metastatic tissue. Endogenous TSH induce Tg release from thyroid bed or metastatic tissue. This means that the Tg release is dependent by TSH (8). The aim of this study was to investigate the potential value of pre-ablative stimulated Tg and Tg/TSH to identify LNM or DM prior to RAI treatment.

Materials and Methods

Patients

Patients treated with RAI for thyroid cancer in Fırat University Hospital between 2012 and 2018 were reviewed in this retrospective analysis. One hundred patients without metastasis were included in group 1, eighty-three patients with lymph node metastasis were included in group 2 and 23 patients with DM were included in group 3. Metastasis was diagnosed by pathologic involvement in whole body RAI scan after treatment, with or without positive findings on other imaging modalities [computed tomography (CT), magnetic resonance (MR), and positron emission tomograph/CT]. Patients with positive anti-Tg antibodies (TgAb) were excluded from the study, since their Tg levels could have been affected. This retrospective analysis has been approved by the Fırat University Research Committee (06.09.2018/14-10).

Radioiodine Therapy and Follow-up

Thyroid hormone replacement was withdrawn for 3-4 weeks prior to RAI treatment, and patients' TSH levels were increased over 30 IU/mL if possible. Patients followed a low-iodine diet for 10 days before I-131 treatment. The doses of radioiodine were determined by performing post-op neck ultrasonography (USG) with or without MR, Tc-99m thyroid scan, along with Tg values. For radioiodine ablation, a dose of 3.7 GBq was administered to eliminate thyroid remnants. When lymph node metastases were detected, patients were treated with radioiodine at a dose of 5.55 GBq. If DM was detected, patients were treated with radioiodine at a dose of 7.4 GBq. I-131 WBS was performed 7-8 days after treatment of I-131.

Tg and TSH Measurement

Tg and TSH were measured approximately 4 hours before RAI administration. Tg levels were determined by chemiluminescence immunoassay (IMMULITE® 2000 XPi Immunoassay System, US/Wales, UK). Measuring ranges were 0.20 to 30000 ng/mL (with 1/100 dilution). TSH levels were determined by chemiluminescence immunoassay (ADVIA Centaur CP Immunoassay System/US) Measuring ranges were 0.010 to 150 µIU/L. TgAb were determined by chemiluminescence microparticle immunoassay (ARCHITECT i2000SR). Measuring ranges were 20 to 1000 IU/mL. Positivity for TgAb was accepted as more than 40 IU/mL, and patients with TgAb levels above 40 IU/mL were excluded from the study.

Statistical Analysis

Continuous variables are reported as mean ± standard deviation or median values and ranges, while categorical variables are reported as absolute numbers. Between groups, differences were assessed with the Kruskal-Wallis test (and Mann-Whitney U pair-wise comparisons) or the chi-square test (categorical variables). A p value less than 0.05 was considered as significant. Receiver-operating characteristic (ROC) curve analysis was used to define the best cut-off value for serum Tg in terms of showing the presence of metastases. For the established cut-off value, we calculated the sensitivity, specificity, and area under the curve (AUC). All analyses were performed with SPSS Software (version 20.0).

Results

Of the 206 patients included in the study, 155 were female and 51 were male. The mean age was 45.88±13.59. Characteristics of study subjects are presented in Table 1.

There was a significant difference between group 3 and other groups (group 1 and group 2) in terms of Tg (p<0.001) and Tg/TSH (p<0.001). In group 3, Tg and Tg/TSH were higher than the other groups. But there was no significant difference between group 1 and group 2 (Figure1). There was also a significant difference in terms of gender (p<0.001) and age (p<0.001) between groups (Table 2). In group 3, the tumor size was significantly lower than group 1 and group 2 (p<0.001).

The diagnostic accuracy of serum Tg and Tg/TSH was evaluated using ROC analysis. The ROC curve is illustrated in Figure 2. The areas under ROC for Tg level and Tg/TSH ratios were 0.990 [95% confidence interval (CI): 0.979-1] and 0.991 (95% CI: 0.981-1), respectively. The cut-off

Table 1. Characteristics of study subjects

Age (mean ± SD)	45.88±13.59
Gender n (%)	
Male	51 (24.8%)
Female	155 (75.2%)
Pathology n (%)	180 (87.4%)
Papillary	10 (4.9%)
Follicular	7 (3.4%)
Hurthle cell	9 (4.4)
Poorly differentiated	
Tumor size mm (median/min-max)	12 (0.5-100)
Metastasis localization	63 (76%)
Lymph node	10 (12%)
Cervical	5 (6%)
Mediastinal	1 (1.2%)
Cervical + mediastinal	4 (4.8%)
Submental	13 (56.5%)
Supraclavicular	7 (30.5%)
Distant metastasis	3 (13%)
Lung	
Bone	
Multiple organ metastasis	
Tg (ng/mL) (median/min-max)	7.32 (0.1-30000)
TSH (IU/mL) (median/min-max)	75 (23-150) 0.093 (0.001-41.74)
Tg/TSH (median/min-max)	

SD: Standard deviation, Tg: Thyroglobulin, TSH: Thyroid-stimulating hormone, Min: Minimum, Max: Maximum

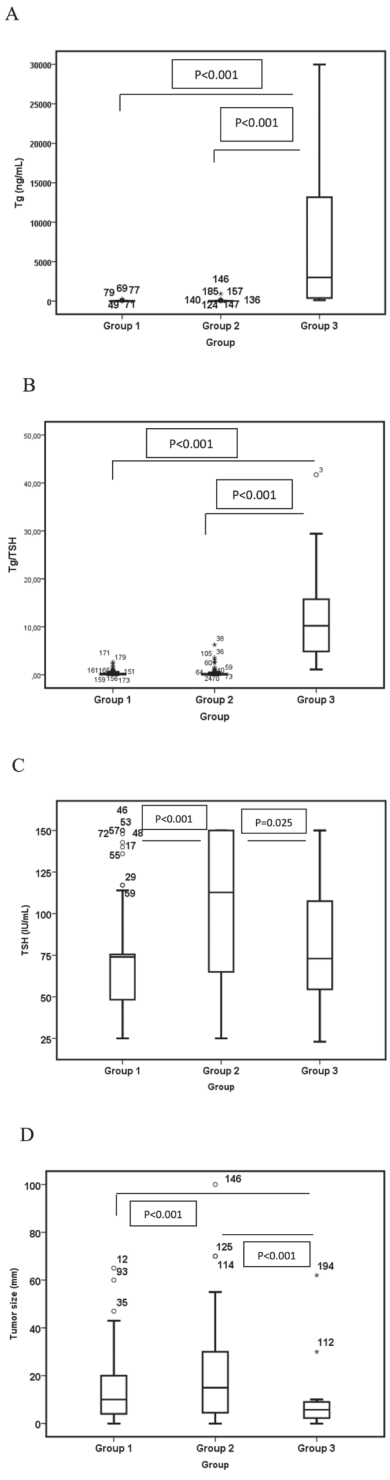

Figure 1. Association of characteristics between groups by Kruskal-Wallis test and Mann-Whitney U pair-wise comparisons: A) Comparison of groups in terms of thyroglobulin (Tg) values. B) Comparison of groups in terms of Tg/thyroid-stimulating hormone (TSH). C) Comparison of groups in terms of TSH. D) Comparison of groups in terms of tumor size

point was specified from the ROC curve using the optimal intersection of specificity and sensitivity. Based on the drawn ROC curve, the cut-off point for Tg was at 102 ng/mL (sensitivity; 100%, specificity; 94.5%) and for Tg/TSH was at 1.06 (sensitivity; 100%, specificity; 92.3%).

Discussion

LNM is known as a risk factor for poor clinical outcome in thyroid carcinoma. Decreased survival and increased mortality rates have been demonstrated among patients with DTC with lymph node metastasis (9). 10-15% of patients with DTC present with or subsequently develop DM. In these patients, the 10-year disease-specific survival rate drops to 40% (10). Early detection and treatment have been found to have a substantial effect on the survival rate of patients with DTC (11). Detection of metastasis of DTC patients is important for better treatment planning. USG, chest radiography, CT, MR and diagnostic WBS are imaging modalities used for LNM and DM diagnosis. Nevertheless, sometimes it may not be visualized on these imaging techniques (11) and the metastasis can only be detected in WBS after treatment.

Table 2. Comparison of characteristics between groups

Characteristics	Group 1 (n=100)	Group 2 (n=83)	Group 3 (n=23)	p
<40 years	35 (35%)	34 (41%)	3 (%13)	0.046*
≥40 years	65 (65%)	49 (59%)	20 (87%)	
Gender				
Female	87 (87%)	55 (66.3%)	13 (56.5%)	<0.001**
Male	13 (13%)	28 (33.7%)	10 (43.5%)	

*p<0.05, **p<0.001

Tg is the specific marker of thyroid tissue. Tg levels significantly decrease after surgical removal of thyroid tissue, while Tg levels remain high in case of residual tissue or DM in thyroid cancer (7). Therefore Tg is a tumor marker for therapy monitoring and a significant parameter used in the follow-up of subjects with DTC. Excluding thyroid cell damage, two factors determine Tg concentration in most clinical situations. These factors are thyroid cell mass and activation of TSH receptors (12). TSH secretion induced by LT4 withdrawal increases the sensitivity of Tg measurement in terms of neoplastic tissue detection (13). Since TSH values of pre-ablative patients may be different, Tg values may also be affected accordingly. For this reason, in our study, we included Tg/TSH ratio in our study parameters in addition to Tg to investigate the predictive value for metastasis in patients with DTC.

According to the results of our study; there was a significant difference between the group without metastasis and with DM in terms of both Tg and Tg/TSH values. ROC analysis of Tg and Tg/TSH also showed good accuracy (0.990 and

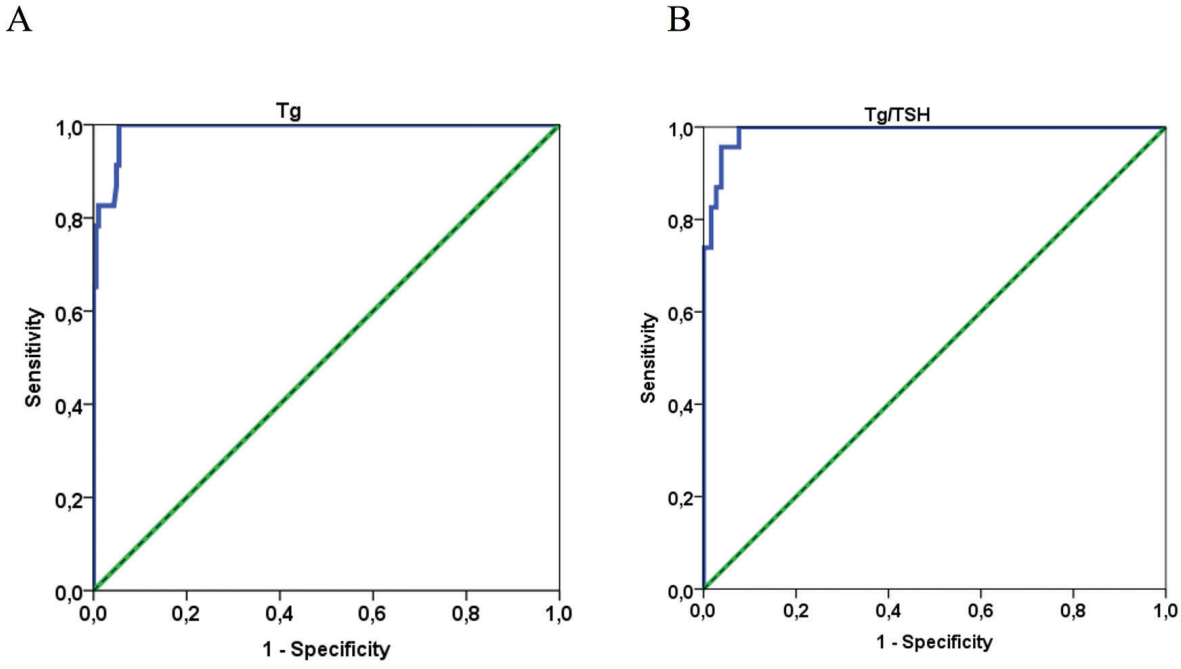

Figure 2. Receiving operator characteristic (ROC) curve for thyroglobulin (Tg) and Tg/thyroid-stimulating hormone (TSH) to detect distant metastatic differentiated thyroid carcinoma. A) ROC curve for Tg level. B) ROC curve for Tg/TSH ratio

0.991) as diagnostic markers for DM. In a similar study by Lin et al. (14), they reported that both Tg and Tg/TSH ratios could be considered predictors of DTC DM after TT prior to the first I-131 ablative therapy. Area under the ROC curve for Tg concentrations and Tg/TSH ratios were 0.913 and 0.916, respectively, in this study.

In a study which investigates the value of pre-ablation stimulated Tg in predicting DM of papillary thyroid cancer (15), it was reported that area under the ROC curve for Tg levels was 0.893 and the cut-off value of Tg was 52.75 µg/L with a sensitivity of 78.90% and specificity of 91.70%. In our study, we found that the areas under ROC for Tg level was 0.990, the cut-off point for Tg was at 102 ng/mL. We think that this difference in Tg cut-off may be related to the Tg measurement method.

In an analysis of Tg doubling time (Tg-DT), which is the time required to double the amount of Tg, Rössing et al. (16) have suggested that Tg-DT is not a single predictor of progressive disease but that it creates significant differences in the survival of patients with high tumor burden in patients with progressive DTC. They reported that there is a significant difference in survival rates patients with Tg levels greater than 100 ng/mL and with Tg levels lower than 100 ng/mL. This result suggested that one of the reasons for the difference in survival rate detected in their study might be DM. Zhao et al. (17) suggested that pre-ablative Tg levels may be affected by TSH and residual tissue after surgery, therefore, the difference between serial Tg measurements (at an average 8-day interval) could be a better marker of DM. The area under the ROC curve for ΔTg (ΔTg <0, ΔTg >0) and ΔTg/ΔTSH (ΔTg/ΔTSH <0, ΔTg/ΔTSH >0) parameters in their study was 0.907, 0.856 and 0.911, 0.905, respectively. Based on the drawn ROC curve, the cut-off point for ΔTg was at -6.55–3.90 ng/mL and for ΔTg/ΔTSH was at -0.40–0.41 ng/µIU.

In our study, there was no significant difference between patients with lymph node metastasis and those without metastasis in terms of Tg and Tg/TSH values. This result suggests that these parameters could not be used to predict LNM. In the literature, the group of patients with metastasis are classified as those with combined lymph node and DM or with DM alone. To the best of our knowledge, there aren't any studies comparing patients with and without lymph node metastases in terms of postoperative stimulated Tg values. Ronga et al. (18) reported that the mean Tg value was not significantly different between those with lymph node metastases and those with DM. In our study, both Tg and Tg/TSH values were significantly different between these two groups.

Conclusion

In conclusion, our results suggest that preablative Tg and Tg/TSH values can be used to estimate DM. On the other hand, these values do not contribute significantly to the estimation of lymph node metastasis; therefore, we think that patients should be evaluated carefully for LNM even if their Tg levels are low.

Ethics

Ethics Committee Approval: This retrospective analysis has been approved by the Fırat University Research Committee (06.09.2018/14-10).

Informed Consent: Retrospective study.

Peer-review: Externally and internally peer-reviewed.

Authorship Contributions

Surgical and Medical Practices: F.D., F.S.Ş., T.A.B., Concept: F.D., F.S.Ş., T.A.B., Design: F.D., F.S.Ş., T.A.B., Data Collection or Processing: F.D., F.S.Ş., T.A.B., Analysis or Interpretation: F.D., F.S.Ş., T.A.B., Literature Search: F.D., F.S.Ş., T.A.B., Writing: F.D., F.S.Ş., T.A.B.

Conflict of Interest: No conflict of interest was declared by the authors.

Financial Disclosure: The authors declared that this study received no financial support.

References

1. Siegel RL, Miller KD, Jemal A. Cancer statistics, 2016. CA Cancer J Clin 2016;66:7-34.
2. McLeod DS, Sawka AM, Cooper DS. Controversies in primary treatment of low-risk papillary thyroid cancer. Lancet 2013;381:1046-1057.
3. Mitchell AL, Gandhi A, Scott-Coombes D, Perros P. Management of thyroid cancer: United kingdom national multidisciplinary guidelines. Laryngol Otol 2016;130:S150-S160.
4. Durante C, Haddy N, Baudin E, Leboulleux S, Hartl D, Travagli JP, Caillou B, Ricard M, Lumbroso JD, De Vathaire F, Schlumberger M. Long-Term Outcome of 444 Patients with Distant Metastases from Papillary and Follicular Thyroid Carcinoma: Benefits and Limits of Radioiodine Therapy. J Clin Endocrinol Metab 2006;91:2892-2899.
5. Haugen BR, Alexander EK, Bible KC, Doherty GM, Mandel SJ, Nikiforov YE, Pacini F Randolph GW, Sawka AM, Schlumberger M, Schuff KG, Sherman SI, Sosa JA, Steward DL, Tuttle RM, Wartofsky L. 2015 American Thyroid Association Management Guidelines for Adult Patients with Thyroid Nodules and Differentiated Thyroid Cancer: The American Thyroid Association Guidelines Task Force on Thyroid Nodules and Differentiated Thyroid Cancer. Thyroid 2016;26:1-133.
6. Amdur RJ, Dan T, Mazzaferri E. Absence of Bone Marrow Toxicity in Elderly Patients Treated With Recombinant Human Thyroid-stimulating Hormone and Empirically Dosed Radioiodine for Thyroid Cancer. Am J Clin Oncol 2013;36:348-353.
7. Tian JJ, Tao R, Shen YF, Xia SY, Li C. Correlation of serum thyroglobulin and anti-thyroglobulin antibody levels with pulmonary metastasis and bone metastasis in patients with thyroid cancer. Journal of Hainan Medical University 2017;23:101-104.
8. Spencer CA, Lopresti JS, Fatemi S, Nicoloff JT. Detection of

Residual and Recurrent Differentiated Thyroid Carcinoma by Serum Thyroglobulin Measurement. Thyroid 1999;9:435-441.
9. Cao CJ, Dou CY, Lian J, Luan ZS, Zhou W, Xie W, Chen L, Zhou K, Lai H. Clinical outcomes and associated factors of radioiodine-131 treatment in differentiated thyroid cancer with cervical lymph node metastasis. Oncol Lett 2018;15:8141-8148.
10. Kim DH, Jung JH, Son SH, Kim CY, Hong CM, Jeong SY, Lee SW, Lee J, Ahn BC. Difference of Clinical and Radiological Characteristics According to Radioiodine Avidity in Pulmonary Metastases of Differentiated Thyroid Cancer. Nucl Med Mol Imaging 2014;48:55-62.
11. Qutbi M, Shafeie B, Amoui M, Tabeie F, Azizmohammadi Z, Mahmoud-Pashazadeh A, Javadi H, Assadi M, Asli IN. Evaluation of Prognostic Factors Associated With Differentiated Thyroid Carcinoma With Pulmonary Metastasis. Clin Nucl Med 2016;41:917-921.
12. Giovanella L, Ceriani L, Suriano S, Ghelfo A, Maffiolis M. Thyroglobulin measurement before rhTSH-aided 131 I ablation in detecting metastases from differentiated thyroid carcinoma. Clin Endocrinol 2008;69:659-663.
13. Schlumberger M, Baudin E. Serum thyroglobulin determination in the follow-up of Patients with differentiated thyroid carcinoma. Eur J Endocrinol 1998;138:249-252.
14. Lin Y, Li T, Liang J, Li X, Qiu L, Wang S, Chen Y, Kang Z, Li F. Predictive Value of Preablation Stimulated Thyroglobulin and Thyroglobulin/ Thyroid-Stimulating Hormone Ratio in Differentiated Thyroid Cancer. Clin Nucl Med 2011;36:1102-1105.
15. Li T, Lin Y, Liang J, Li X, Qiu L, Wang S, Chen Y, Kang Z, Li F. The value of pre-ablation stimulated thyroglobulin in predicting distant metastasis of papillary thyroid cancer. Chin J Nucl Med Mol İmaging 2012;32:189-191.
16. Rössing RM, Jentzen W, Nagarajah J, Bockisch A, Görges R. Serum Thyroglobulin Doubling Time in Progressive Thyroid Cancer. Thyroid 2016;26:1712-1718.
17. Zhao T, Liang J, Li T, Gao W, Lin Y. Serial stimulated thyroglobulin measurements are more specific for detecting distant metastatic differentiated thyroid cancer before radioiodine therapy. Chin J Cancer Res 2017;29:213-222.
18. Ronga G, Filesi M, Ventroni G, Vestri AR, Signore A. Value of the first serum thyroglobulin level after total thyroidectomy for the diagnosis of metastases from differentiated thyroid carcinoma. Eur J Nucl Med 1999;26:1448-1452.

Interesting Image
Mol Imaging Radionucl Ther 2019;28:27-29 DOI:10.4274/mirt.galenos.2018.55264

Unexpected Hepatic Uptake of Tc-99m-MAA in Lung Perfusion Scintigraphy in a Patient with End-stage Renal Disease

Son Dönem Böbrek Hastalığı Olan Hastanın Akciğer Perfüzyon Sintigrafisinde Tc-99m-MAA'nın Beklenmedik Karaciğer Tutulumu

Kadir Alper Küçüker[1], İsa Burak Güney[1], Kairgeldy Aikimbaev[2], Saime Paydaş[3]
[1]*Çukurova University Faculty of Medicine, Department of Nuclear Medicine, Adana, Turkey*
[2]*Çukurova University Faculty of Medicine, Department of Radiology, Adana, Turkey*
[3]*Çukurova University Faculty of Medicine, Department of Internal Medicine, Adana, Turkey*

Abstract

Extra-pulmonary accumulation of Tc-99m-macroaggregated albumin (MAA) is described as uptake areas out of the lung in perfusion scintigraphy. If the particles spread throughout the body before reaching the lung via venous collaterals or due to right-to-left shunt, or if the particles are too small to occlude the pulmonary capillaries, then the agent can be seen at different locations of the body. Extra-pulmonary accumulation of Tc-99m-MAA can be detected mostly in the liver as well as in the brain, kidney, thyroid, myocardium, spleen and vertebra. Herein, we present lung scanning images with unexpected hepatic accumulation of Tc-99m-MAA. This pulmonary perfusion scintigraphy was performed in a patient with end-stage renal disease due to dyspnea in the post-operative period of kidney transplantation.

Keywords: Tc-99m-macroaggregated albumin, perfusion scintigraphy, collateral circulation, liver, end-stage renal disease

Öz

Tc-99m-kümelenmiş albüminin (MAA) ekstrapulmoner birikimi, akciğer perfüzyon sintigrafisinde akciğer dışında radyoaktif madde tutulumu olması şeklinde tanımlanır. Eğer Tc-99m-MAA partikülleri venöz kollateraller sayesinde ya da sağdan sola şant nedeniyle akciğere ulaşamadan vücuda yayılırsa veya partiküller akciğer kapillerini tıkayamayacak kadar küçük ise radyoaktif ajan vücudun farklı alanlarında izlenebilir. Tc-99m-MAA'nın ekstrapulmoner birikimi en sık karaciğerde izlenmekle birlikte, literatürde bazı çalışmalarda beyin, böbrek, tiroid, miyokard, dalak ve vertebralarda da gösterilmiştir. Burada, Tc-99m-MAA'nın beklenmedik hepatik birikiminin tespit edildiği akciğer perfüzyon sintigrafisi görüntülerini sunuyoruz. Bu akciğer perfüzyon sintigrafisi, son dönem böbrek yetmezliği bulunan bir hastaya böbrek transplantasyonu operasyonu sonrası döneminde gelişen nefes darlığı nedeniyle uygulanmıştır.

Anahtar kelimeler: Tc-99m kümelenmiş albümin, perfüzyon sintigrafi, kollateral dolaşım, karaciğer, son-dönem böbrek hastalığı

Address for Correspondence: Kadir Alper Küçüker MD, Çukurova University Faculty of Medicine, Department of Nuclear Medicine, Adana, Turkey
Phone: +90 322 338 32 19 E-mail: alper_kucuker@hotmail.com ORCID ID: orcid.org/0000-0003-2535-7498
Received: 09.11.2017 **Accepted:** 15.10.2018

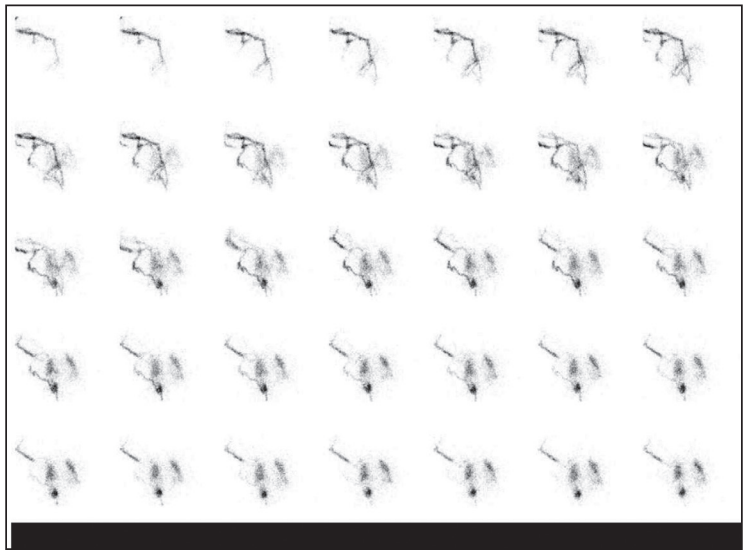

Figure 1. A 25 year-old female patient has been undergoing hemodialysis therapy for 11 years. During hemodialysis period, her arteriovenous fistulas have occluded and aneurysms have developed many times in different vascular locations. Thus, her vascular access was altered to a central venous catheter in 2015. Various venous sites such as bilateral jugular, subclavian and femoral veins had been used for blood exchange due to repetitive venous stenoses. After failure of central venous catheters, she has eventually undergone cadaveric kidney transplantation on May in 2017. She developed dyspnea in the post-operative period. The graft was functioning very well. She was referred to our department for pulmonary perfusion scintigraphy with suspicion of pulmonary embolism. A two head gamma camera (Siemens Symbia T16 SPECT/CT, Germany) was used for scintigraphy, with 80 Mbq of MAA administered intravenously for perfusion imaging. In static and SPECT/CT images, we detected an area that uptakes macroaggregated albumin (MAA) that corresponded to segment 4B in the liver in addition to three filling defects in the lung. After this finding, we acquired dynamic images that focused on the right chest and axillar region, and determined collateral circulation from the axillary region to the liver via lateral chest wall veins. When we injected the radioactive agent into the cephalic vein, an amount of radiopharmeutical was taken by liver via collaterals and caused an uptake in liver parenchyma. Since the superior vena cava (SVC) was not totally occluded, rest of the radioactive agent taken by lungs. There was no uptake in other organs since any connection to the systemic arterial circulation was lacking.

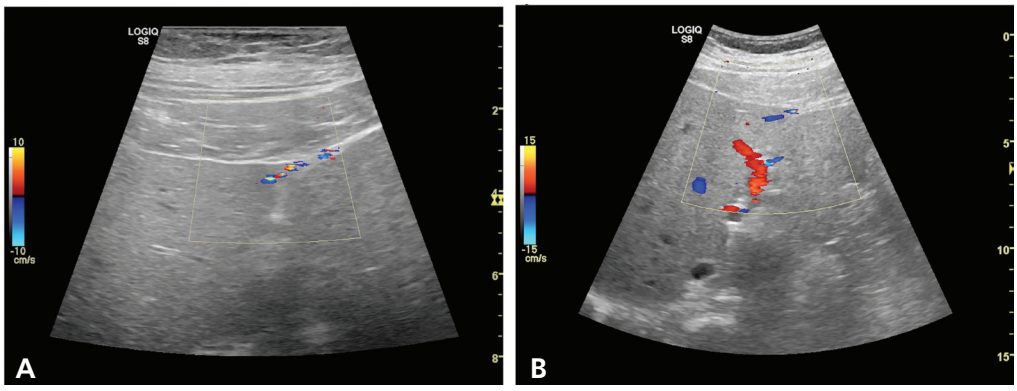

Figure 2. A venography could not be performed due to the risks of nephrotoxicity and embolus. Therefore, we planned for a color doppler ultrasound (CDUS) study. In CDUS, an unusual venous structure that perforated the capsule and entered to the liver parenchyma from segment 4 has been identified (A). Any other pathologic sign could not be seen in the liver parenchyma, the flow direction of that vein was towards the liver, which excluded any liver pathology such as portal hypertension or cirrhosis (B). These findings suggest a collateral circulation via the lateral thoracic veins between the right upper extremity and the liver. When SVC is obstructed, collateral pathways can emerge in the internal mammary, the azygos, the lateral thoracic and the vertebral venous pathways. In addition to SVC obstruction, presence of collateral circulation has been shown following inferior vena cava (IVC) occlusions. A caval-portal shunt is provided by the inferior mesenteric vein, umbilical vein and left renal vein. Intrahepatic collateral veins between proximal and distal segments of the obstruction is also specific to IVC obstructions (1). Extra-pulmonary accumulation of Tc-99m-MAA can be detected if the agent is shunted to the liver directly via venous–venous collaterals before reaching the right atrium, due to right-to-left shunt in the heart or lung and when the particles are degraded into sub-micron sizes. It has been reported that extra-pulmonary accumulation of Tc-99m-MAA was less than 4% among 378 lung scan patients (2). Extra-pulmonary accumulation of Tc-99m-MAA can be detected mostly in the liver as well as the brain, kidney, thyroid, myocardium, spleen and vertebra in several studies (3,4,5,6).

Ethics

Informed Consent: Consent form was filled out by all participants.

Peer-review: Externally peer-reviewed.

Authorship Contributions

Surgical and Medical Practices: K.A.K., İ.B.G., K.A., S.P., Concept: K.A.K., İ.B.G., Design: K.A.K., İ.B.G., Data Collection or Processing: K.A.K., İ.B.G., K.A., S.P., Analysis or Interpretation: K.A.K., İ.B.G., K.A., S.P., Literature Search: K.A.K., İ.B.G., Writing: K.A.K., İ.B.G.

Conflict of Interest: No conflict of interest was declared by the authors.

Financial Disclosure: The authors declared that this study received no financial support.

References

1. Kapur S, Paik E, Rezaei A, Vu DN. Where there is blood, there is a way: unusual collateral vessels in superior and inferior vena cava obstruction. Radiographics 2010;30:67-78.
2. Kume N, Suga K, Uchisako H, Matsui M, Shimizu K, Matsunaga N. Abnormal extra pulmonary accumulation of Tc-99m-MAA during lung perfusion scanning. Ann Nucl Med 1995;9:179-184.
3. Gale B, Chen C, Chun KJ, Lan J, Cynamon J, Freeman LM. Systemic to Pulmonary Venous Shunting in Superior Vena Cava Obstruction: Unusual Myocardial and Thyroid Visualization. Clin Nucl Med 1990;15:246-250.
4. Esser JP, Oei HY, de Bruin HG, Krenning EP. Liver and vertebral uptake of Tc-99m macroaggregated albumin (MAA). Clin Nucl Med 2004;29:793-794.
5. Karls S, Hassoun H, Derbekyan V. Vertebral Uptake of Tc-99m Macroaggregated Albumin (MAA) with SPECT/CT Occurring in Superior Vena Cava Obstruction. Nucl Med Mol Imaging 2016;50:266-269.
6. Goshen E, Oksman Y, Rotenberg G, Zwas ST. Absent pulmonary uptake on Tc-99m-MAA perfusion lung scan due to severe right to left shunt. Semin Nucl Med 2004;34:157-158.

Interesting Image
Mol Imaging Radionucl Ther 2019;28:30-33 DOI:10.4274/mirt.galenos.2018.72677

A Diagnostic Challenge: Erdheim Chester Disorder

Zor Bir Tanı: Erdheim Chester Hastalığı

Mairah Razi[1], Maria Qubtia[2], Aamna Hassan[1], Mudassar Hussain[3], Abdul Hameed[2]
[1]Shaukat Khanum Memorial Cancer Hospital and Research Centre, Clinic of Nuclear Medicine, Lahore, Pakistan
[2]Shaukat Khanum Memorial Cancer Hospital and Research Centre, Clinic of Medical Oncology, Lahore, Pakistan
[3]Shaukat Khanum Memorial Cancer Hospital and Research Centre, Clinic of Pathology, Lahore, Pakistan

Abstract

Erdheim-Chester disease (ECD) is a rare, multisystemic, idiopathic disease often associated with *BRAF* V600E mutation. Its diagnosis is typically delayed and challenging due to its variable manifestations. Although it has an indolent course, advanced stages can manifest fulminant behavior with multiple vital organ involvement. It is a class 2a, non-Langerhans cell histiocytosis with characteristic radiological appearance. Whole body imaging might be helpful, particularly, to assess skeletal lesions. Although widespread disease with typical skeletal involvement on imaging can prompt diagnosis, histopathology with immunohistochemistry is required for confirmation. The disease can also manifest itself with a large variety of central nervous system related or orbital symptoms. Cardiac involvement is quite common. We present an interesting image of a patient with ECD who underwent PET/CT. Informed consent of the subject described in this image is waived by the Institutional Review Board.

Keywords: Erdheim-Chester disease, non-Langerhans cell histiocytosis, positron emission tomography

Öz

Erdheim-Chester hastalığı (ECD), çoğunlukla *BRAF* V600E mutasyonu ile ilişkili, nadir, multisistemik ve idiyopatik bir bozukluktur. Tipik olarak farklı belirtileri nedeniyle geç ve zor tanı konulur. Her ne kadar sessiz bir klinik seyri olsa da ileri evrelerde multipl vital organ tutulumu ile fulminan seyir gösterebilir. Karakteristik radyolojik özellikleri olan, sınıf 2a, non-Langerhans hücreli histiyositozlardandır. Tüm vücut görüntüleme, özellikle iskelet lezyonlarını göstermek için, yararlı olabilir. Her ne kadar görüntülemede tipik yaygın iskelet tutulumu tanıyı öne sürse de kesin tanı için histopatolojik doğrulama gereklidir. Hastalık aynı zamanda kraniyal ya da orbital farklı bulgularla da ortaya çıkabilir. Kardiyak tutulum sıktır. Bu yayında ECD'nin PET/BT görüntülerini sunmaktayız.

Anahtar kelimeler: Erdheim-Chester hastalığı, non-Langerhans hücreli histiyositoz, pozitron emisyon tomografisi

Address for Correspondence: Mairah Razi MD, Shaukat Khanum Memorial Cancer Hospital and Research Centre, Clinic of Nuclear Medicine, Lahore, Pakistan
Phone: +924235905000 E-mail: m_sdr@yahoo.com ORCID ID: orcid.org/0000-0002-7914-4925
Received: 01.03.2018 **Accepted:** 25.09.2018

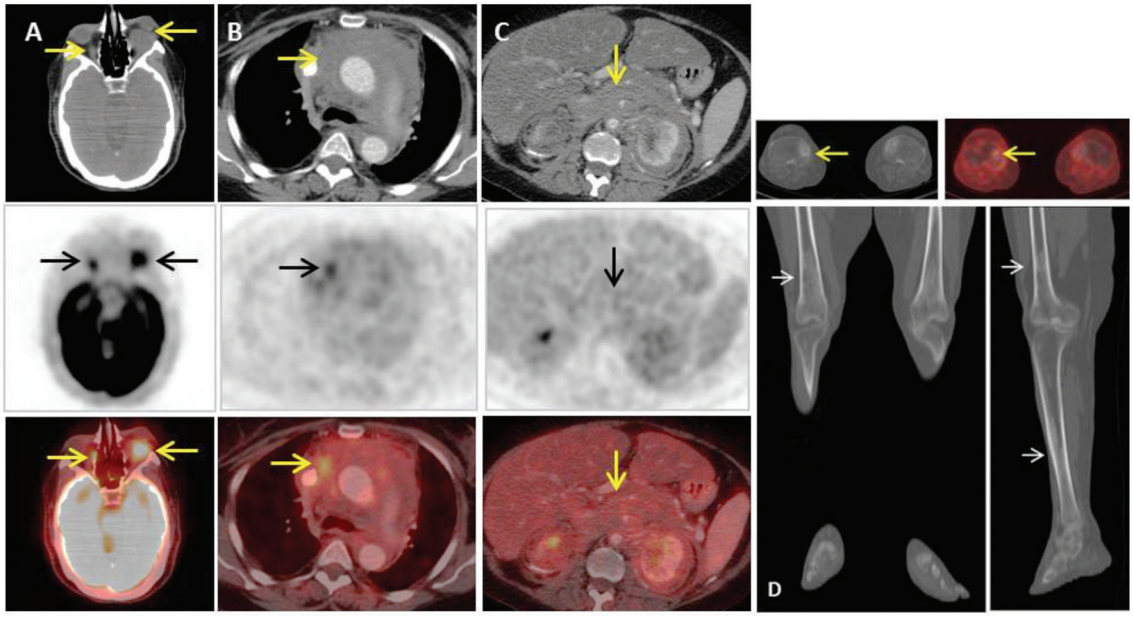

Figure 1. A 59-year-old diabetic, hypertensive, hypothyroid female with cardiac pacemaker for complete heart block, was diagnosed with retroperitoneal fibrosis. Tarsorrhaphy was performed for left eye swelling for corneal/visual protection. Subsequently, she developed renal damage along with lower limb swelling. Baseline non-contrast computed tomography (CT) scan revealed diffuse soft tissue mass around the descending aorta and kidneys, resulting in bilateral hydronephrosis. Follow-up CT scan revealed retroperitoneal mass extending up to the posterior mediastinum. PET/CT was performed with intravenous injection of 10 mCi of ^{18}F-FDG. Scan features were suggestive of Erdheim-Chester disease (ECD) in correlation with history and widespread skeletal disease.
Axial contrast enhanced PET/CT images (upper row; CT, middle; ^{18}F-FDG PET & lower; fusion PET/CT) through orbits (A) showed hypermetabolic intraconal left orbital soft tissue mass (SUV_{max}: 6.1) causing proptosis, inseparable from the optic nerve and extraocular muscles. Hypermetabolic thickening of the right optic nerve is also shown. (B) In the mediastinum, diffuse heterogeneously avid infiltrative soft tissue mass (SUV_{max}: 4.4) is insinuating between great vessels. (C) Abdominal sections show diffuse retroperitoneal soft tissue mass (SUV_{max}: 2.9) encasing branches of the abdominal aorta, infiltrating bilaterally into perinephric space with renal encasement. (D) Coronal and sagittal sections of lower extremities show osteosclerotic changes along long bones. Representative axial PET/CT fusion images show focal avidity overlying sclerosis at medial plateau of the right tibia.

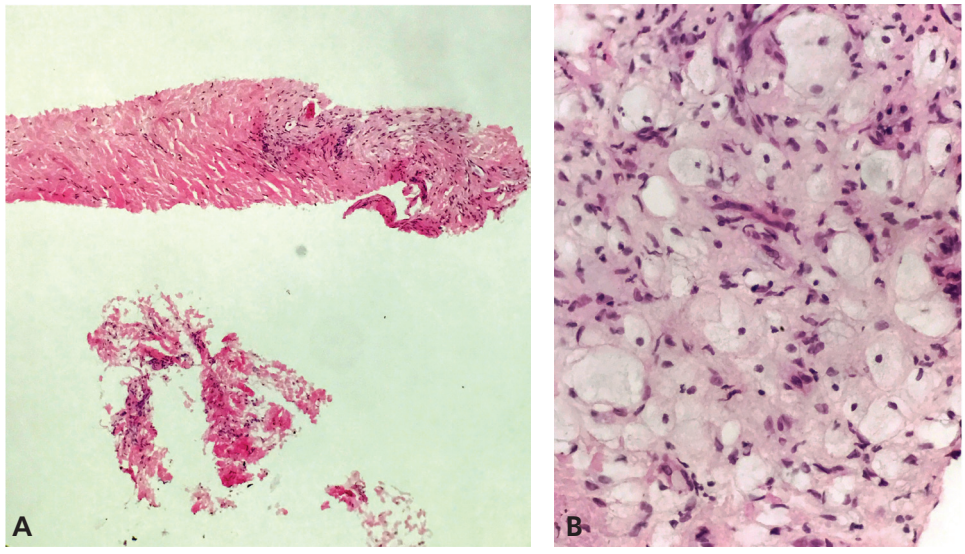

Figure 2. Histopathologic examination of the mediastinal mass revealed dense fibrosis and foamy macrophages. Hematoxylin and eosin (H&E) staining, at 10X and 40X magnifications. Positive CD68 (histiocyte marker) and negative S100 (neural marker), confirming diagnosis of ECD (A; H&E 10X, B; H&E 40X).

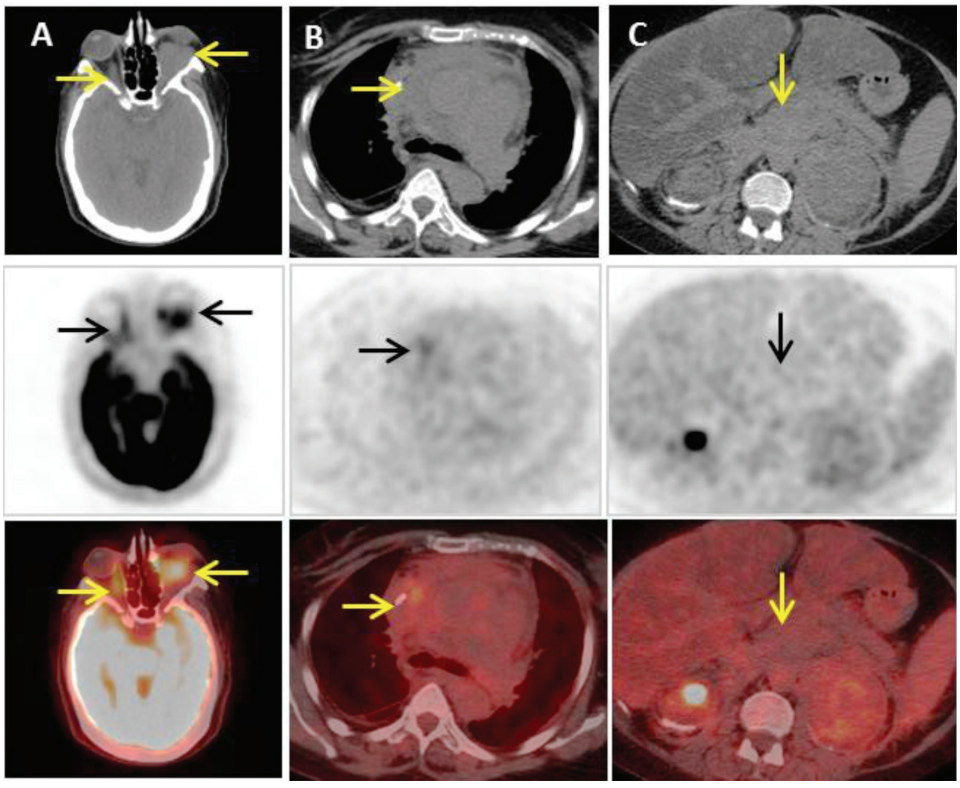

Figure 3. The patient was treated with pegylated interferon-alpha (IFN). Her performance status significantly improved within three weeks along with orbital pain and swelling, pedal edema, and renal functions. Re-evaluation non-contrast PET/CT at six months post IFN initiation; axial CT, PET and fusion images through orbit (A), mediastinum (B) and abdomen (C) demonstrate interval reduction in metabolic activity with stable morphological disease within orbits (SUV_{max}: 5.2), mediastinum (SUV_{max}: 3.9) and retroperitoneal stations (SUV: 2.4) reflecting stable response. She had good quality of life and tolerated IFN for almost 23 months. Subsequently, she developed cardiac and renal decompensation and died.

ECD is a rare chronic disease with delayed presentation, first described by Jakob Erdheim and William Chester as lipid granulomatosis in 1930 (1). Typically, it manifests with characteristic osteosclerosis of diaphysis and metaphysis with epiphyseal sparing of long bones which can be picked up by bone scintigraphy or CT or PET/CT scan (2). Partial involvement of epiphysis has also been reported in the literature (3). ECD indolently involves various organs or fulminant multisystem failure; central nervous system 40-50%, cardiac 75% (4), pulmonary (43%) or pleural involvement (5). Retroperitoneal fibrosis and renal involvement are the commonest presentations (6).

^{18}F-FDG PET/CT gained potential importance in early diagnosis of ECD with multisystem involvement enabling whole body acquisition in a single session. Studies have shown excellent specificity of PET scans ranging from 69.2 to 100%; however, sensitivity varies among different organs (range 4.3 to 78.3%) contrary to other imaging modalities (7). PET/CT provides useful information in appreciation of therapy response earlier, depicting metabolic disease activity. One of the recent studies reported effectiveness of PET/CT in management as 48% of cases (8,9). ^{18}F-FDG PET scanning depicts metabolic response earlier in neurologic and osseous disease than morphologic changes detected on magnetic resonance imaging (7). Despite characteristic skeletal findings and multisystem involvement, imaging may help in diagnosis, but histologic evaluation is required for confirmation. Our case presents a rare disease in which multidisciplinary approach and appropriate imaging are essential for timely diagnosis and patient management.

Ethics

Informed Consent: Consent form was filled out by all participants.

Peer-review: Externally and internally peer-reviewed.

Authorship Contributions

Surgical and Medical Practices: M.R., M.Q., A.Has., M.H., A.H., Concept: M.R., M.Q., A.Has., M.H., A.H., Design: M.R., M.Q., A.H., M.H., A.H., Data Collection or Processing: M.R., M.Q., A.Has., M.H., A.H., Analysis or Interpretation: M.R., M.Q., A.Has., M.H., A.H., Literature Search: M.R., M.Q., A.Has., M.H., A.H., Writing: M.R., M.Q., A.Has., M.H., A.H.

Conflict of Interest: No conflict of interest was declared by the authors.

Financial Disclosure: The authors declared that this study received no financial support.

References

1. Chester W. Über Lipoidgranulomatose. Virchows Archiv für pathologische Anatomie und Physiologie und für klinische Medizin 1930;279:561-602.
2. Diamond EL, Dagna L, Hyman DM, Cavalli G, Janku F, Estrada-Veras J, Ferrarini M, Abdel-Wahab O, Heaney ML, Scheel PJ, Feeley NK, Ferrero E, McClain KL, Vaglio A, Colby T, Arnaud L, Haroche J. Consensus guidelines for the diagnosis and clinical management of Erdheim-Chester disease. Blood 2014;124:483-492.
3. Haroche J, Arnaud L, Cohen-Aubart F, HervierB, Charlotte F, Emile JF, Amoura Z. Erdheim-Chester disease. Curr Rheumatol Rep 2014;16:412.
4. Haroche J, Charlotte F, Arnaud L, von Deimling A, Hélias-Rodzewicz Z, Hervier B, Cohen-Aubart F, Launay D, Lesot A, Mokhtari K, Canioni D, Galmiche L, Rose C, Schmalzing M, Croockewit S, Kambouchner M, Copin MC, Fraitag S, Sahm F, Brousse N, Amoura Z, Donadieu J, Emile JF. High prevalence of BRAF V600E mutations in Erdheim–Chester disease but not in other non-Langerhans cell histiocytoses. Blood 2012;120:2700-2703.
5. Kenn W, Eck M, Allolio B, Jakob F, Illg A, Marx A, Mueller-Hermelink HK, Hahn D. Erdheim-Chester disease: evidence for a disease entity different from Langerhans cell histiocytosis? Three cases with detailed radiological and immunohistochemical analysis. Hum Pathol 2000;31:734-739.
6. Cavalli G, Guglielmi B, Berti A, Campochiaro C, Sabbadini MG, Dagna L. The multifaceted clinical presentations and manifestations of Erdheim-Chester disease: comprehensive review of the literature and of 10 new cases. Ann Rheum Dis 2013;72:1691-1695.
7. Arnaud L, Hervier B, Neel A, Hamidou MA, Kahn JE, Wechsler B, Perez-Pastor G, Blomberg B, Fuzibet JG, Dubourguet F, Marinho A, Magnette C, Noel V, Pavic M, Casper J, Beucher AB, Costedoat-Chalumeau N, Aaron L, Salvatierra J, Graux C, Cacoub P, Delcey V, Dechant C, Bindi P, Herbaut C, Graziani G, Amoura Z, Haroche J. CNS involvement and treatment with interferon-alpha are independent prognostic factors in Erdheim-Chester disease: a multicenter survival analysis of 53 patients. Blood 2011;117:2778-2782.
8. Pan A, Doyle T, Schlup M, Lubcke R, Schultz M. Unusual manifestation of Erdheim-Chester disease. BMC Gastroenterol 2011;11:77.
9. Haroche J, Cohen-Aubart F, Emile JF, Arnaud L, Maksud P, Charlotte F, Cluzel P, Drier A, Hervier B, Benameur N, Besnard S, Donadieu J, Amoura Z. Dramatic efficacy of vemurafenib in both multisystemic and refractory Erdheim-Chester disease and Langerhans cell histiocytosis harboring the BRAF V600E mutation. Blood 2013;121:1495-1500.

Interesting Image
Mol Imaging Radionucl Ther 2019;28:34-37 DOI:10.4274/mirt.galenos.2018.09821

False-positive I-131 Uptakes at Pulmonary Wedge-resection Site and Soft Tissue Lateral to the Femoral Heads in a Patient with Papillary Thyroid Carcinoma

Papiller Tiroid Kanserli Bir Hastada Akciğerde Kama-Rezeksiyon Alanında ve Femur Başlarının Lateralinde Yumuşak Dokuda Yanlış-Pozitif I-131 Tutulumları

Bülent Yazıcı[1], Aylin Oral[1], Şeyma Alçiçek[1], İpek Tamsel[2], Ayşegül Akgün[1]
[1]*Ege University Faculty of Medicine, Department of Nuclear Medicine, İzmir, Turkey*
[2]*Ege University Faculty of Medicine, Department of Radiology, İzmir, Turkey*

Abstract

A hyper-metabolic pulmonary nodule was detected on ^{18}F-FDG PET/CT in a 65-year-old woman who had been followed up for 12 years without any complaints following treatment for papillary thyroid cancer (PTC). Wedge resection was performed to the pulmonary nodule and the pathologic examination revealed PTC metastasis. On the post-therapeutic I-131 scan after radioiodine treatment, focal I-131 uptake was detected at the site of pulmonary wedge resection. At first, this finding was thought to be related to the residual lesion but diagnostic CT demonstrated only focal traction bronchiectasis at that region. In addition, a false-positive I-131 uptake was also detected at the soft tissue just lateral to the femoral heads probably due to inflammation.

Keywords: Thyroid, cancer, false-positive, iodine, I-131

Öz

On iki yıldır sorunsuz takip edilen tiroid papiller kanserli 65 yaşındaki kadın hastaya çekilen ^{18}F-FDG PET/BT'de hipermetabolik bir akciğer nodülü saptandı. Nodül kama-rezeksiyon yöntemiyle çıkarıldı. Patoloji sonucunda bu nodülde tiroid papiller kanseri metastazı saptandı. Radyoaktif iyot tedavisinden sonra yapılan tüm vücut I-131 tarama sintigrafisinde akciğerde rezeksiyon alanında fokal I-131 tutulumu görüldü. Bu bulgunun öncelikle kalıntı bir lezyona bağlı olabileceği düşünüldü ancak daha sonra yapılan tanısal BT'de bu alanda sadece traksiyon bronşektazisi olduğu görüldü. Ayrıca, femur başlarının lateralinde yumuşak dokularda da enflamatuvar nedenlere bağlı olduğu düşünülen yanlış-pozitif I-131 tutulumları saptandı.

Anahtar kelimeler: Tiroid, kanser, yanlış pozitif, iyot, I-131

Address for Correspondence: Bülent Yazıcı MD, Ege University Faculty of Medicine, Department of Nuclear Medicine, İzmir, Turkey
Phone: +90 505 221 16 27 E-mail: bulentayseyazici@yahoo.com ORCID ID: orcid.org/0000-0001-6207-9162
Received: 01.06.2018 **Accepted:** 07.09.2018

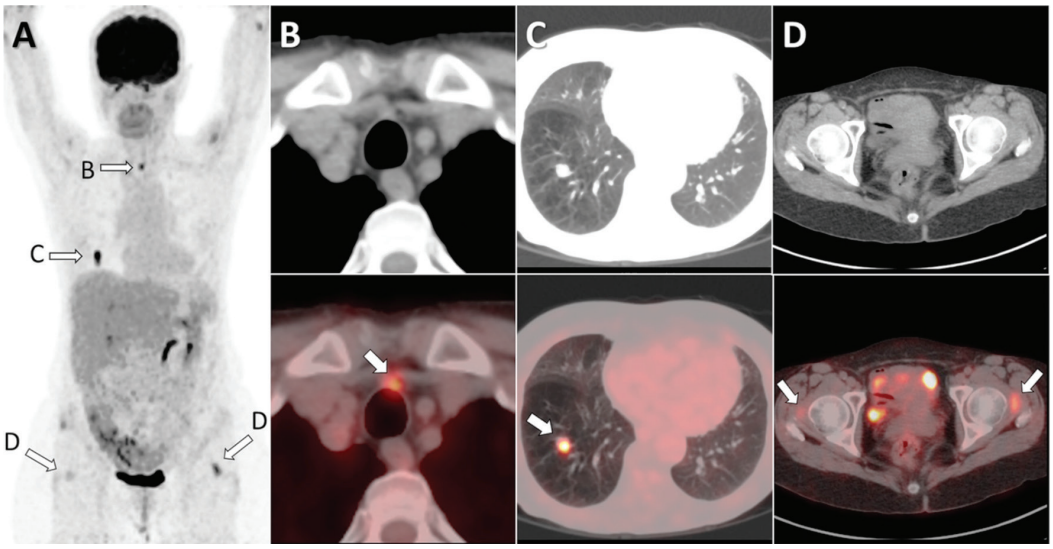

Figure 1. Total thyroidectomy was performed to a 65-year-old woman 12 years ago with a diagnosis of papillary thyroid cancer (PTC) with central lymph node metastasis. After the operation, 150 mCi of I-131 was given to the patient. Follow-up I-131 whole body scans (WBS) at 1-year, 3-year and 5-year were all negative. Thyroglobulin (Tg) and anti-Tg values were also negative during the WBSs. The patient had been followed for 12 years with annual ultrasound (US) without any complaints. However, a recent cervical US detected a suspicious pre-tracheal 9 mm lymph node and its biopsy revealed PTC metastasis. When thorax computed tomography (CT) was performed, a 13 mm pulmonary nodule was found in the right lower lobe. At first, since Tg was negative, the nodule was thought to be due to a lung neoplasm. Thus, ^{18}F-FDG PET/CT was performed (A). PET/CT showed the hypermetabolic pre-tracheal lymph node (B) and the hypermetabolic pulmonary nodule in the right lower lobe (C). In addition, increased uptakes were detected at soft tissues lateral to the femoral heads (D) probably due to some inflammatory processes. The pulmonary nodule was completely removed by wedge-resection and pathology revealed PTC metastasis.

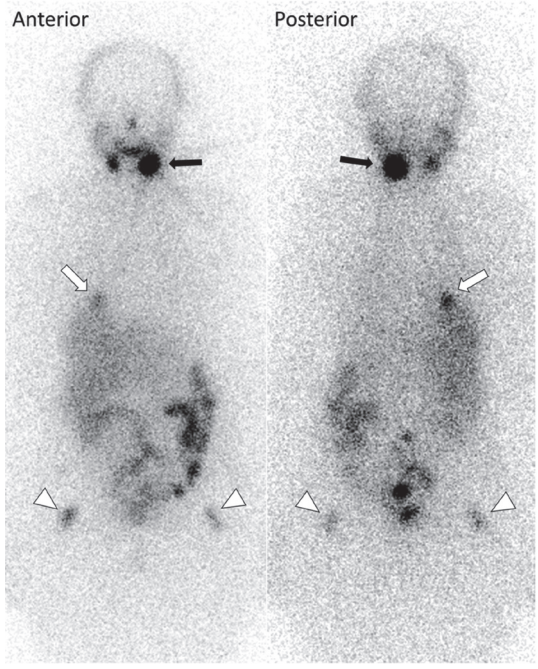

Figure 2. After the diagnosis of metastases, 200 mCi I-131 was applied. Tg was 77.2 ng/mL while TSH was 79 μIU/mL on the day of treatment. Post-therapeutic I-131 WBS showed focal uptakes on the right lower hemi-thorax (white-arrows) and around the hips (arrow-heads) in addition to hyperactivity on the left submandibular gland (black-arrows) and physiological gastrointestinal activities. FDG-avid metastatic pre-tracheal lymph node was false-negative on I-131 WBS.

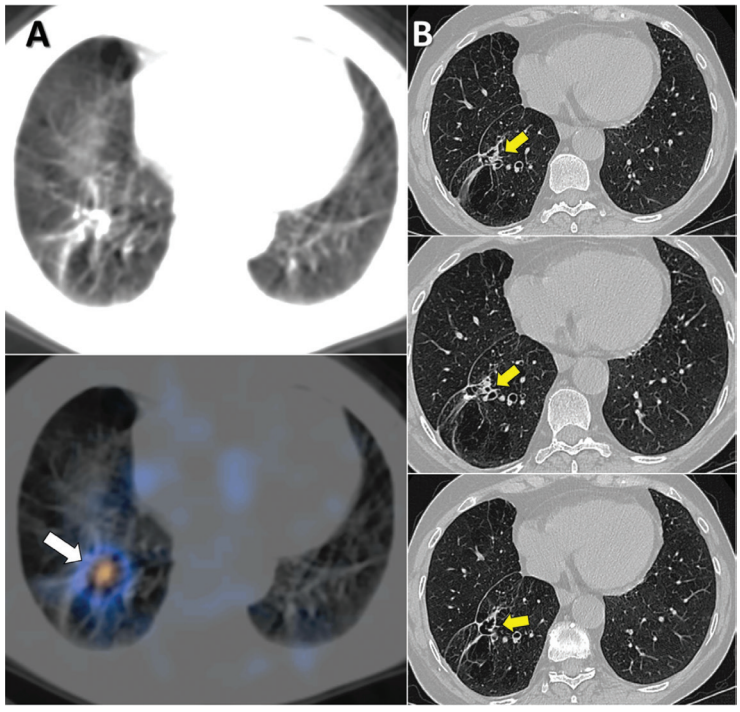

Figure 3. SPECT/CT images showed focal I-131 uptake at the wedge-resection site (A). A diagnostic CT was performed due to the possibility of residual lesion. Sequential slices demonstrated only focal traction bronchiectasis due to wedge-resection (B). A few case reports showed incidental detection of I-131 uptake in bronchiectasis (1,2,3). However, this case was different because we observed focal uptake at the metastasectomy site, which could be thought to be due to a residual lesion. Since the CT component of our SPECT/CT was not enough to clarify this issue, a diagnostic CT was obtained.

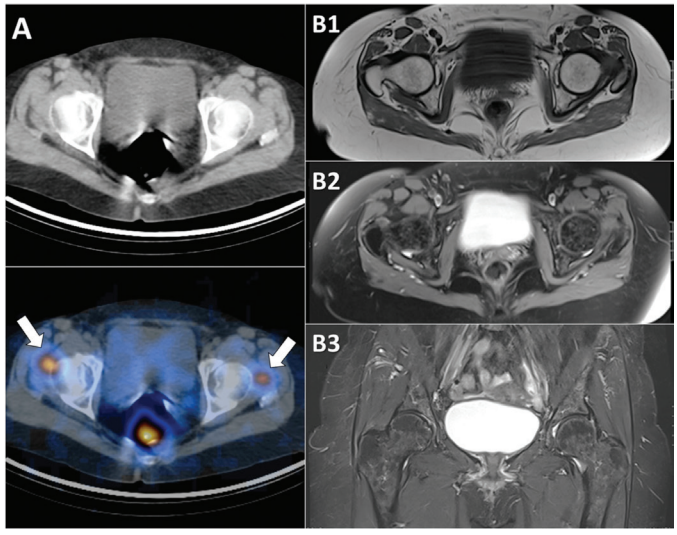

Figure 4. Similar to FDG-PET/CT (Figure 1 D), SPECT/CT images also showed focal uptakes on the soft tissues lateral to the femoral heads (A), which might be due to inflammation but the exact reason couldn't be found because T1-weighted (B1) and fat-suppressed T2-weighted (B2, B3) images of magnetic resonance imaging were normal. Informed consent of the patient was obtained for all procedures. Many false-positive findings in I-131 scans due to physiological variants, inflammation or some non-thyroidal neoplasms have been reported (4,5,6,7,8). As a result, the following interesting/rare situations were seen in combination in this case: false-positive I-131 uptakes at wedge-resection site and soft tissues, false-negative I-131 for FDG-avid lymph metastasis, and detection of metastases after 12 years of disease-free follow-up that emphasizes the importance of long term follow-up. Our experience in this case also underlines the importance of careful interpretation of WBS. Focal I-131 uptake at the pulmonary wedge-resection site could be a false-positive finding due to focal traction bronchiectasis. Diagnostic CT should be performed to clarify this suspicious finding in order to determine if there is a residual lesion.

Ethics

Informed Consent: Consent form was filled out by all participants.

Peer-review: Externally peer-reviewed.

Authorship Contributions

Medical Practices: B.Y., A.O., Ş.A., İ.T., A.A., Concept: B.Y., A.O., Ş.A., Design: B.Y., A.O., Ş.A., Data Collection or Processing: B.Y., Analysis or Interpretation: B.Y., A.O., İ.T., A.A., Literature Search: B.Y., Ş.A., Writing: B.Y.

Conflict of Interest: No conflict of interest was declared by the authors.

Financial Disclosure: The authors declared that this study received no financial support.

References

1. Jong I, Taubman K, Schlicht S. Bronchiectasis simulating pulmonary metastases on iodine 131 scintigraphy in well-differentiated thyroid carcinoma. Clin Nucl Med 2005;30:688-689.
2. Gargya A, Chua E. Focal bronchiectasis causing abnormal pulmonary radioiodine uptake in a patient with well-differentiated papillary thyroid carcinoma. Case Rep Endocrinol 2012;2012:1-3.
3. Jia C, Moadel R, Freeman LM. Focal thoracic uptake mimicking lung metastasis on 131I post-therapy whole-body scan in patients with thyroid carcinoma. Clin Nucl Med 2014;39:360-362.
4. Oh JR, Ahn BC. False-positive uptake on radioiodine whole-body scintigraphy: physiologic and pathologic variants unrelated to thyroid cancer. Am J Nucl Med Mol Imaging 2012;2:362-385.
5. Carlisle MR, Lu C, McDougall IR. The interpretation of 131I scans in the evaluation of thyroid cancer, with an emphasis on false positive findings. Nucl Med Commun 2003;24:715-735.
6. Yazici B, Oral A, Eraslan C, Argin M, Ömür Ö. False-Positive 131I Uptake in a Benign Bone Lesion on Post-therapy Scan. Clin Nucl Med 2016;41:63-65.
7. Çayır D, Araz M, Apaydın M, Cakal E. Inguinal Endometriosis Visualized on I-131 Whole Body Scan. Mol Imaging Radionucl Ther 2018;27:52-54.
8. Garger YB, Winfeld M, Friedman K, Blum M. In thyroidectomized thyroid cancer patients, false-positive I-131 whole body scans are often caused by inflammation rather than thyroid cancer. J Investig Med High Impact Case Rep 2016;4:2324709616633715.

Interesting Image
Mol Imaging Radionucl Ther 2019;28:38-40 DOI:10.4274/mirt.galenos.2018.44227

Splenosis Mimicking Lymphoma Relapse Confirmed by ^{18}F-FDG PET/CT and Tc-99m Nano-colloid Scintigraphy Thirty Years After Splenectomy for Trauma

Travma ve Splenektomiden Otuz Yıl Sonra Ortaya Çıkarak Lenfoma Relapsını Taklit Eden ve ^{18}F-FDG PET/BT ve Tc-99m Nanokolloid Sintigrafisi ile Doğrulanan Splenozis

Zehra Pınar Koç[1], Pelin Özcan Kara[1], Anıl Tombak[2]
[1]*Mersin University Faculty of Medicine, Department of Nuclear Medicine, Mersin, Turkey*
[2]*Mersin University Faculty of Medicine, Department of Hematology, Mersin, Turkey*

Abstract

Splenosis is implantation of the splenic tissue in the abdominal region or elsewhere in the body as a consequence of trauma or splenectomy, which might mimic intra-abdominal involvement of several malignancies. This case report presents a patient with abdominal implants without ^{18}F-FDG accumulation confirmed to be splenosis by Tc-99m nano-colloid scintigraphy.

Keywords: Splenosis, nano-colloid, FDG, PET, lymphoma

Öz

Splenozis bazı durumlarda malign hastalıkların karın içi tutulumunu taklit edebilen splenik dokunun travma veya splenektomi sonucu karın içi veya başka bölgelere implantasyonudur. Bu olgu sunumunda abdominal implantları olan ve ^{18}F-FDG tutulumu göstermeyip Tc-99m nanokolloid sintigrafisi ile splenozis tanısı doğrulanan hastayı sunmak istedik.

Anahtar kelimeler: Splenozis, nanokolloid, FDG, PET, lenfoma

Address for Correspondence: Zehra Pınar Koç MD, Mersin University Faculty of Medicine, Department of Nuclear Medicine, Mersin, Turkey
Phone: +90 324 241 00 00 E-mail: zehrapinarkoc@gmail.com ORCID ID: orcid.org/0000-0002-3274-5790
Received: 15.03.2018 **Accepted:** 06.09.2018

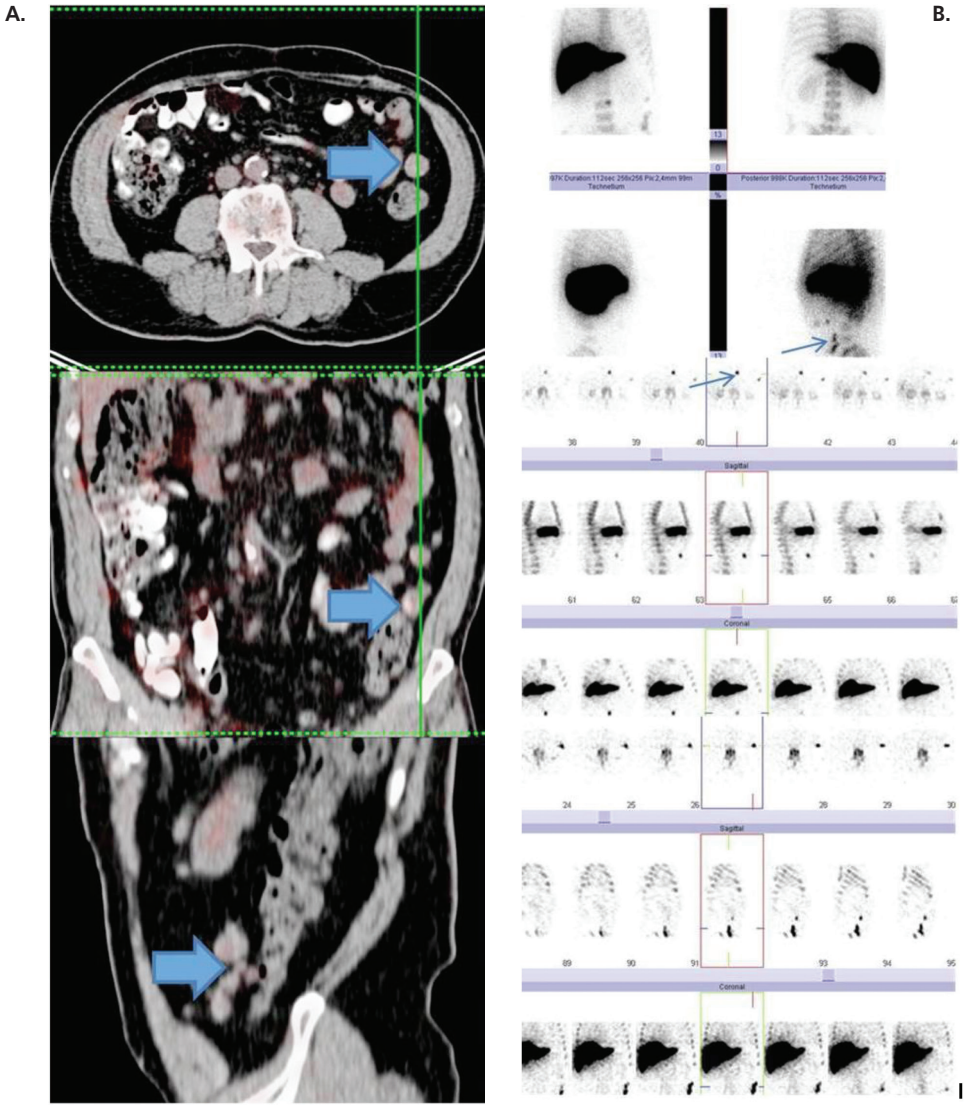

Figure 1. A) Upper to lower; trans-axial, horizontal and sagittal PET/CT fusion images showing faint activity accumulation in intra-abdominal lesions (wide arrows). B) Upper to lower; Tc-99m nano-colloid planar antero-posterior and lateral, SPECT trans-axial, coronal and sagittal projection images of two lesions pointed by narrow arrows.

A 64 year-old male patient with a history of chemotherapy for Non-Hodgkin lymphoma had undergone splenectomy following an abdominal trauma due to a traffic accident thirty-years ago and has had an eventless follow-up since then. The patient was also positive for hepatitis C virus. His follow-up abdominal contrast-enhanced CT showed abdominal implants. The patient was referred for Tc-99m nano-colloid scintigraphy and ^{18}F-FDG PET/CT at the same time with suspicion of splenosis and relapse. Sequential Tc-99m nano-colloid scintigraphy, SPECT and ^{18}F-FDG PET/CT showed an intra-abdominal lesion at midline and multiple lesions in the left lateral area (Figure 1). Due to the increased activity accumulation at spleen scintigraphy and relatively low metabolic activity in the PET/CT the patient was diagnosed as splenosis.

Although previous studies have shown that splenosis is not characterized by significantly high FDG activity accumulation (1,2), there are exceptions (3). Recent imaging modalities in the field of nuclear medicine include Ga-68 based imaging that exhibits significantly high splenic uptake which might not differentiate tumor involvement from ectopic splenic tissue, thus requiring further scintigraphic imaging and attention to this particular issue. In a recent case report, peritoneal metastasis was ruled out by selective spleen SPECT/CT imaging in a patient who showed significant intra-abdominal Ga-68 PSMA uptake (4). Although in general splenosis presents with disseminated abdominal lesions, various sites of occurrence have been reported as case reports (5). In a previous case report, hepatic involvement as shown by selective spleen scintigraphy was described (6). Another case report of hepatic splenosis was identified by PET and diagnosed by histopathologic examination (7). False positive somatostatin imaging of a solitary pulmonary nodule and intrathoracic splenosis has also been reported (8).

Although the presentation of the patient presented herein was not an unusual manifestation, splenosis is generally not expected after such a long period. To the best of our knowledge, with a diagnosis of splenosis 30 years after splenectomy, this is the longest interval reported in the literature.

Ethics

Informed Consent: Consent form was filled out by all participants.

Peer-review: Externally peer-reviewed.

Authorship Contributions

Surgical and Medical Practices: Z.P.K., P.Ö.K., A.T., Concept: Z.P.K., P.Ö.K., Design: Z.P.K., P.Ö.K., Data Collection or Processing: Z.P.K., P.Ö.K., A.T., Analysis or Interpretation: Z.P.K., P.Ö.K., A.T., Literature Search: Z.P.K., P.Ö.K., Writing: Z.P.K., P.Ö.K.

Conflict of Interest: No conflict of interest was declared by the authors.

Financial Disclosure: The authors declared that this study received no financial support.

References

1. Martínez Lorca A, Coronado Poggio M, Hernández Pérez I, Ramírez Escalante Y, Rizkallal Monzon S, Marín Ferrer MD. [Utility of (^{99}m)Tc-labelled heat-denatured erythrocyte scintigraphy and ^{18}F-FDG PET-CT to differentiate accessory spleens from tumoral metastases. A case report]. Rev Esp Med Nucl Imagen Mol 2015;34:68-69.
2. Ake AC, Menzli A, Lecomte JC, Mampassi-Makaya A, Valleix D. Peritoneal splenosis mimicking peritoneal carcinomatosis: a case report. Diagn Interv Imaging 2012;93:890-893.
3. Kellert B, Caster M, Des Jean R, Vaccarello L. Diffuse intra-abdominal splenosis presenting as carcinomatosis exhibiting positron emitted tomography hypermetabolic activity. Gynecol Oncol Case Rep 2013;5:46-48.
4. Demirci E, Has Simsek D, Kabasakal L, Mülazimoğlu M. Abdominal Splenosis Mimicking Peritoneal Metastasis in Prostate-Specific Membrane Antigen PET/CT, Confirmed With Selective Spleen SPECT/CT. Clin Nucl Med 2017;42:e504-e505.
5. Treglia G, Giovanella L, Muoio B, Caldarella C. Splenosis Mimicking Relapse of a Neuroendocrine Tumor at Gallium-68-DOTATOC PET/CT. Nucl Med Mol Imaging 2014;48:163-165.
6. Kok J, Lin M, Lin P, Ngu C, Sam S, Loh C, Kociuba K. Splenosis presenting as multiple intra-abdominal masses mimicking malignancy. ANZ J Surg 2008;78:406-407.
7. Krawczyk M, Schneider G, Farmakis G, Zimmer V, Lammert F. Splenosis mimicking hepatic adenoma. J Clin Exp Hepatol 2013;3:351-352.
8. Leong CW, Menon T, Rao S. Post-traumatic intrahepatic splenosis mimicking a neuroendocrine tumour. BMJ Case Rep 2013;2013.

Interesting Image
Mol Imaging Radionucl Ther 2019;28:41-43 DOI:10.4274/mirt.galenos.2018.06977

Doughnut Shaped Parathyroid Adenoma

Doughnut Görünümlü Paratiroid Adenomu

Derya Çayır[1], Mehmet Bozkurt[1], Mehmet Erdoğan[2], Salih Sinan Gültekin[1], Cem Azılı[3], Ata Türker[4]
[1]*University of Health Sciences, Dışkapı Yıldırım Beyazıt Training and Research Hospital, Clinic of Nuclear Medicine, Ankara, Turkey*
[2]*Süleyman Demirel University Faculty of Medicine, Department of Nuclear Medicine, Isparta, Turkey*
[3]*University of Health Sciences, Dışkapı Yıldırım Beyazıt Training and Research Hospital, Department of General Surgery, Ankara, Turkey*
[4]*University of Health Sciences, Dışkapı Yıldırım Beyazıt Training and Research Hospital, Department of Pathology, Ankara, Turkey*

Abstract

A 52-year-old woman presented with a complaint of neck swelling. The patient showed signs of hyperparathyroidism: hypercalcemia, and hypophosphatemia. Tc-99m MIBI dual-phase parathyroid scintigraphy and SPECT revealed increased activity in a regular-bordered, "doughnut"-shaped mass on the left side of the thyroid gland with a central hypoactive area. The cervical ultrasound identified a mixed echoic thyroid nodule with a central large cystic portion, and no parathyroid gland abnormality. Total thyroidectomy and parathyroid exploration was performed. Pathological evaluation of the resected thyroid specimen reported a giant intra-thyroidal hemorrhagic parathyroid adenoma.

Keywords: Parathyroid adenoma, Tc-99m sestamibi, SPECT

Öz

Boyunda şişlik şikayeti ile başvuran elli iki yaşında kadın hastada hiperkalsemi, hipofosfatemi ile hiperparatiroidizm saptandı. Yapılan Tc-99m MIBI dual faz paratiroid sintigrafisinde ve SPECT çalışmasında tiroid bezinin sol lobunu kaplayan, ortasında hipoaktif alanlar izlenen, artmış aktivite tutulumu gösteren "doughnut" görünümlü lezyon izlendi. Boyun ultrasonografide sol lobun üst ve orta kesiminde ortasında kistik komponent görülen, karışık ekoda tiroid nodülü gözlendi, ancak paratiroid patolojisi izlenmedi. Hastaya total tiroidektomi ve paratiroid eksplorasyonu yapıldı. Tiroid cerrahi spesimeninin patolojik deperlendirmesi dev intratiroidal hemorajik paratiroid adenomu olarak raporlandı.

Anahtar kelimeler: Paratiroid adenomu, Tc-99m sestamibi, SPECT

Address for Correspondence: Derya Çayır MD, University of Health Sciences, Dışkapı Yıldırım Beyazıt Training and Research Hospital, Clinic of Nuclear Medicine, Ankara, Turkey
Phone: +90 535 568 10 66 E-mail: drderyaors@hotmail.com ORCID ID: orcid.org/0000-0002-7756-3210
Received: 19.04.2018 **Accepted:** 27.07.2018

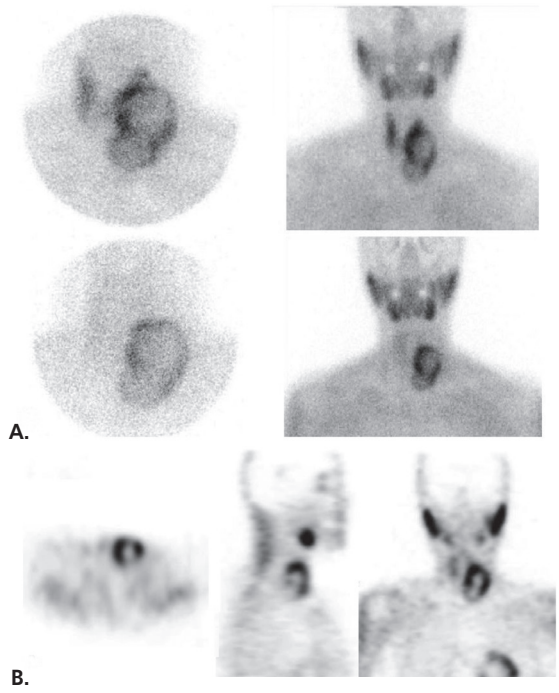

Figure 1. A 52-year-old woman presented with a complaint of neck swelling. The patient's laboratory examinations showed high levels of serum parathormone [356.5 pg/mL (normal range: 12-88)], hypercalcemia [12.37 mg/dL (normal: 8.8-10.6)], and hypophosphatemia [2.29 mg/dL (normal: 2.5-4.5)]. Primary hyperparathyroidism is the most frequent reason of hyperparathyroidism, and the most common cause of hyperparathyroidism is solitary parathyroid adenoma (1). Tc-99m MIBI parathyroid scintigraphy and cervical ultrasound (US) are the methods of choice for parathyroid imaging (2), while Tc-99m MIBI parathyroid scintigraphy shows good correlation with parathyroid hormone level and histopathologic diagnosis (3). Accordingly, we performed Tc-99m MIBI dual-phase parathyroid scintigraphy (A) and SPECT (B), on which an increased activity including a central hypoactive area as a regular round doughnut-shaped mass on the left side of the thyroid gland, extending through inferior part of the neck, was observed.

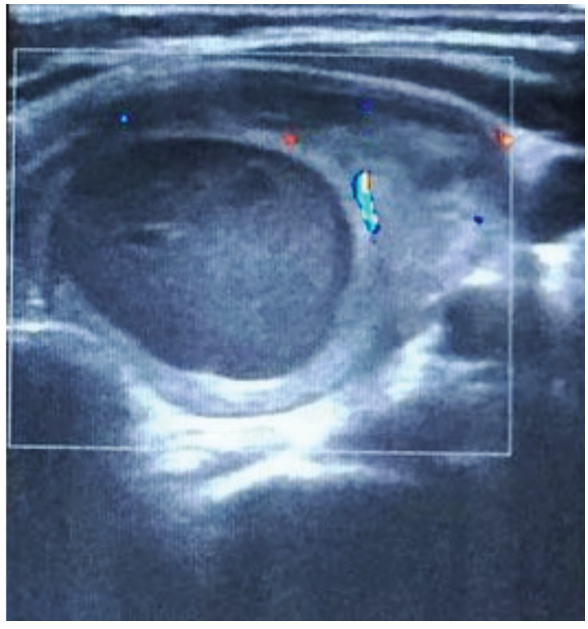

Figure 2. After finding out this MIBI active mass, cervical US was carried out to identify the lesion characteristics. The US revealed a mixed echoic intrathyroidal lesion, with a polar vascularity on color doppler US that was 36 mm in dimension with a central large cystic portion. The curative treatment for primary hyperparathyroidism is the surgical excision of the hyper-functioning parathyroid tissue (4).

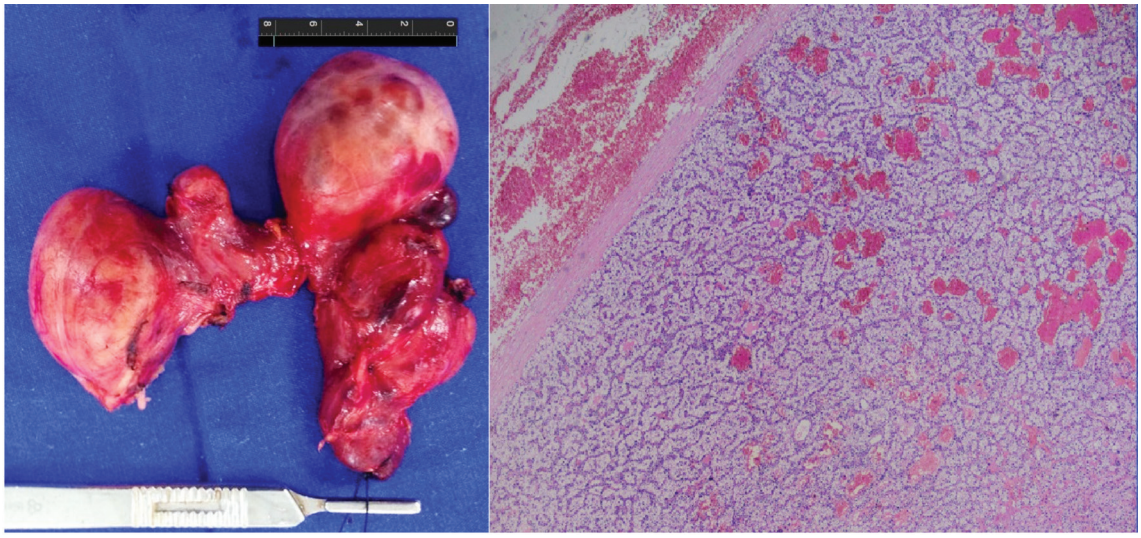

Figure 3. Consequently, the patient underwent total thyroidectomy and parathyroid exploration. Pathologic evaluation of the resected thyroid specimen revealed parathyroid adenoma of about 8 cm in diameter with extensive bleeding, localized within the left lobe. The prevalence of intrathyroidal parathyroid adenoma is around 1% in surgical series (5), and giant intrathyroidal parathyroid adenomas are extremely rare (6).
Whenever the diagnosis of a parathyroid adenoma is in question, Tc-99m MIBI dual-phase scan and SPECT or SPECT/CT can help to identify the parathyroid adenoma in patients with hyperparathyroidism.

Ethics

Informed Consent: Consent form was filled out by all participants.

Peer-review: Externally peer-reviewed.

Authorship Contributions

Surgical and Medical Practices: C.A., A.T., Concept: D.Ç., M.B., Design: D.Ç., Data Collection or Processing: D.Ç., M.B., M.E., Analysis or Interpretation: D.Ç., S.S.G., Literature Search: D.Ç., M.B., Writing: D.C., M.B.

Conflict of Interest: No conflict of interest was declared by the authors.

Financial Disclosure: The authors declared that this study received no financial support.

References

1. Ruda JM, Hollenbeak CS, Stack BC Jr. A systematic review of the diagnosis and treatment of primary hyperparathyroidism from 1995 to 2003. Otolaryngol Head Neck Surg 2005;132:359-372.
2. Hindié E, Ugur O, Fuster D, O'Doherty M, Grassetto G, Ureña P, Kettle A, Gulec SA, Pons F, Rubello D; Parathyroid Task Group of the EANM. 2009 EANM parathyroid guidelines. Eur J Nucl Med Mol Imaging 2009;36:1201-1216.
3. Silov G, Özdal A, Erdoğan Z, Turhal Ö, Karaman H. The Relationship Between Technetium-99m-Methoxyisobutyl Isonitrile Parathyroid Scintigraphy and Hormonal and Biochemical Markers in Suspicion of Primary Hyperparathyroidism. Mol Imaging Radionucl Ther 2013;22:8-13.
4. Silverberg SJ, Shane E, Jacobs TP, Siris E, Bilezikian JP. A 10-year prospective study of primary hyperparathyroidism with or without parathyroid surgery. N Engl J Med 1999;341:1249-1255.
5. Goodman A, Politz D, Lopez J, Norman J. Intrathyroid parathyroid adenoma: incidence and location the case against thyroid lobectomy. Otolaryngol Head Neck Surg 2011;144:867-871.
6. Vilallonga R, Zafón C, Migone R, Baena JA. Giant intrathyroidal parathyroid adenoma. J Emerg Trauma Shock 2012;5:196-198.

Letter to the Editor
Mol Imaging Radionucl Ther 2019;28:44-45 DOI:10.4274/mirt.galenos.2018.04127

Role of ^{18}F-FDG Positron Emission Tomography/Computed Tomography Imaging in Testicular Lymphoma

Testis Lenfomasında ^{18}F-FDG Pozitron Emisyon Tomografi/Bilgisayarlı Tomografi Görüntülemenin Rolü

Kamal Kant Sahu[1], Ajay Mishra[1], James O'shea[2]
[1]*Department of Internal Medicine, Saint Vincent Hospital, 123 Summer Street, Worcester, MA, 01608, United States*
[2]*Division of Hematology and Medical Oncology, Saint Vincent Cancer and Wellness Center, 1 Eaton Place, 01608, Worcester USA*

Keywords: Testis, DLBCL, R-CHOP, PET scan

Anahtar kelimeler: Testis, DLBCL, R-CHOP, PET görüntüleme

Dear Editor,

We read with great interest the recent article by Okuyucu et al. (1) regarding the role of ^{18}F-FDG PET/CT in the management of testicular lymphoma. Hereby, we would like to share our experience with regards to the diagnostic approach in a case of testicular lymphoma.

^{18}F-FDG PET/CT scan has a pivotal role as an initial modality to investigate non-Hodgkin's lymphoma. PET scan is now even considered the standard of care in follow-up, to assess the response and for tailoring the subsequent therapy. Thanks to the newer diagnostic modalities, oncologists are now diagnosing malignancies in rare sites as well (2,3,4). It is important to note that due to rare location, there are no standard guidelines to follow and, in such situations, oncologists investigate and treat based on their individual experience and available literature.

Testicular lymphoma is unique with regards to its location, aggressive nature and high rate of relapse to contralateral testis/central nervous system. In the testis, unlike the other sites, fine needle aspiration cytology and biopsy are not considered as the diagnostic tool and orchiectomy has both diagnostic and therapeutic implications PET scan provides essential information about the side of involvement (unilateral vs bilateral), extent and pattern of disease involvement (intense, mild, focal diffuse SUV uptake), risk of relapse (SUV_{max} uptake in brain parenchyma or contralateral testis), need of intrathecal methotrexate, radiation therapy to the contralateral testis etc.

Sidhu et al. (5) recently mentioned the different patterns of ^{18}F-FDG uptake (i.e. normal, focal, multifocal, symmetrically diffuse, asymmetrically diffuse) in their institutional study of 12 cases of lymphoma with secondary testicular involvement. Important to note that five out of 12 patients in their study had concurrent CT scans which were reported as normal. This fact again signifies the impeccable role of PET/CT. Recently, Ollila and Olszewski (6) studied the role of radiotherapy in primary testicular lymphoma. PET/CT would again be a good tool to guide radiation oncologists to determine the radiation field.

Address for Correspondence: Kamal Kant Sahu MD, Department of Internal Medicine, Saint Vincent Hospital, 123 Summer Street, Worcester, MA, 01608, United States
Phone: +1 508 363 50 00 E-mail: drkksahu85@gmail.com ORCID ID: orcid.org/0000-0002-0382-6882
Received: 05.08.2018 **Accepted:** 29.08.2018

Radiotherapy, addition of rituximab, prophylactic intrathecal chemotherapy and use of PET/CT scan have certainly improved progression free survival and overall survival in testicular lymphoma. Till today, data regarding testicular lymphoma are mostly derived from small case series and retrospective studies. Involvement of extramedullary sites especially reproductive organs can be extremely challenging due to their masquerading, atypical clinical presentations and impact to fertility (7,8,9). More studies and randomized clinical trials are required and would be helpful in formulating uniform guidelines for the management of testicular lymphoma.

Ethics

Informed Consent: Not needed.

Preer-review: Internally peer-reviewed.

Authorship Contributions

Concept: K.K.S., A.M., J.O., Design: K.K.S., A.M., J.O., Data Collection or Processing: K.K.S., A.M., J.O., Analysis or Interpretation: K.K.S., A.M., J.O., Literature Search: K.K.S., A.M., J.O., Writing: K.K.S., A.M., J.O.

Conflict of Interest: No conflict of interest was declared by the authors.

Financial Disclosure: The authors declared that this study received no financial support.

References

1. Okuyucu K, İnce S, Alagöz E, Ataş E, Arslan N. Utility of FDG PET/CT in the Management of Primary Testicular Lymphoma. Mol Imaging Radionucl Ther 2018;27:61-65.
2. Sahu KK, Thakur K. Role of Positron Emission Tomography Imaging in Myeloid Sarcoma. Indian J Nucl Med 2018;33:90.
3. Gautam A, Sahu KK, Alamgir A, Siddiqi I, Ailawadhi S. Extramedullary Solitary Plasmacytoma: Demonstrating the Role of (18)F-FDG PET Imaging. J Clin Diagn Res 2017;11:XD01-XD03.
4. Sahu KK, Gautam A, Ailawadhi S. Re: FDG PET/CT Findings of Intracardiac Myeloid Sarcoma. Clin Nucl Med 2017;42:242-245.
5. Sidhu P, Lin P, Son H, Rosenfeld D, Lin M. Testicular fluorine-18 fludeoxyglucose uptake on positron emission tomography CT in patients with lymphoma: clinical significance and management impact. Br J Radiol 2014;87:20140472.
6. Ollila TA, Olszewski AJ. Radiation therapy in primary testicular lymphoma: does practice match the standard of care? Leuk Lymphoma 2018:1-4.
7. Sahu KK, Jain A, Yanamandra U, Varma SC, Malhotra P. Myeloid Sarcoma of Vulva: A Short Update. Indian J Hematol Blood Transfus 2016;32(Suppl 1):69-71.
8. Sahu KK, Singh P, Malhotra P, Srinivasan R. Thyroid Plasmacytoma: A Rare Cause of Hoarseness of Voice. Indian J Nucl Med. 2019;34:78-80.
9. Sahu KK, Prakash G, Sanamandra P, Khadwal A, Dey P, Sharma P, Varma SC, Malhotra P. An Unusual Site of Acute Lymphoblastic Leukaemia Relapse: Challenge for Gynaecologists. J Obstet Gynaecol India. 2016;66(Suppl 2):656-661.